

HONG KONG

MEDICAL JOURNAL

香港醫學雜誌

The official publication of the
Hong Kong Academy of Medicine and
the Hong Kong Medical Association

25(S9)

HONG KONG MEDICAL JOURNAL

香港醫學雜誌

Volume 25 Number 6 December 2019

Supplement 9

Health and Medical Research Fund

Research Dissemination Reports

醫療衛生研究基金

研究成果報告

Vision Science
視覺科學

Infectious Disease
傳染病

Cancer
癌症



ISSN 1024-2708

香港醫學專科學院出版社
HONG KONG ACADEMY OF MEDICINE PRESS

MEDICAL JOURNAL

香港醫學雜誌

EDITOR-IN-CHIEF

Martin CS Wong 黃至生

SENIOR EDITORS

LW Chu 朱亮榮
 Albert KK Chui 徐家強
 Michael G Irwin
 Eric CH Lai 賴俊雄
 KY Leung 梁國賢
 Anthony CF Ng 吳志輝
 TW Wong 黃大偉

EDITORS

KS Chan 陳健生
 Kelvin KL Chong 莊金隆
 Jacqueline PW Chung 鍾佩樺
 James TK Fung 馮德焜
 Brian SH Ho 何思灝
 Ellis KL Hon 韓錦倫
 KW Huang 黃凱文
 WK Hung 熊維嘉
 Bonnie CH Kwan 關清霞
 Arthur CW Lau 劉俊穎
 PY Lau 婁培友
 Danny WH Lee 李偉雄
 Thomas WH Leung 梁慧康
 WK Leung 梁惠強
 Kenneth KW Li 李啟煌
 Janice YC Lo 羅懿之
 Herbert HF Loong 龍浩鋒
 James KH Luk 陸嘉熙
 Arthur DP Mak 麥敦平
 Henry KF Mak 麥嘉豐
 Martin W Pak 白威
 Walter WK Seto 司徒偉基
 Regina WS Sit 薛詠珊
 William YM Tang 鄧旭明
 Jeremy YC Teoh 張源津
 KY Tse 謝嘉瑜
 Harry HX Wang 王皓翔
 HL Wong 黃學良
 Kenneth KY Wong 黃格元
 Patrick CY Woo 胡釗逸
 Hao Xue 薛浩
 Bryan PY Yan 甄秉言
 TK Yau 游子覺
 Kelvin KH Yiu 姚啟恒

EPIDEMIOLOGY ADVISERS

Daniel SY Ho 何世賢
 Eman Leung 梁以文
 Edmond SK Ma 馬紹強
 Gary Tse 謝家偉
 Shelly LA Tse 謝立亞
 Ian YH Wong 王逸軒
 Esther YT Yu 余懿德
 Hunter KL Yuen 袁國禮

STATISTICAL ADVISERS

Marc KC Chong 莊家俊
 William B Goggins
 Eddy KF Lam 林國輝
 Carlos KH Wong 黃競浩

HONORARY ADVISERS

David VK Chao 周偉強
 Paul BS Lai 賴寶山

Health and Medical Research Fund**Research Dissemination Reports****Editorial**

3

VISION SCIENCE**Diabetic retinopathy screening for specialist care**

4

*KKW Li, L Wong, SM McGhee, YW Kam, R Gangwani, JX Lian, DSH Wong***Improving the current diabetic macular oedema screening programme**

8

*I Wong, R Wong, R Gangwani, V Chong, R Kawasaki***Genetic prediction models for primary open-angle glaucoma: translational research**

12

*LJ Chen, CP Pang, CCY Tham, CKS Leung***INFECTIOUS DISEASE****Surveillance of biologic sources of hepatitis E viruses in community**

17

*MCW Chan, PKS Chan***Antiviral activity of human $\gamma\delta$ -T cells against enterovirus 71**

21

*KT Lam, J Zheng, Z Xiang, YP Liu, YL Lau, WW Tu***Pre-pandemic live-attenuated influenza vaccine**

24

DH He, APY Chiu, JTK Wu, BJ Cowling

**INTERNATIONAL EDITORIAL
ADVISORY BOARD**

Sabarathnam Arulkumaran
United Kingdom

Robert Atkins
Australia

Peter Cameron
Australia

Daniel KY Chan
Australia

David Christiani
United States

Andrew Coats
Australia

James Dickinson
Canada

Willard Fee, Jr
United States

Robert Hoffman
United States

Sean Hughes
United Kingdom

Roger Jones
United Kingdom

Michael Kidd
Australia

Arthur Kleinman
United States

Stephen Leeder
Australia

Xiaoping Luo
PR China

William Rawlinson
Australia

Jonathan Samet
United States

Yaojiang Shi
PR China

David Weller
United Kingdom

Max Wintermark
United States

Atsuyuki Yamataka
Japan

Homer Yang
Canada

KG Yeoh
Singapore

Matthew Yung
United Kingdom

Zhijie Zheng
PR China

Full details of the Editorial Board
are available online at
<https://www.hkmj.org/about/eo.html>

MANAGING EDITOR

Alan Purvis

DEPUTY MANAGING EDITOR

Betty Lau 劉薇薇

ASSISTANT MANAGING EDITOR

Warren Chan 陳俊華

CANCER

| | |
|---|-----------|
| PEGylated recombinant human arginase as a drug for breast cancer <i>SL Leung, MK Ho, YM Lam, HY Chow, YH So, YC Leung</i> | 28 |
| Detection of methylated septin 9 DNA in blood for diagnosis, prognosis, and surveillance of colorectal cancer <i>WK Leung, VY Shin, WL Law</i> | 32 |
| M2 macrophages on tumour growth and metastasis in hepatocellular carcinoma <i>K Man, CM Lo, XB Liu</i> | 35 |
| Computational platform for modelling, analysis, and prediction of anti-EGFR drug resistance for lung cancer <i>H Yan, GY Zhu, M Wong, V Lee</i> | 40 |
| Combined use of <i>Andrographis paniculata</i> and chemotherapeutics for metastatic oesophageal cancer: a pre-clinical study <i>L Li, GGL Yue, KP Fung, J Yu, CBS Lau, PWY Chiu</i> | 43 |
| Author index | 47 |
| Disclaimer | 48 |

Editorial

Dissemination reports are concise informative reports of health-related research supported by the Health and Medical Research Fund (and its predecessor funds) administered by the Food and Health Bureau. In this edition, we present 11 dissemination reports of projects related to vision science, infectious disease, and cancer. In particular, three projects are highlighted due to their potentially significant findings, impact on healthcare delivery and practice, and/or contribution to health policy formulation in Hong Kong.

Diabetic retinopathy (DR) is a complication of diabetes mellitus. Screening for DR is very cost-effective. In the Hong Kong public healthcare system, people with diabetes mellitus are screened at least once every 6 months. However, patients attending specialist clinics or a private general practitioner for diabetes care may not be screened. Li et al¹ aimed to identify the prevalence of DR in a sample of attendees at specialist clinics and factors that could disrupt the continuity of complication monitoring. They found that the weighted prevalence of DR and sight-threatening DR was 41.8% and 10.4%, respectively. The authors identified system factors that affected access to DR screening, which should be emphasised to improve the preventive care for those at high risk of avoidable vision loss.

Hepatitis E virus (HEV) is transmitted mainly through the faecal-oral route. HEV is genetically classified into at least seven genotypes (HEV 1-7).

In Hong Kong, hepatitis E is a notifiable disease and the number of cases has been increasing since 2001. Chan and Chan² reported the prevalence of HEV in different food items over a 2-year period and genotyped HEV from clinical cases over the same period. They provided molecular evidence suggesting that contaminated pig liver is one possible source of local human cases of HEV infections.

Breast cancer is the most common cancer in women. Safe and effective treatments against triple-negative breast cancer (ie not expressing oestrogen receptor, progesterone receptor, or HER2) are in demand. Arginine is essential for the growth of a variety of tumours and depleting arginine leads to inhibition of tumour growth. Leung et al³ developed a PEGylated recombinant human arginase that was effective in a triple-negative xenograft model. The drug is safe and effective and should present fewer immunological problems compared with other bacterial-derived arginine-depleting enzymes.

We hope you will enjoy this selection of research dissemination reports. Electronic copies of these dissemination reports and the corresponding full reports can be downloaded individually from the Research Fund Secretariat website (<https://rfs2.fhb.gov.hk/>). Researchers interested in the funds administered by the Food and Health Bureau also may visit the website for detailed information about application procedures.

Supplement editor



Dr Richard A Collins
Chief Scientific Reviewer
(Research Office)
Food and Health Bureau

References

1. Li KKW, McGhee SM, Kam YW, Gangwani R, Lian JX. Diabetic retinopathy screening for specialist care. *Hong Kong Med J* 2019;25(Suppl 9):S4-7.
2. Chan MCW, Chan PKS. Surveillance of biologic sources of hepatitis E viruses in community. *Hong Kong Med J* 2019;25(Suppl 9):S17-20.
3. Leung SL, Ho MK, Lam YM, Chow HY, So YH, Leung YC. PEGylated recombinant human arginase as a drug for breast cancer. *Hong Kong Med J* 2019;25(Suppl 9):S28-31.

Diabetic retinopathy screening for specialist care

KKW Li *, L Wong, SM McGhee, YW Kam, R Gangwani, JX Lian, DSH Wong

KEY MESSAGES

1. The weighted prevalence of diabetic retinopathy (DR) and sight-threatening diabetic retinopathy (STDR) among subjects was 41.8% and 10.4%, respectively.
2. Around 20% of subjects with diabetes who attended the studied hospital reported not having been offered DR screening before. The others had been offered it by the hospital diabetic clinic (41.0%, 431/1051), a general outpatient clinic (GOPC, 13.7%, 144/1051), the hospital ophthalmology department (8.4%, 88/1051) or the hospital family medicine clinic (8.4%, 88/1051).
3. Subjects attending the renal clinic and the cardiac clinic were less likely to be offered DR screening (renal: OR=0.48, $P<0.001$; cardiac: OR=0.60, $P=0.003$) and less likely to have appropriate DR screening in place (renal: OR=0.49, $P<0.001$; cardiac: OR=0.61, $P=0.004$) when compared to those attending the family medicine clinic. Subjects attending the renal clinic were more likely to have DR (OR=3.85, $P<0.001$) and STDR (OR=6.14, $P<0.001$) than those attending the family medicine clinic.
4. Subjects who attended a GOPC for diabetes care as well as a specialist clinic were more likely to have been offered DR screening (OR=2.05, $P=0.001$) and have appropriate DR screening in place (OR=2.09, $P<0.001$) than those who do not attend a GOPC. However, access to a GOPC was not significantly associated with the presence of DR and STDR.

Hong Kong Med J 2019;25(Suppl 9):S4-7
HMRF project number: 11121381

¹KKW Li, ^{1,4}L Wong, ²SM McGhee, ³YW Kam, ⁴R Gangwani, ^{4,5}JX Lian, ⁴DSH Wong

¹ Department of Ophthalmology, United Christian Hospital

² School of Public Health, The University of Hong Kong

³ Department of Medicine and Geriatrics, United Christian Hospital

⁴ Department of Ophthalmology, The University of Hong Kong

⁵ School of Optometry, The Hong Kong Polytechnic University

* Principal applicant and corresponding author: lkw856@ha.org.hk

Introduction

Diabetic retinopathy (DR) is a complication of diabetes mellitus (DM); screening for DR is one of the most cost-effective health procedures available.¹⁻³ The Hospital Authority of Hong Kong have set up screening services within General Outpatient Clinics (GOPCs), at which people with DM are screened at least once every 6 months to 2 years depending on individual risk factors.^{4,5} However, some patients who attend some specialist clinic or a private general practitioner for diabetes care may not be screened. These people probably have risk factors (such as longer duration of diabetes, high blood pressure, and high cholesterol levels) of avoidable blindness.

In a previous pilot study at Queen Mary Hospital, among 3276 patients screened for DR, 17% were identified to have sight-threatening diabetic retinopathy (STDR) at screening and required specialist confirmation and about 4% had maculopathy (unpublished results). These patients were from a variety of other specialist clinics. We did not know how many of them had been screened and how many were under ophthalmologist care. In the present study, we aimed to (1) identify the prevalence of DR in a representative sample of attenders at specialist clinics in a general hospital, (2) collect data on previous and current screening and/or care for

DR, usual source of care for DM, and other factors that could disrupt the continuity of complication monitoring, and (3) identify the characteristics of those who went through the net of complication screening so as to improve service provision.

Methods

Patients with DM who had an appointment in any cardiac, renal, diabetic, or family medicine specialist clinic in the United Christian Hospital in the subsequent 9 months were identified. They were contacted by telephone to obtain consent to participate, complete a structured telephone interview, and be invited for DR screening by an optometrist using a non-mydratic retinal camera. Based on the UK National Screening Programme for Diabetic Retinopathy grading scheme, DR grading was classified as no retinopathy, background retinopathy, pre-proliferative retinopathy, proliferative retinopathy, maculopathy, or photocoagulation. STDR was defined as pre-proliferative retinopathy to photocoagulation. For those who had been screened but did not take up DR screening, their DR status was extracted from their medical records. Univariate and multivariate logistic regression models were used to investigate whether system factors (ie, specialist clinic attendance and access to a GOPC for

diabetes care) were associated with (1) being offered DR screening, (2) having appropriate DR screening in place (defined as screening attended within the last 2 years and offered by a public GOPC or ophthalmologist, an optometrist (public or private), a diabetic clinic (public or private), or a public family medicine specialist clinic, (3) presence of any DR, and (4) presence of STDR.

Results

A total of 2136 patients were contacted. Of 1761 patients eligible, 1313 (74.6%) agreed to participate, of whom 411 attended screening. Of the remaining 902 subjects who did not attend screening, 778 had their DR records extracted for analysis. Of 1313 patients, 1051 (80.1%) reported that they had been offered DR screening before, most commonly by the hospital diabetic clinic (41.0%, n=431), followed by the GOPC (13.7%, n=144), the hospital ophthalmology department (8.4%, n=88), and the hospital family medicine clinic (8.4%, n=88). Among 262 patients who reported never having been offered DR screening, only 44 (16.8%) knew where they could have it done. Of 1313 patients, only 738 (56.2%) had appropriate DR screening in place. Of 1189 DR results available (411 attended screening and 778 had medical records extracted), 17 were ungradable and 1172 were gradable. Of the latter, the overall unweighted prevalence of DR and STDR was 48.6% (n=570) and 16.3% (n=191), respectively, compared with 41.8% (95% CI=37.5%-46.1%) and 10.4% (95% CI=8.1%-12.7%) after weighting by the number of patients with appointments in the clinic in the same period.

Compared with those attending the family medicine clinic, those attending the renal clinic (odds ratio [OR]=0.48, $P<0.001$) and cardiac clinic (OR=0.60, $P=0.003$) were less likely to be offered DR screening and have appropriate DR screening in place (OR=0.49, $P<0.001$ and OR=0.61, $P=0.004$, respectively) [Table]. Compared with those attending the family medicine clinic, those attending the renal clinic were more likely to have DR (OR=3.85, $P<0.001$) and STDR (OR=6.14, $P<0.001$) [Table]. Those attending the GOPC for diabetes care and the specialist clinic were more likely to have been offered DR screening (OR=2.05, $P=0.001$) and have appropriate DR screening in place (OR=2.09, $P<0.001$) than those who did not attend a GOPC (Table). However, access to GOPC was not associated with presence of DR and STDR (Table).

Discussion

Most participants who claimed never to have been offered screening did not know where to access DR screening and only half of them had appropriate screening being in place. There is room

for improvement to ensure those with diabetes can access regular screening for DR with a maximum interval of 2 years, based on retinal photographs. Specialist awareness of the importance of referring those with diabetes to DR screening should be heightened, especially for those at high risk of DR and STDR. Our findings on prevalence of DR at specialist clinics are similar to those reported in a study of 164 755 primary care patients after excluding ungradable results, in which 41.3% (95% CI=41.1%-41.5%) and 10.4% (95% CI=10.2%-10.5%) were found to have DR and STDR, respectively.⁴

There were limitations to this study. A large number of patients refused our screening and claimed that they had already been screened. We extracted their DR results from medical records. They had not been randomly selected for screening and may represent a biased sample. Patients with DR results extracted from medical records had longer duration of diabetes (12.4 vs 10.1 months, $P<0.001$) and higher haemoglobin A1c value (7.5% vs 7.2%, $P=0.005$) than those attending our screening. They also had a higher rate of DR and STDR; they were selected for screening by doctors probably because of higher risk. Excluding them might have resulted in a lower risk sample at screening. We therefore combined the two groups for analysis. Whether patients have ever been offered DR screening or appropriate DR screening in place was based on self-reported data collected retrospectively and may be subject to recall bias. We tried to reduce this bias by confirming the information with a series of questions on specifications (who offered screening, the name of place, the date of screening, and whether screened with a camera). We followed up the DR status in STDR cases detected by our screening, but we did not have follow-up results of STDR cases detected by other programmes. This may have resulted in overreporting.

Conclusion

Both system factors of specialist clinic attendance and access to a GOPC for diabetes care affected access to DR screening. Those attending specialist clinics (rather than family medicine clinic in the hospital) and those not attending a GOPC with DR screening settings may have been missed to be screened for DR. These system factors should be emphasised to improve the preventive care for those at high risk of avoidable vision loss, especially for those attending renal and cardiac clinics.

Acknowledgements

This study was supported by the Health and Medical Research Fund, Food and Health Bureau, Hong Kong SAR Government (11121381). We thank Prof David Wong for contributing to the design and set

TABLE. Multivariate analyses of factors associated with screening being offered, appropriate screening in place, diabetic retinopathy, and sight-threatening diabetic retinopathy

| Variable | Screening being offered (n=1311) | | Appropriate screening in place (n=1311) | | Diabetic retinopathy (n=1165) | | Sight-threatening diabetic retinopathy (n=1166) | |
|---|--------------------------------------|---------|---|---------|--------------------------------------|---------|---|---------|
| | Odds ratio (95% confidence interval) | P value | Odds ratio (95% confidence interval) | P value | Odds ratio (95% confidence interval) | P value | Odds ratio (95% confidence interval) | P value |
| Age, y | 0.98 (0.96-0.99) | <0.001 | 0.97 (0.96-0.99) | <0.001 | 0.98 (0.97-1) | 0.023 | 0.95 (0.93-0.97) | <0.001 |
| Sex | | | | | | | | |
| Female | 1.00 | | 1.00 | | 1.00 | | 1.00 | |
| Male | 1.03 (0.75-1.42) | 0.847 | 1.01 (0.73-1.38) | 0.959 | 2.59 (1.82-3.7) | <0.001 | 1.89 (1.15-3.1) | 0.012 |
| Marital status | | | | | | | | |
| Never married | 1.00 | | 1.00 | | 1.00 | | 1.00 | |
| Married | 1.30 (0.83-2.04) | 0.249 | 1.32 (0.85-2.07) | 0.219 | 0.99 (0.62-1.6) | 0.982 | 0.75 (0.41-1.37) | 0.35 |
| Divorced/separated/widowed | 1.38 (0.82-2.33) | 0.227 | 1.39 (0.83-2.35) | 0.213 | 1.38 (0.79-2.44) | 0.259 | 1.08 (0.52-2.25) | 0.84 |
| Education level | | | | | | | | |
| No schooling/pre-primary | 1.00 | | 1.00 | | 1.00 | | - | |
| Primary | 1.12 (0.73-1.73) | 0.596 | 1.16 (0.76-1.78) | 0.496 | 0.73 (0.45-1.19) | 0.203 | - | - |
| Secondary lower (Forms 1-5) | 0.98 (0.61-1.57) | 0.93 | 1.04 (0.65-1.67) | 0.859 | 0.76 (0.45-1.29) | 0.31 | - | - |
| Form 6 and above | 1.75 (0.96-3.19) | 0.066 | 1.85 (1.02-3.34) | 0.043 | 0.41 (0.22-0.8) | 0.008 | - | - |
| Monthly family income | | | | | | | | |
| <\$9999 | 1.00 | | 1.00 | | 1.00 | | 1.00 | |
| \$10000-19999 | 0.95 (0.64-1.42) | 0.816 | 0.95 (0.64-1.41) | 0.8 | 1.16 (0.75-1.8) | 0.497 | 1.13 (0.64-1.99) | 0.665 |
| \$20000-29999 | 1.06 (0.67-1.67) | 0.816 | 1.06 (0.67-1.67) | 0.808 | 0.69 (0.42-1.12) | 0.135 | 0.91 (0.47-1.76) | 0.779 |
| \$30000-39999 | 1.36 (0.74-2.49) | 0.322 | 1.35 (0.73-2.47) | 0.337 | 1.67 (0.92-3.05) | 0.094 | 1.50 (0.69-3.26) | 0.301 |
| ≥\$40000 | 0.65 (0.38-1.1) | 0.107 | 0.64 (0.38-1.1) | 0.106 | 0.81 (0.46-1.43) | 0.47 | 0.60 (0.26-1.39) | 0.237 |
| Refuse to answer/don't know | 0.96 (0.69-1.33) | 0.804 | 0.95 (0.69-1.32) | 0.779 | 1.11 (0.77-1.59) | 0.581 | 0.80 (0.47-1.35) | 0.408 |
| Receiving Comprehensive Social Security Assistance | | | | | | | | |
| No | 1.00 | | 1.00 | | 1.00 | | - | |
| Yes | 0.79 (0.55-1.14) | 0.205 | 0.77 (0.54-1.1) | 0.155 | 1.72 (1.14-2.57) | 0.009 | - | - |
| Currently access to general outpatient clinic | | | | | | | | |
| No | 1.00 | | 1.00 | | 1.00 | | 1.00 | |
| Yes | 2.05 (1.36-3.1) | 0.001 | 2.09 (1.38-3.15) | <0.001 | 0.97 (0.63-1.52) | 0.909 | 0.57 (0.24-1.36) | 0.208 |
| Attended specialist clinic | | | | | | | | |
| Family medicine clinic | 1.00 | | 1.00 | | 1.00 | | 1.00 | |
| Cardiac clinic | 0.60 (0.43-0.84) | 0.003 | 0.61 (0.44-0.85) | 0.004 | 1.26 (0.87-1.81) | 0.225 | 0.93 (0.46-1.88) | 0.839 |
| Diabetic clinic | 1.47 (0.98-2.21) | 0.06 | 1.50 (1-2.24) | 0.05 | 1.20 (0.79-1.83) | 0.394 | 1.56 (0.81-3.02) | 0.186 |
| Renal clinic | 0.48 (0.34-0.67) | <0.001 | 0.49 (0.35-0.69) | <0.001 | 3.85 (2.61-5.69) | <0.001 | 6.14 (3.46-10.89) | <0.001 |
| Know diabetes could affect blindness (diabetic retinopathy) | | | | | | | | |
| No | 1.00 | | 1.00 | | - | | - | |
| Yes | 1.39 (0.68-2.82) | 0.362 | 0.73 (0.54-1) | 0.05 | - | - | - | - |
| Don't know | 0.93 (0.43-1.99) | 0.853 | 0.69 (0.51-0.93) | 0.015 | - | - | - | - |
| Think early diabetic retinopathy symptomatic | | | | | | | | |
| No | 1.00 | | - | | - | | 1.00 | |
| Yes | 0.72 (0.53-0.99) | 0.04 | - | - | - | - | 0.79 (0.51-1.21) | 0.28 |
| Don't know | 0.71 (0.52-0.98) | 0.034 | - | - | - | - | 0.60 (0.36-0.98) | 0.04 |

TABLE. (cont'd)

| Variable | Screening being offered (n=1311) | | Appropriate screening in place (n=1311) | | Diabetic retinopathy (n=1165) | | Sight-threatening diabetic retinopathy (n=1166) | |
|--|--------------------------------------|---------|---|---------|--------------------------------------|---------|---|---------|
| | Odds ratio (95% confidence interval) | P value | Odds ratio (95% confidence interval) | P value | Odds ratio (95% confidence interval) | P value | Odds ratio (95% confidence interval) | P value |
| Aware that there is treatment for diabetic retinopathy | | | | | | | | |
| No | 1.00 | | - | | 1.00 | | 1.00 | |
| Yes | 0.91 (0.71-1.18) | 0.49 | - | - | 1.54 (1.18-2.01) | 0.002 | 3.25 (2.18-4.84) | <0.001 |
| Smoking status | | | | | | | | |
| Non-smoker | 1.00 | | 1.00 | | 1.00 | | 1.00 | |
| Ex-smoker | 1.21 (0.86-1.7) | 0.281 | 1.20 (0.86-1.69) | 0.284 | 0.89 (0.61-1.29) | 0.532 | 1.18 (0.7-1.99) | 0.534 |
| Current smoker | 0.96 (0.62-1.48) | 0.845 | 0.96 (0.62-1.49) | 0.865 | 0.77 (0.48-1.24) | 0.282 | 0.49 (0.24-1.03) | 0.061 |
| Alcohol intake | | | | | | | | |
| Never | 1.00 | | 1.00 | | 1.00 | | 1.00 | |
| Ex-drinker | 0.96 (0.65-1.41) | 0.832 | 0.97 (0.66-1.42) | 0.887 | 1.07 (0.7-1.64) | 0.747 | 1.39 (0.79-2.42) | 0.251 |
| Drink less than once a month (eg special occasions) | 1.12 (0.76-1.65) | 0.555 | 1.12 (0.76-1.65) | 0.557 | 0.99 (0.65-1.49) | 0.944 | 0.63 (0.33-1.19) | 0.154 |
| Current drinker | 1.78 (1.05-3.05) | 0.034 | 1.76 (1.03-2.99) | 0.038 | 0.80 (0.46-1.38) | 0.415 | 0.43 (0.17-1.06) | 0.068 |
| Duration of diabetes, y | 1.04 (1.02-1.05) | <0.001 | 1.04 (1.02-1.05) | <0.001 | 1.06 (1.04-1.08) | <0.001 | 1.06 (1.04-1.09) | <0.001 |
| Type of diabetes | | | | | | | | |
| Type 1 | 1.00 | | 1.00 | | 1.00 | | 1.00 | |
| Type 2 | 0.47 (0.19-1.11) | 0.084 | 0.47 (0.2-1.12) | 0.089 | 2.28 (1.18-4.37) | 0.014 | 14.25 (3.93-51.66) | <0.001 |
| Others | 0.89 (0.12-6.34) | 0.908 | 0.84 (0.12-6.08) | 0.864 | | | | |
| Haemoglobin A1c, % | 1.07 (0.98-1.17) | 0.113 | 1.07 (0.98-1.17) | 0.12 | 1.18 (1.07-1.29) | 0.001 | 1.07 (0.95-1.2) | 0.293 |
| Systolic blood pressure, mm Hg | 1.00 (1-1.01) | 0.371 | 1.00 (1-1.01) | 0.362 | 1.01 (1-1.02) | 0.004 | 1.03 (1.02-1.04) | <0.001 |
| Diastolic blood pressure, mm Hg | 0.99 (0.97-1) | 0.038 | 0.99 (0.97-1) | 0.044 | 0.98 (0.96-0.99) | 0.003 | 0.96 (0.94-0.98) | 0.001 |
| Self-perceived health | | | | | | | | |
| Excellent | - | | - | | 1.00 | | - | |
| Good | - | - | - | - | 1.54 (0.52-4.53) | 0.436 | - | - |
| Average | - | - | - | - | 1.75 (0.62-4.95) | 0.295 | - | - |
| Fair | - | - | - | - | 2.38 (0.82-6.86) | 0.109 | - | - |
| Poor | - | - | - | - | 1.84 (0.6-5.64) | 0.288 | - | - |

up of this study. We also thank Dr Chan Kin-sang, Department of Medicine, Haven of Hope Hospital for his support in collaborative studies between Department of Ophthalmology and Department of Medicine and Geriatrics, Ms Monica Lee, Ward Manager, Department of Ophthalmology, United Christian Hospital, and Ms Maisy Mok Pik-hung, Nurse Consultant, Diabetes Ambulatory Care Centre, United Christian Hospital for their help in subject recruitment and logistical support.

References

1. Tung TH, Chen SJ, Liu JH, et al. A community-based follow-up study on diabetic retinopathy among type 2

diabetics in Kinmen. *Eur J Epidemiol* 2005;20:317-23.
 2. Stefansson E, Bek T, Porta M, Larsen N, Kristinsson JK, Agardh E. Screening and prevention of diabetic blindness. *Acta Ophthalmol Scand* 2000;78:374-85.
 3. American Academy of Ophthalmology Retina Panel. Preferred Practice Pattern Guidelines. Diabetic Retinopathy. San Francisco: American Academy of Ophthalmology; 2008.
 4. Lian JX, Gangwani RA, McGhee SM, et al. Systematic screening for diabetic retinopathy (DR) in Hong Kong: prevalence of DR and visual impairment among diabetic population. *Br J Ophthalmol* 2016;100:151-5.
 5. Gangwani RA, Lian JX, McGhee SM, Wong D, Li KK. Diabetic retinopathy screening: global and local perspective. *Hong Kong Med J* 2016;22:486-95.

Improving the current diabetic macular oedema screening programme

I Wong*, R Wong, R Gangwani, V Chong, R Kawasaki

KEY MESSAGES

1. The current diabetic retinopathy screening strategy is very effective at detecting maculopathy, but it has low sensitivity and positive predictive value.
2. Under the current strategy, up to 87.1% of patients referred to ophthalmologists for maculopathy screening were found to be false positives.
3. Three newly proposed screening strategies were compared with the current strategy in terms of sensitivity index and cost-effectiveness.
4. Strategy D that incorporated macular optical coherence tomography for all patients into the

current strategy was most cost-effective.

Hong Kong Med J 2019;25(Suppl 9):S8-11
HMRF project number: 11121801

¹ I Wong, ² R Wong, ¹ R Gangwani, V Chong, ⁴ R Kawasaki

¹ Department of Ophthalmology, LKS Faculty of Medicine, The University of Hong Kong

² Department of Ophthalmology, The Hong Kong Eye Hospital

³ Department of Ophthalmology, Oxford University, UK

⁴ Department of Public Health, Yamagata University Graduate School of Medical Science, Japan

* Principal applicant and corresponding author: wongyhi@hku.hk

Introduction

Diabetic retinopathy (DR) is a common cause of blindness. Diabetic macular oedema (DME) and proliferative diabetic retinopathy are the two major causes of vision loss in DR. Timely treatment is effective at preventing vision loss due to DME.¹ From a public health standpoint, prevention is more cost-effective than treatment.

In Hong Kong, the current DR screening strategy is based on fundus photograph grading.² Diabetic patients who attend general outpatient clinics are offered annual fundus photography screening. Those with maculopathy are referred for clinical assessment by ophthalmologists at specialist outpatient clinics. Those confirmed to have DME are offered treatments as appropriate.

Accurate diagnosis of DME requires stereopsis and detection of macular thickening. Even with stereo fundus photography, detection of DME may be difficult. Determining the presence of surrogate markers in the macula (ie, retinal exudates and/or haemorrhages) is the recommended first step in predicting the presence of macular oedema. Nonetheless, these surrogate markers may not be perfectly correlated with DME.

We have reported the DR screening results among 174532 diabetic patients over 3.5 years.² The prevalence of DR was 39%. Of all patients, 8.6% (15009) had fundus photographs graded as maculopathy. This accounted for up to 87.4% of all cases referred to specialist outpatient clinics during those 3.5 years.² This indicates that maculopathy is

the most prevalent diagnosis of sight-threatening diabetic retinopathy among those with diabetes. Owing to the limitation of fundus photography to visualising retinal thickening in DME, false-positive maculopathy cases are a concern. Based on the current screening strategy, we devised three additional strategies to enhance the overall sensitivity and cost-effectiveness of screening. This study aimed to compare different screening strategies with the current strategy in terms of the sensitivity index and cost-effectiveness of DME detection.

Methods

Patients were recruited from the Diabetic Complications Screening Programme of the Hong Kong West Cluster, Hospital Authority from 1 February 2014 to 31 January 2016. Strategy A was the current screening protocol. Strategy B did not consider retinal haemorrhage in the macula as a surrogate marker for maculopathy; patients with haemorrhage only were not considered to have maculopathy. Strategy C used best-corrected visual acuity instead of visual acuity and used optical coherence tomography (OCT) for referred cases with suspicion of maculopathy only if positive for maculopathy. Strategy D used OCT of the macula for all cases in addition to all components of strategy A. The screening procedures have been reported previously.² Best-corrected visual acuity assessment and measurement of macular volume using OCT (Cirrus HD OCT 4000, Carl Zeiss Meditec, Dublin [CA], USA) were performed on all patients.

Reports of all patients were reviewed by investigators other than the initial grading optometrist(s). All assessments were reviewed separately by two independent investigators, and the results were recorded as the reference standard.

The current screening protocol (strategy A) was the benchmark and compared with the three

other screening strategies. A model was formulated to simulate the current practice. The model estimated the costs for each patient until 12 months after being seen by an ophthalmologist. As there were no real-life data to show the exact probability that a patient underwent a particular management step, estimates were based on interviews with local retinal experts

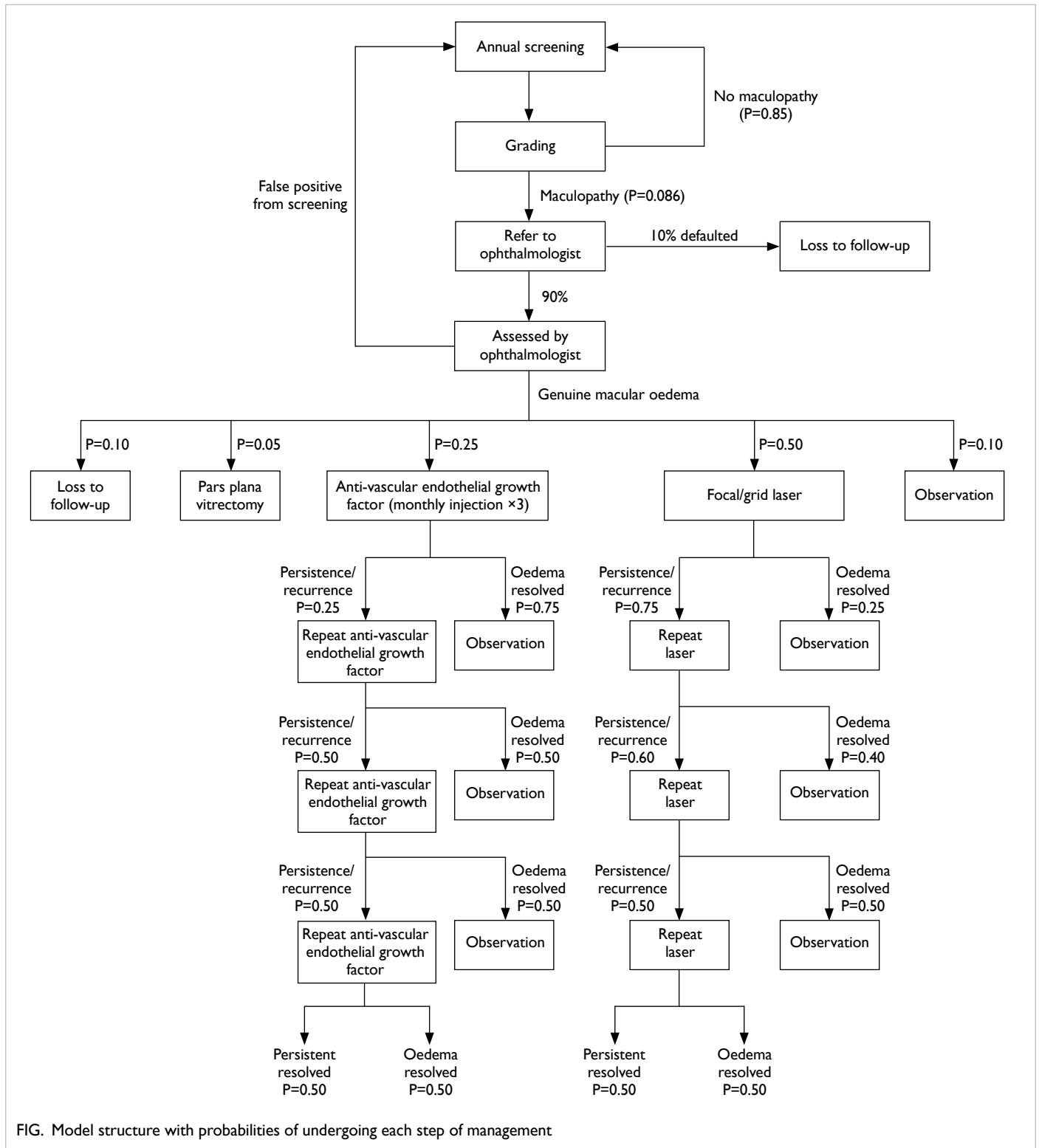


FIG. Model structure with probabilities of undergoing each step of management

and a review of medical records and the literature.¹ The per-person health provider costs of (1) the screening programme, (2) retinal examination at specialist outpatient clinics, and (3) treatment costs until 1 year after screening were used in the analysis (Fig).

The four strategies were compared in terms of sensitivity index, quality-adjusted life-years (QALYs) gained, and cost-effectiveness. Reference values were the gross domestic product (GDP) per capita of Hong Kong in 2014 (HK\$310 113 or US\$39 963)⁵ and US\$50 000/QALY gained.³ Strategies that costs <1, 1 to 3, and >3 times the GDP per capita were considered as 'very cost-effective', 'cost-effective', and 'not cost-effective', respectively.⁴

Results

A total of 2277 patients (mean age, 62.80±11.75

years) were recruited; 996 (43.7%) of them were male. The outcomes and sensitivities of the four screening strategies are shown in Table 1. The QALY gained per patient was 0.45. The total QALY gained, costs involved, and incremental cost-effectiveness ratio for each strategy are shown in Table 2. The four strategies were all considered 'very cost-effective'; strategy D was the most cost-effective.

Discussion

We estimated the outcomes of each strategy for the same pool of screening-naïve diabetic patients. The difference in screening procedures resulted in varying sensitivity indices. With strategy A, the false-positive rate of maculopathy was high (87.1%) and resulted in unnecessary referrals (HK\$740 [US\$95.4] per consultation), the opportunity cost of using specialist outpatient clinics, and increased

TABLE 1. Outcomes of the four screening strategies for diabetic macular oedema (DME)*

| Parameter | Strategy A | | Strategy B | | Strategy C | | Strategy D | |
|--|------------|--------------|------------|--------------|------------|--------------|------------|--------------|
| | Normal | DME-positive | Normal | DME-positive | Normal | DME-positive | Normal | DME-positive |
| Fundus photograph grading | | | | | | | | |
| Negative retinopathy, negative maculopathy | 1007 | 38 | 1007 | 38 | 1007 | 38 | 1007 | 38 |
| Positive retinopathy, negative maculopathy | 874 | 24 | 1070 | 43 | 1165 | 33 | 1165 | 33 |
| Positive retinopathy, positive maculopathy | 291 | 43 | 95 | 24 | 0 | 34 | 0 | 34 |
| Optical coherence tomography grading | | | | | | | | |
| Negative | 1881 | 62 | 2077 | 81 | 2172 | 71 | 2172 | 0 |
| Positive | 291 | 43 | 95 | 24 | 0 | 34 | 0 | 105 |
| Sensitivity | 40.95% | | 22.86% | | 32.38% | | 100.00% | |
| Specificity | 86.60% | | 95.63% | | 100.00% | | 100.00% | |
| Positive predictive value | 12.87% | | 20.17% | | 100.00% | | 100.00% | |
| Negative predictive value | 96.81% | | 96.25% | | 96.83% | | 100.00% | |

* Data are presented as No. of patients unless otherwise indicated

TABLE 2. Cost-effectiveness analysis of the four screening strategies*

| | Strategy A | Strategy B | Strategy C | Strategy D |
|---|------------|------------|------------|------------|
| Quality-adjusted life-years gained, y | 19.4983 | 10.8828 | 15.4173 | 47.6123 |
| Total cost, HK\$ | 1 125 408 | 710 893 | 715 986 | 1 517 867 |
| Unit cost, HK\$ | 494.25 | 312.21 | 314.44 | 666.61 |
| Total cost, US\$ | 145 213.9 | 91 728.1 | 92 385.3 | 195 853.8 |
| Cost per quality-adjusted life-years gained, US\$ | 7447.5 | 8428.7 | 5992.3 | 4113.5 |
| Incremental quality-adjusted life-years gained, y | Reference | -8.62 | -4.08 | 28.11 |
| Incremental cost, US\$ | Reference | -53 485.8 | -52 828.7 | 50 639.9 |
| Incremental cost-effectiveness ratio, US\$ | Reference | 6208.1 | 12 944.9 | 1801.2 |

* Cost estimates (per patient per visit): best-corrected visual acuity assessment HK\$83.3, fundus photography HK\$65.5, optical coherence tomography of the macula HK\$208.3, ophthalmologist consultation HK\$740, laser procedure HK\$1 500, anti-vascular endothelial growth factor injection HK\$660, vitrectomy HK\$30 000, hospital stay HK\$3290.

waiting time for patients in need. Although the cost per QALY gained is still 'very cost-effective' from the health provider standpoint, strategy A has low sensitivity and positive predictive value. In strategy D, comprehensive OCT screening increases the sensitivity and positive predictive value. Although its total cost is highest, it yields the highest QALY gained. Strategy D's cost/QALY gained is US\$4113.5, which is the lowest of the four strategies.

Given the fact that 95.4% of patients screened did not have DME, strategy D appears to waste OCT resources on normal diabetic patients. Nonetheless, every normal diabetic patient may be at risk of having developed DME by the next annual screening. A baseline OCT can be used as a reference for subsequent screening visits. In addition, when OCT is performed at the time of screening, specialists can read the report upon referral and make necessary decisions.

In strategy D, fundus photograph screening could be removed to save costs. Nonetheless, OCT is only good at detecting macular pathologies and cannot detect neovascularisation in sight-threatening diabetic retinopathy. Despite that, strategy D remained the most cost-effective of the four strategies. Strategies B and C were less cost-effective. For details on these two strategies, please refer to the full report.

There are limitations to the study. The disability weight of DR for DME differed from the genuine disability weight of DME. The disability weight reported in Global Burden of Disease was probably a combined disability weight of both sight-threatening diabetic retinopathy and DME. Nonetheless, in real-life situations, most referred cases of DR were due to DME. The cost estimates and probabilities of treatment were largely based on expert opinion and medical records, which may have been biased and incorrect.

More precise data on the epidemiology of DR in Hong Kong are needed. Validation of the costs and probabilities of treatment is needed, as are data on diabetic patients' compliance with the screening programme. A clear definition of cost-

effectiveness specific to Hong Kong is important to facilitate interpretation of economic evaluation. In 2015, Hong Kong ranked 17th in the world in terms of GDP per capita; using this as a reference may not be reasonable. If the GDP per capita of China (US\$7429.7) had been used as a reference,⁵ strategies A and B would have become 'cost-effective', and strategies C and D would have remained 'very cost-effective'.

Conclusion

Strategy D that incorporates OCT of all patients in addition to all components of the current strategy is the most cost-effective of the four strategies investigated.

Acknowledgements

This study was supported by the Health and Medical Research Fund, Food and Health Bureau, Hong Kong SAR Government (#11121801). We thank Mr Hang Lam and Ms Mandy Law for their help with data collection and analysis. We also thank Mr Jordy Lau, Ms Man-Yee Lee, Dr Wing-Sun Chow, and Prof Karen Lam for providing support to facilitate patient screening visits.

References

1. Diabetic Retinopathy Clinical Research Network, Wells JA, Glassman AR, et al. Aflibercept, bevacizumab, or ranibizumab for diabetic macular edema. *N Engl J Med* 2015;372:1193-203.
2. Lian JX, Gangwani RA, McGhee SM, et al. Systematic screening for diabetic retinopathy (DR) in Hong Kong: prevalence of DR and visual impairment among diabetic population. *Br J Ophthalmol* 2016;100:151-5.
3. World Health Organization. Cost effectiveness and strategic planning (WHO-CHOICE); 2016. Available from: http://www.who.int/choice/costs/CER_levels/en/. Accessed 2 August 2016.
4. Hong Kong – the Facts. Available from: <http://www.gov.hk/en/about/abouthk/facts.htm>. Accessed 2 August 2016.
5. The World Bank. GDP per capita (current US\$). Available from: http://data.worldbank.org/indicator/NY.GDP.PCAP.CD?view=map&year_high_desc=true. Accessed 2 August 2016.

Genetic prediction models for primary open-angle glaucoma: translational research

LJ Chen*, CP Pang, CCY Tham, CKS Leung

KEY MESSAGES

1. This study investigated the association of 48 genetic markers in multiple genes with primary open-angle glaucoma (POAG).
2. This study confirmed the association of variant rs4236601 in the *CAVI/CAV2* gene locus with POAG in Chinese, and suggested a common variant in this locus, rs3801994, as a new genetic biomarker for POAG in Chinese.
3. This study revealed the association of the *CDNK2B* gene variant rs3217986 with normal-tension POAG, and rs2157719 with high-tension POAG in Chinese.
4. This study confirmed the association of variant

rs33912345 in the *SIX6* gene with POAG, and identified a new variant rs12436579 for the disease in Chinese.

5. This study simulated a genetic prediction model that can incorporate multiple gene variants for the prediction of individual risk of POAG.

Hong Kong Med J 2019;25(Suppl 9):S12-6
HMRF project number: 11120801

LJ Chen, CP Pang, CCY Tham, CKS Leung

Department of Ophthalmology and Visual Sciences, The Chinese University of Hong Kong

* Principal applicant and corresponding author: lijia_chen@cuhk.edu.hk

Introduction

Glaucoma is a leading cause of irreversible blindness worldwide. Most glaucoma cases are primary open-angle glaucoma (POAG), estimated to affect ~2% of the world population. Development of POAG is resulted from the interaction of multiple environmental and genetic risk factors. Nonetheless, a single gene variant is of limited value for genetic counselling or identifying individuals at risk. A combination of multiple gene variants can significantly increase the predictive value for POAG. Therefore, we aimed to identify a relatively complete set of gene variants that are associated with POAG. These variants are useful in establishing genetic prediction model for POAG.

Methods

We recruited over 600 Hong Kong Chinese POAG patients with variable age of onset, highest intraocular pressure, and disease severity. We also recruited >1000 Hong Kong healthy controls. In addition, data were collected for over 300 POAG patients and 600 controls from Shantou, China, over 300 POAG patients and 400 controls from Beijing, China, and over 200 POAG and 200 controls from Osaka, Japan.

A total of 48 single-nucleotide polymorphisms (SNPs) were selected: (1) 13 SNPs from genes identified by genome-wide association studies: 2 SNPs in *CAVI/CAV2*, 2 SNPs in *TMCO1*, 4 SNPs in *CDKN2B-AS1*, 1 SNP each in *SRBD1* and *ELOVL5*, and 1 SNP each in chromosomal regions 8q22

and 14q23; (2) 5 SNPs from our previous studies, including *APOE* epsilon4, *TNF* rs1800629, TP53 rs1042522, *TLR4* rs7037117, and 2p16 rs1533428; (3) 20 SNPs from genes previously reported to be associated with POAG in other populations by candidate gene approaches; and (4) 10 SNPs in genes associated with endophenotypes of glaucoma, including *ZNF469*, *COL5A1*, *AKAP13*, and *AVGR8* for central corneal thickness, *ATOH7*, *RFTN1*, *TGFBR3*, *CARD10*, *CDC7*, and *SIX1/SIX6* for optic disc parameters.

After identification of the associated SNPs in the *CAVI/CAV2*, *CDNK2B*, and *SIX6* genes, we expanded the number of SNPs to enable more comprehensive evaluation of the three genes. We conducted a related study to evaluate the association of the *TCF4* and *PTPRG* genes with Fuchs corneal dystrophy, which is associated with POAG risk. We found that *TCF4* rs613872 was strongly associated with Fuchs corneal dystrophy in Caucasians but not in Chinese, whereas SNPs in *PTPRG* were not associated with Fuchs corneal dystrophy in Caucasians or Chinese populations.¹

The selected SNPs were genotyped in all Hong Kong samples using TaqMan genotyping assays (Applied Biosystems). SNPs that are significantly associated with POAG were genotyped in the replication cohorts using the same platform.

For each selected SNP, Hardy-Weinberg equilibrium was evaluated by Chi-squared test. The association of each SNP with POAG was assessed by Chi-squared tests or Fisher exact tests. Odds ratios (OR) of significant sequence alterations were

estimated. For SNP data generated in different cohorts, genotypes were combined using a Mantel-Haenszel model. An individual or pooled P value of <0.05 was considered statistically significant.

Fifty SNPs from our POAG genome-wide association study were adopted for the simulation of genetic model, involving 341 POAG patients and 1141 controls. The samples were randomly assigned into training and validation groups with a ratio of 7 to 3, respectively. Genotype was re-coded as the number of risk alleles for a SNP. The genetic risk score was the total number of risk alleles a subject had. Prediction equations were fitted using logistic regression with different combinations of age, sex, and re-coded genotypes/genetic risk scores. The discriminative accuracy of fitted equations was evaluated with the area under curve of the receiver operating characteristic analysis.

Results

Among the 48 SNPs, only the SNPs in the *CAV1/CAV2*, *CDNK2B*, and *SIX6* genes were significantly associated with POAG. The other SNPs were not significantly associated with POAG.

Association of *CAV1/CAV2* with POAG

In the Hong Kong cohort, the SNP rs4236601 conferred an increased risk of POAG² (A allele, P=0.0072, OR=4.72, Table 1), with a population

attributable risk of 1.47%. A common SNP, rs3801994, showed a borderline association with POAG (A allele, P=0.036, OR=1.31, Table 1). This SNP presented in 18% of patients and 15% of controls, conferring a population attributable risk of 4.33%.

SNP rs4236601 was associated with POAG in the Shantou cohort (P=0.0079, OR=4.23). It had a minor allele frequency of 0.49% in controls and 2.0% in patients. Also, rs4236601 showed a significant association with POAG in the Beijing cohort (P=0.030, OR=3.92). The minor allele frequency was higher in the Beijing cohort: 1.3% in controls and 3.6% in POAG patients. In contrast, rs3801994 was not significantly associated with POAG in the Shantou or Beijing cohort, but their ORs were toward the same direction with that in the Hong Kong cohort (OR=1.14 in the Shantou cohort and 1.09 in the Beijing cohort, Table 1). By pooling the data of rs4236601 and rs3801994 from the three Chinese cohorts, the SNP rs4236601 was strongly associated with POAG (P=1.1 ×10⁻⁴, OR=3.80), whereas SNP rs3801994 showed a borderline association with POAG (P=0.022, OR=1.23, I²=0).³

Association of the *CDNK2B* gene SNPs with POAG

We genotyped 11 SNPs of the *CDNK2B* gene. Among the nine candidate SNPs, rs3217986 was associated with normal-tension glaucoma, and

TABLE 1. Allelic association of the *CAV1/CAV2* single nucleotide polymorphisms (SNPs) with primary open-angle glaucoma (POAG) in Chinese and Japanese populations

| SNP | Predicted function | MA | MAF | | POAG vs control | | POAG vs control (adjusted for age and sex) | |
|---------------------|--------------------|-------|---------|-------|-----------------|-------------------|--|-------------------|
| | | | Control | POAG | P value | OR (95% CI) | P value | OR (95% CI) |
| Chinese - Hong Kong | | n=436 | n=454 | | | | | |
| rs6466579 | Intergenic | T | 0.18 | 0.19 | 0.52 | 1.08 (0.85-1.37) | 0.46 | 1.10 (0.85-1.42) |
| rs7801950 | Intergenic | T | 0.12 | 0.14 | 0.22 | 1.19 (0.90-1.58) | 0.21 | 1.21 (0.90-1.62) |
| rs4236601 | Intergenic | A | 0.0043 | 0.020 | 0.0072 | 4.72 (1.36-16.36) | 0.0086 | 6.25 (1.60-24.50) |
| rs3779512 | c.102+4320T>G | T | 0.061 | 0.056 | 0.68 | 0.92 (0.62-1.37) | 0.93 | 0.98 (0.65-1.49) |
| rs3807989 | c.103-12759A>G | A | 0.22 | 0.25 | 0.083 | 1.21 (0.97-1.51) | 0.11 | 1.21 (0.96-1.53) |
| rs3801994 | c.103-8531G>A | A | 0.15 | 0.18 | 0.036 | 1.31 (1.02-1.69) | 0.042 | 1.32 (1.01-1.74) |
| rs1049337 | c.*1246C>T | C | 0.46 | 0.49 | 0.21 | 1.13 (0.93-1.36) | 0.091 | 1.19 (0.97-1.46) |
| Chinese - Shantou | | n=731 | n=123 | | | | | |
| rs4236601 | Intergenic | A | 0.0049 | 0.020 | 0.0079 | 4.23 (1.33-13.43) | 0.0037 | 6.09 (1.80-20.63) |
| rs3801994 | c.103-8531G>A | A | 0.19 | 0.21 | 0.44 | 1.14 (0.82-1.59) | 0.54 | 1.11 (0.80-1.54) |
| Chinese - Beijing | | n=192 | n=170 | | | | | |
| rs4236601 | Intergenic | A | 0.013 | 0.036 | 0.057 | 2.86 (0.92-8.85) | 0.030 | 3.92 (0.71-21.49) |
| rs3801994 | c.103-8531G>A | A | 0.19 | 0.20 | 0.67 | 1.09 (0.72-1.66) | 0.85 | 1.04 (0.49-2.20) |
| Japanese - Osaka | | n=207 | n=101 | | | | | |
| rs4236601 | Intergenic | - | - | - | - | - | - | - |
| rs3801994 | c.103-8531G>A | A | 0.33 | 0.28 | 0.22 | 0.79 (0.55-1.15) | 0.033 | 0.58 (0.35-0.96) |

rs2157719 with high-tension glaucoma in the Chinese cohort (Table 2). SNP rs3217986 (OR=0.67, 95% CI=0.46-0.99, P=0.045) was for the first time identified for normal-tension glaucoma. It did not alter the risk of high-tension glaucoma (P=0.857) or POAG (P=0.386). SNP rs2157719 reduced the risk of high-tension glaucoma (OR=0.69, 95% CI=0.48-0.98, P=0.040), but not POAG (P=0.084) or normal-tension glaucoma (P=0.542).

Association of the SIX6 gene with POAG

We identified a new SNP, rs12436579, for normal-tension glaucoma (P=0.021), high-tension glaucoma (P=0.017), and POAG (P=0.0064) in Hong Kong Chinese (Table 3). The SNP rs33912345 showed significant association with normal-tension

glaucoma (P=0.044). However, rs10483727 and the other eight SNPs (rs7152532, rs1010053, rs4400969, rs2179970, rs10148202, rs10133871, rs761557, and rs7156317) did not show significant association with POAG (P≥0.11, Table 3).

We tested the two significant SNPs (rs33912345 and rs12436579) and one significant SNP (rs10483727) in the Shantou Chinese and Japanese populations. All three SNPs were associated with POAG in Shantou Chinese (P≤0.015, Table 3). The OR of these three SNPs in Japanese pointed to the same direction as that in the Chinese populations. In the pool-analysis, we confirmed the associations: rs33912345 (P=0.0023, OR=0.78, I²=0), rs10483727 (P=0.0020, OR=0.78, I²=0), and rs12436579 (P=0.00081, OR=0.79, I²=10%).

TABLE 2. Allelic association of genotyped single nucleotide polymorphisms (SNP) with primary open-angle glaucoma (POAG) in Chinese and Japanese populations

| SNP | Associated allele | Allele frequency | | | | High-tension glaucoma vs control | | Normal-tension glaucoma vs control | | POAG vs control | |
|---|-------------------|------------------|-----------------------|-------------------------|-------|----------------------------------|------------------|------------------------------------|------------------|------------------|------------------|
| | | Control | High-tension glaucoma | Normal-tension glaucoma | POAG | OR (95% CI) | P _{emp} | OR (95% CI) | P _{emp} | OR (95% CI) | P _{emp} |
| Association analysis in Chinese cohort | | n=733 | n=437 | n=285 | n=722 | | | | | | |
| rs2518723 | T | 0.337 | 0.326 | 0.333 | 0.329 | 0.95 (0.77-1.19) | 0.727 | 0.99 (0.77-1.25) | 1.000 | 0.97 (0.79-1.18) | 1.000 |
| rs3217992 | C | 0.465 | 0.458 | 0.430 | 0.447 | 0.97 (0.79-1.19) | 1.000 | 0.87 (0.69-1.09) | 0.236 | 0.93 (0.77-1.12) | 0.778 |
| rs3217986 | G | 0.115 | 0.112 | 0.081 | 0.100 | 0.97 (0.70-1.34) | 0.857 | 0.67 (0.46-0.99) | 0.045 | 0.85 (0.63-1.15) | 0.386 |
| rs573687 | A | 0.103 | 0.069 | 0.089 | 0.085 | 0.79 (0.55-0.99) | 0.035 | 0.86 (0.58-1.27) | 0.483 | 0.81 (0.59-1.12) | 0.244 |
| rs545226 | A | 0.415 | 0.395 | 0.354 | 0.379 | 0.92 (0.75-1.13) | 0.386 | 0.77 (0.61-0.98) | 0.028 | 0.86 (0.71-1.04) | 0.171 |
| rs10965215 | G | 0.309 | 0.282 | 0.277 | 0.280 | 0.87 (0.70-1.10) | 0.317 | 0.86 (0.67-1.10) | 0.217 | 0.87 (0.71-1.07) | 0.353 |
| rs2157719 | C | 0.107 | 0.077 | 0.093 | 0.083 | 0.69 (0.48-0.98) | 0.040 | 0.85 (0.58-1.25) | 0.542 | 0.75 (0.55-1.03) | 0.084 |
| rs17694493 | C | 0.015 | 0.011 | 0.023 | 0.016 | 0.79 (0.32-1.95) | 0.750 | 1.61 (0.68-3.80) | 0.294 | 1.11 (0.51-2.41) | 0.750 |
| rs4977756 | G | 0.207 | 0.211 | 0.190 | 0.202 | 1.02 (0.79-1.32) | 1.000 | 0.90 (0.67-1.19) | 0.469 | 0.97 (0.77-1.23) | 1.000 |
| rs10757278 | A | 0.489 | 0.489 | 0.493 | 0.490 | 1.00 (0.81-1.23) | 1.000 | 1.02 (0.81-1.28) | 1.000 | 1.01 (0.83-1.21) | 1.000 |
| rs1333049 | G | 0.490 | 0.490 | 0.493 | 0.491 | 1.00 (0.81-1.23) | 1.000 | 1.01 (0.81-1.27) | 1.000 | 1.00 (0.83-1.21) | 1.000 |
| Association analysis in Japanese cohort | | n=207 | n=102 | n=154 | n=256 | | | | | | |
| rs2518723 | T | 0.377 | 0.352 | 0.333 | 0.341 | 0.90 (0.63-1.27) | 0.539 | 0.83 (0.61-1.13) | 0.221 | 0.85 (0.65-1.12) | 0.231 |
| rs3217992 | C | 0.466 | 0.460 | 0.422 | 0.437 | 0.98 (0.70-1.37) | 0.727 | 0.83 (0.62-1.12) | 0.455 | 0.89 (0.68-1.15) | 0.321 |
| rs3217986 | G | 0.043 | 0.069 | 0.062 | 0.065 | 1.64 (0.80-3.37) | 0.233 | 1.46 (0.75-2.82) | 0.386 | 1.53 (0.85-2.76) | 0.196 |
| rs573687 | A | 0.118 | 0.139 | 0.092 | 0.110 | 1.20 (0.73-1.97) | 0.441 | 0.75 (0.46-1.22) | 0.278 | 0.92 (0.61-1.39) | 0.857 |
| rs545226 | A | 0.391 | 0.411 | 0.353 | 0.376 | 1.09 (0.77-1.53) | 0.611 | 0.85 (0.62-1.15) | 0.378 | 0.94 (0.72-1.22) | 0.778 |
| rs10965215 | G | 0.358 | 0.332 | 0.284 | 0.303 | 0.89 (0.63-1.27) | 0.469 | 0.71 (0.52-0.98) | 0.038 | 0.78 (0.59-1.03) | 0.108 |
| rs2157719 | C | 0.116 | 0.134 | 0.095 | 0.110 | 1.18 (0.71-1.95) | 0.571 | 0.80 (0.49-1.30) | 0.360 | 0.94 (0.63-1.42) | 0.857 |
| rs17694493 | C | 0.029 | 0.020 | 0.023 | 0.022 | 0.68 (0.22-2.13) | 0.600 | 0.78 (0.31-2.02) | 0.857 | 0.74 (0.32-1.70) | 0.370 |
| rs4977756 | G | 0.225 | 0.238 | 0.222 | 0.228 | 1.08 (0.72-1.60) | 1.000 | 0.99 (0.69-1.41) | 1.000 | 1.02 (0.75-1.39) | 0.857 |
| rs10757278 | A | 0.544 | 0.465 | 0.431 | 0.445 | 0.73 (0.52-1.02) | 0.065 | 0.64 (0.47-0.86) | 0.003 | 0.67 (0.52-0.87) | 0.003 |
| rs1333049 | G | 0.515 | 0.460 | 0.431 | 0.443 | 0.81 (0.57-1.13) | 0.221 | 0.72 (0.53-0.96) | 0.022 | 0.75 (0.58-0.97) | 0.021 |

TABLE 3. Allelic association of the SIX6/SIX1 locus with normal-tension glaucoma, high-tension glaucoma, and primary open-angle glaucoma (POAG) in Chinese and Japanese populations

| No. | SNP | MA | MA frequency | | | | Normal-tension glaucoma vs control | | High-tension glaucoma vs control | | POAG vs control | |
|---------------------|------------|----|--------------|-------------------------|-----------------------|-------|------------------------------------|---------|----------------------------------|---------|------------------|---------|
| | | | Control | Normal-tension glaucoma | High-tension glaucoma | POAG | OR (95% CI) | P value | OR (95% CI) | P value | OR (95% CI) | P value |
| Chinese - Hong Kong | | | n=375 | n=349 | n=436 | n=785 | | | | | | |
| 1 | rs33912345 | A | 0.209 | 0.168 | 0.185 | 0.177 | 0.76 (0.58-0.99) | 0.044 | 0.86 (0.67-1.10) | 0.22 | 0.82 (0.65-1.02) | 0.067 |
| 2 | rs12436579 | A | 0.313 | 0.259 | 0.260 | 0.259 | 0.76 (0.61-0.96) | 0.021 | 0.77 (0.62-0.95) | 0.017 | 0.77 (0.63-0.93) | 0.0064 |
| 3 | rs7152532 | C | 0.445 | 0.423 | 0.428 | 0.426 | 0.91 (0.74-1.12) | 0.39 | 0.93 (0.77-1.13) | 0.49 | 0.92 (0.78-1.10) | 0.38 |
| 4 | rs1010053 | A | 0.449 | 0.430 | 0.456 | 0.445 | 0.92 (0.75-1.14) | 0.46 | 1.03 (0.85-1.25) | 0.79 | 0.98 (0.82-1.17) | 0.83 |
| 5 | rs4400969 | A | 0.136 | 0.150 | 0.148 | 0.149 | 1.12 (0.83-1.50) | 0.45 | 1.10 (0.83-1.45) | 0.51 | 1.11 (0.86-1.42) | 0.42 |
| 6 | rs2179970 | C | 0.110 | 0.100 | 0.090 | 0.094 | 0.90 (0.63-1.27) | 0.54 | 0.80 (0.58-1.12) | 0.19 | 0.84 (0.63-1.13) | 0.25 |
| 7 | rs10148202 | A | 0.241 | 0.244 | 0.240 | 0.242 | 1.01 (0.80-1.29) | 0.92 | 0.99 (0.79-1.25) | 0.95 | 1.00 (0.82-1.23) | 0.99 |
| 8 | rs10133871 | A | 0.253 | 0.264 | 0.257 | 0.260 | 1.06 (0.84-1.34) | 0.64 | 1.02 (0.82-1.28) | 0.86 | 1.04 (0.85-1.27) | 0.72 |
| 9 | rs10483727 | C | 0.207 | 0.174 | 0.183 | 0.179 | 0.81 (0.62-1.05) | 0.117 | 0.86 (0.67-1.10) | 0.22 | 0.84 (0.67-1.04) | 0.11 |
| 10 | rs761557 | T | 0.138 | 0.144 | 0.146 | 0.145 | 1.05 (0.78-1.42) | 0.73 | 1.07 (0.81-1.41) | 0.63 | 1.06 (0.83-1.37) | 0.63 |
| 11 | rs7156317 | G | 0.153 | 0.166 | 0.163 | 0.164 | 1.10 (0.83-1.45) | 0.52 | 1.08 (0.83-1.41) | 0.58 | 1.09 (0.86-1.38) | 0.50 |
| 12 | rs3783820 | T | 0.429 | 0.463 | 0.482 | 0.474 | 1.15 (0.93-1.41) | 0.20 | 1.24 (1.02-1.51) | 0.031 | 1.20 (1.01-1.43) | 0.043 |
| Chinese - Shantou | | | n=731 | n=34 | n=123 | n=157 | | | | | | |
| 1 | rs33912345 | A | 0.208 | 0.152 | 0.126 | 0.131 | 0.68 (0.34-1.35) | 0.27 | 0.55 (0.37-0.82) | 0.0029 | 0.58 (0.41-0.82) | 0.0020 |
| 2 | rs12436579 | A | 0.294 | 0.235 | 0.213 | 0.218 | 0.74 (0.42-1.31) | 0.29 | 0.65 (0.47-0.90) | 0.0091 | 0.67 (0.50-0.89) | 0.0064 |
| 3 | rs10483727 | C | 0.209 | 0.162 | 0.126 | 0.134 | 0.73 (0.38-1.41) | 0.35 | 0.55 (0.37-0.81) | 0.0025 | 0.58 (0.41-0.83) | 0.0024 |
| Japanese - Osaka | | | n=207 | n=154 | n=102 | n=256 | | | | | | |
| 1 | rs33912345 | A | 0.198 | 0.171 | 0.172 | 0.171 | 0.84 (0.57-1.23) | 0.37 | 0.84 (0.54-1.31) | 0.45 | 0.84 (0.60-1.18) | 0.31 |
| 2 | rs12436579 | A | 0.316 | 0.311 | 0.297 | 0.305 | 0.97 (0.71-1.34) | 0.86 | 0.91 (0.63-1.32) | 0.63 | 0.95 (0.72-1.26) | 0.71 |
| 3 | rs10483727 | C | 0.203 | 0.170 | 0.168 | 0.169 | 0.80 (0.55-1.18) | 0.26 | 0.80 (0.51-1.23) | 0.31 | 0.80 (0.57-1.12) | 0.19 |

Simulation of genetic modelling using multiple SNPs

Equations using more SNPs performed better. Equations using re-coded genotypes and genetic risk score of 10 SNPs were comparable. Age and sex contributed minimally to the discriminative power. The best equation used the genetic risk score of 50 SNPs and the area under the curve of 75.1% was attained. The test using a cut-off probability of 0.3 had a sensitivity of 62% and specificity of 83% for detection of subjects at risk of glaucoma.

Discussion

We performed genetic association analysis for POAG in the Hong Kong Chinese and other Asian cohorts. A total of 48 SNPs from multiple genes were screened. After identifying the SNPs in the *CAV1/CAV2*, *CDNK2B*, and *SIX6* genes that were significantly associated with POAG, we expanded the number of SNPs in these three genes and identified new associated SNPs for POAG. These three genes

are important genetic biomarkers for the molecular pathogenesis of POAG in Chinese. For the remaining genes that were not significantly associated with POAG, further studies are warranted to involve more SNP markers to confirm their role in the disease. We have successfully identified disease-associated genes and SNPs by using haplotype-tagging SNP analysis in both glaucoma³ and age-related macular degeneration.^{4,5} This method can be used in future studies of glaucoma gene identification.

The current number of significant SNPs is not sufficient for building up an applicable genetic model. We therefore simulated the genetic model using data from our POAG genome-wide association studies. We demonstrated a method in assessing the risk of POAG using expandable prediction equations based on SNPs. We found that equations using more SNPs performed better. Equations using re-coded genotypes and genetic risk score of 10 SNPs were comparable. The best equation used the genetic risk score of 50 SNPs and the area under the curve of 75.1% was attained. The test using a

cut-off probability of 0.3 had a sensitivity of 62% and specificity of 83% for detection of subjects at risk of POAG. This model sets up a foundation for future establishment of genetic prediction model for POAG. Further studies are warranted to identify more associated gene SNPs for POAG for such models to be applicable.

Understanding glaucoma genetics provides useful information for its management. Discovery of all genetic factors for glaucoma is of great importance. Obtaining a complete and universal picture of glaucoma genetic components will help guide the biological investigations and translational studies. In addition, uncovering the pathogenic mechanisms behind the association between genetic variations and glaucoma should be achieved through studies of multiple disciplines. Furthermore, expanding the options for translation of genetic discoveries into clinical practices should increase the possibilities of creation of a useful product. Gene therapy based on virus vector, genome editing, and prediction model of risk of POAG using genetic information are promising research area.

Conclusion

SNPs at the *CAV1/CAV2* locus, the *CDNK2B* gene, and the *SIX6* gene are associated with POAG in the Hong Kong Chinese population. These SNPs (rs4236601 and rs3801994 in *CAV1/CAV2*, rs3217986 and rs2157719 in *CDNK2b*, and rs33912345 and rs12436579 in *SIX6*) are potentially useful genetic biomarker for POAG. With more SNPs are being identified, they can be incorporated into the genetic model that we simulated and be applied to patient care in future.

Acknowledgements

This study was supported by the Health and Medical Research Fund, Food and Health Bureau, Hong Kong SAR Government (#11120801). We also thank all the participants in this study.

Results from this study have been published in:

(1) Rong SS, Chen LJ, Leung CK, et al. Ethnic specific association of the *CAV1/CAV2* locus with primary open-angle glaucoma. *Sci Rep* 2016;6:27837.

(2) Lau LC, Ma L, Young AL, et al. Association of common variants in *TCF4* and *PTPRG* with Fuchs' corneal dystrophy: a systematic review and meta-analysis. *PLoS One* 2014;9:e109142.

(3) Rong SS, Lu SY, Matsushita K, et al. Association of the *SIX6* locus with primary open angle glaucoma in southern Chinese and Japanese. *Exp Eye Res* 2019;180:129-36.

References

1. Lau LC, Ma L, Young AL, et al. Association of common variants in *TCF4* and *PTPRG* with Fuchs' corneal dystrophy: a systematic review and meta-analysis. *PLoS One* 2014;9:e109142.
2. Thorleifsson G, Walters GB, Hewitt AW, et al. Common variants near *CAV1* and *CAV2* are associated with primary open-angle glaucoma. *Nat Genet* 2010;42:906-9.
3. Rong SS, Chen LJ, Leung CK, et al. Ethnic specific association of the *CAV1/CAV2* locus with primary open-angle glaucoma. *Sci Rep* 2016;6:27837.
4. Chen LJ, Ma L, Chu WK, et al. Identification of *PGF* as a new gene for neovascular age-related macular degeneration in a Chinese population. *Invest Ophthalmol Vis Sci* 2016;57:1714-20.
5. Ma L, Liu K, Tsujikawa M, et al. Association of *ABCG1* with neovascular age-related macular degeneration and polypoidal choroidal vasculopathy in Chinese and Japanese. *Invest Ophthalmol Vis Sci* 2016;57:5758-63.

Surveillance of biologic sources of hepatitis E viruses in community

MCW Chan *, PKS Chan

KEY MESSAGES

1. Food-borne route may play a role in hepatitis E virus (HEV) infection in Hong Kong.
2. HEV contamination is not uncommon in a variety of meat and seafood items for daily consumption.
3. HEV RNA was detected in pig liver, pig intestine, and oyster in local retail settings with a prevalence of 1.5%, 0.4%, and 0.2%, respectively.
4. Local co-circulating human and swine HEV strains were genetically indistinguishable from each other.
5. Local co-circulating human and swine HEV strains belonged to genotype 4 with highly comparable subtype distribution in which subtype 4b predominated over subtype 4d.

Hong Kong Med J 2019;25(Suppl 9):S17-20
HMRF project number: 13120172

MCW Chan, PKS Chan

Department of Microbiology, The Chinese University of Hong Kong

* Principal applicant and corresponding author: martin.chan@cuhk.edu.hk

Introduction

Hepatitis E virus (HEV) is a non-enveloped, positive-sense, single-stranded RNA virus in the family *Hepeviridae* and genus *Orthohepevirus*. HEV is transmitted primarily through the faecal-oral route. Non-travel-associated locally-acquired hepatitis E is re-emerging in developed countries. HEV is genetically classified into at least seven genotypes (HEV-1 to HEV-7). Because HEV-3 and HEV-4 can be detected in both humans and pigs, food-borne virus acquisition from consumption of contaminated food (such as pig liver sausage) and zoonotic transmission via close contact with infected pigs have been implicated.¹

In Hong Kong, hepatitis E is a notifiable disease, and the number of cases has been on an upward trend since 2001.² Study to elucidate genetic relatedness of animal HEV detected in food and human HEV in clinical cases has been lacking. Thus, we reported the prevalence of HEV in different food items (lamb, oyster, pig blood curd, pig intestine, and pig liver) from retail stores over a 24-month period from 1 April 2014 to 31 March 2016 in Hong Kong. We also genotyped HEV from local clinical cases of the same period and provided molecular evidence suggesting that contaminated pig liver is one possible source of local human cases of autochthonous HEV infections.

Methods

From 1 April 2014 to 31 March 2016, five types of food items at risk of HEV contamination were purchased in two local market settings: supermarkets (lamb, oyster, and pig liver) and wet

markets (oyster, pig blood curd, pig large intestine, and pig liver) at five districts (Hong Kong Island, Kowloon East, Kowloon West, New Territories East, and New Territories West) once every 2 weeks. Food tissues were homogenised and tested for HEV RNA by a quantitative RT-PCR assay. To monitor for viral RNA extraction efficiency and carryover of PCR inhibitors, each food sample was spiked with a known amount of TATAA Universal RNA Spike I. Archived human sera collected from hospitalised patients who tested positive for HEV IgM during the study period in our hospitals were retrieved. Viral RNA was extracted. To perform virus genotyping, HEV RNA from food samples and human sera was reverse-transcribed to cDNA, followed by a nested PCR targeting HEV open reading frame 1 (ORF1, 133 nucleotides) and ORF2/3 junction (97 nucleotides). PCR products were Sanger-sequenced. Phylogenetic inference was made using neighbor-joining clustering method. Sequences obtained in this study have been deposited into GenBank under accession numbers KX752737 to KX752775.

Results

A total of 240 lamb, 479 oyster, 240 pig blood curd, 240 pig intestine, and 479 pig liver samples were tested for HEV RNA by RT-qPCR. To monitor for the RNA extraction efficiency and PCR inhibition, 382 food samples were randomly selected for spike RNA detection, and 377 (98.7%) of them were tested positive, indicating satisfactory recovery and PCR efficiency at a 96% confidence level. HEV RNA was detected in seven pig liver, one pig intestine, and one oyster samples from four out of five districts (except

TABLE. Temporal distribution of food samples tested positive for hepatitis E virus RNA.

| | No. of positive samples | | | | | | | | | | | | | | | | | | | | | | | |
|-------------------|-------------------------|--------------------|-------------------|-------------------|-----|-----|-----|-----|-----|---|-----|-----|-----|-------------------|-----|------|-------------------|-----|-----|-------------------|-----|-----|-----|-----|
| | 2014 | | | | | | | | | 2015 | | | | | | 2016 | | | | | | | | |
| | Q2 | | | Q3 | | | Q4 | | | Q1 | | | Q2 | | | Q3 | | | Q4 | | | Q1 | | |
| | Apr | May | Jun | Jul | Aug | Sep | Oct | Nov | Dec | Jan | Feb | Mar | Apr | May | Jun | Jul | Aug | Sep | Oct | Nov | Dec | Jan | Feb | Mar |
| Pig liver | | 1 (supermarket) | | 1 (wet market) | | | | | | 1 (supermarket) & 1 (wet market) | | | | 1 (wet market) | | | 1 (wet market) | | | 1 (wet market) | | | | |
| Pig intestine | | | 1 (wet market) | | | | | | | | | | | | | | | | | | | | | |
| Pig blood curd | | | | | | | | | | | | | | | | | | | | | | | | |
| Oyster | | 1 (wet market) | | | | | | | | | | | | | | | | | | | | | | |
| Lamb | | | | | | | | | | | | | | | | | | | | | | | | |

for New Territories West). The prevalence of HEV in pig liver, pig intestine, oyster, lamb, and pig blood curd samples was 1.5% (95% CI: 0.6%-3.0%), 0.4% (0.0%-2.3%), 0.2% (0.0%-1.2%), 0% (0.0%-1.5%), and 0% (0.0%-1.5%), respectively. In pig liver samples, HEV was detected in both supermarkets and wet markets. There was no significant difference in detection rate between retail settings. Food samples tested HEV RNA positive were collected all year-round with no observable seasonality (Table).

In our hospitals, 24 patients were tested positive for HEV IgM during the study period. The median age was 57 years and the male-to-female ratio was 5:1. A winter seasonality was observed in which 14 (58%) cases were admitted and diagnosed with hepatitis E during winter months from January to March. In contrast, there was only one (4%) case during summer months from July to September. Among these 24 patients, 22 archived HEV IgM positive sera had sufficient volume for further testing, and 18 (82%) of them tested HEV RNA positive. The median Ct value was 30.6 with an interquartile range of 27.6 to 32.8.

Among the nine HEV-positive food samples, three samples with the highest viral load (lowest Ct value) were pig livers. They were successfully genotyped by both nested ORF1 and ORF2/3 PCR. In addition, partial ORF1 sequence was determined from a pig liver sample that had the fourth highest viral load. Among the 18 HEV RNA positive human sera samples, 14 (78%) were successfully genotyped by both nested ORF1 and ORF2/3 PCR. The remaining four human sera samples with lowest HEV viral load were genotyped by nested ORF2/3 PCR only. Genotyping failure was associated with lower HEV viral load ($P < 0.05$). Phylogenetic neighbour-joining trees were constructed using concatenated and individual partial ORF1 and ORF2/3 sequences

(Fig). All HEV from pig liver samples and human sera clustered into genotype 4. All but one swine HEV strains belonged to subtype 4b and the remaining strain grouped into subtype 4d based on partial ORF1 sequence. Pairwise nucleotide identity in concatenated ORF1 and ORF2/3 of swine HEV in subtype 4b ranged from 97.4% to 98.7%. Similarly, in human sera, all but one HEV were assigned to subtype 4b and another strain was assigned to subtype 4d. Pairwise nucleotide identity in concatenated ORF1 and ORF2/3 of human HEV in subtype 4b ranged from 96.5% to 100.0%. The mean pairwise nucleotide identity between human and swine HEV strains was 97.8%. Both human and swine HEV strains interspersed in the subtype 4b lineage, and there was no species-specific sub-lineage observed from the phylogenetic tree.

Discussion

We detected HEV RNA in pig liver, pig intestine, and oyster samples. We provided compelling molecular evidence supporting close genetic relatedness between human and swine HEV genotype 4 strains to the subtype level circulating during the study period.

An increasing number of hepatitis E cases has been reported in non-endemic developed countries.³ Most cases had no recent travel history to hepatitis E endemic area; this implicates a local source of infection and food-borne and zoonotic transmission from pigs. The prevalence of HEV RNA in pig liver samples was 1.5%. There was no observable seasonality or temporal association with human hepatitis E cases after taking into account the long incubation period. Among the seven swine HEV strains, we were able to sequence four of them with the highest viral loads and all belonged to genotype

4. The local HEV RNA prevalence in pig liver samples is comparable to those reported by others in Asia. In China, where HEV genotype 4 strains are predominant,⁴ HEV RNA prevalence in pig herds is around 5%. In Japan, where HEV genotypes 3 and 4 co-circulate, HEV RNA prevalence in retail pig liver products ranges from 2% to 5%. In contrast, the detection rate of HEV in pig livers outside Asia, where HEV genotype 3 predominates, is much higher. In North America, the prevalence of HEV contamination in retail pig livers typically ranges from 5% to 10%. In Europe, the prevalence is even higher and can reach up to over 40% in very high-risk pig liver-derived food products such as figatellu. It is of interest to know whether or not HEV prevalence in pig livers is genotype-dependent.

To better understand association between human and swine HEV strains, an additional 18 human HEV strains from clinical hepatitis cases during the same period were genotyped. Phylogenetic analysis showed that all sequenced human and swine HEV strains were genotype 4. Among both human and swine HEV strains, subtype 4b is predominant whereas subtype 4d is the minority. This concordant HEV genotype distribution indicates possible association between human and swine HEV strains. Interestingly, HEV subtype distribution seems to vary in different cities in China.⁴ For instance, subtype 4b is the predominant type in both humans and pigs in southern China, but subtypes 4a and 4i are predominant in eastern China and subtype 4g is predominant in northeast China. Such a highly matched HEV genotype and subtype distribution between human and swine HEV strains strongly suggest one common HEV reservoir and probable cross-species transmission in our populations.

This is the first report of HEV RNA detection in pig intestine, which is a popular food in Chinese cuisine. It is not surprising to detect HEV in pig intestine as extrahepatic HEV dissemination is common in naturally infected pigs. Our findings extend the range of food items at risk of HEV contamination. We also detected HEV RNA in oysters but at a very low frequency of 0.2%. This is consistent with studies from Croatia, France, and Japan that detected no HEV in oysters. However, a higher HEV prevalence of 8.7% in oysters was reported in South Korea coastal region. Considering that oysters are common vehicles of other food-borne viruses such as norovirus and hepatitis A virus and are consumed raw, the risk of food-borne HEV transmission from oysters and other shellfish cannot be ignored.

Conclusion

HEV contamination is not uncommon in a variety of meat and seafood items for daily consumption. The HEV genotype 4 strains isolated from human

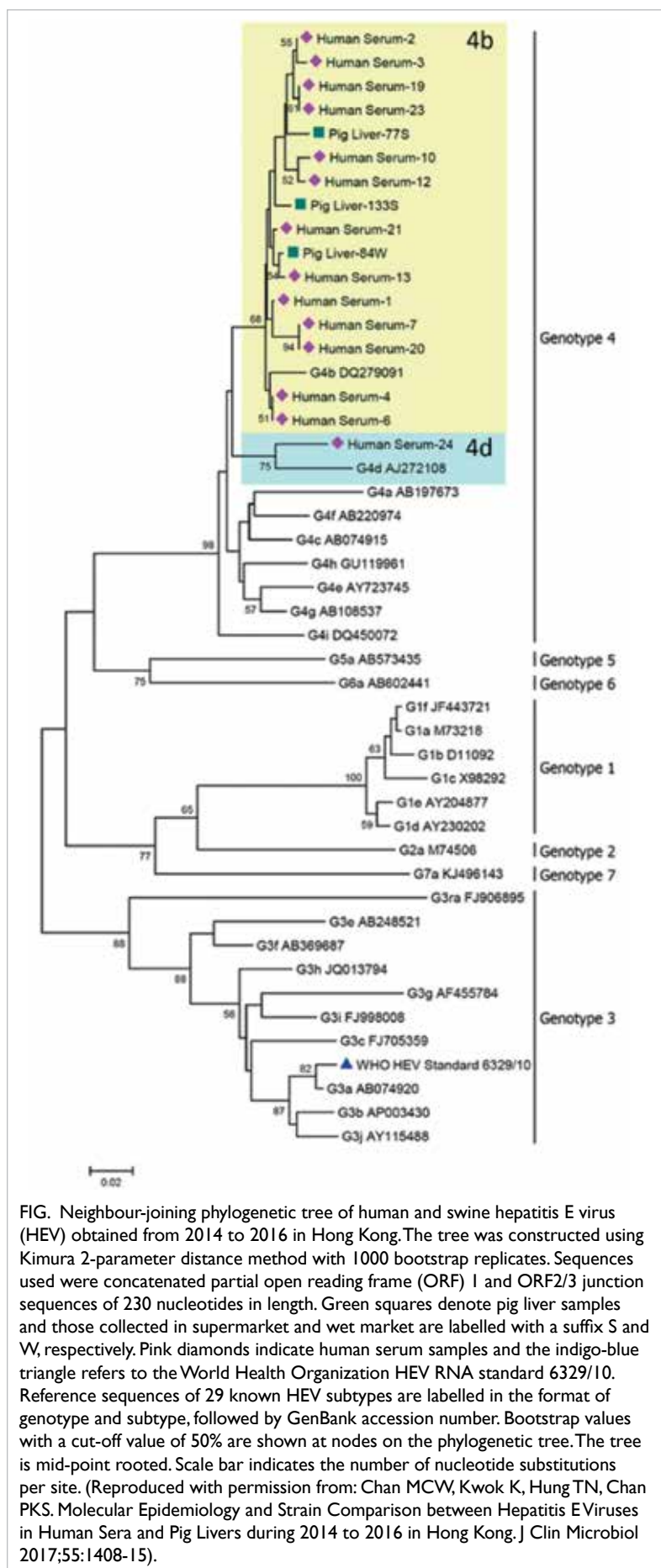


FIG. Neighbour-joining phylogenetic tree of human and swine hepatitis E virus (HEV) obtained from 2014 to 2016 in Hong Kong. The tree was constructed using Kimura 2-parameter distance method with 1000 bootstrap replicates. Sequences used were concatenated partial open reading frame (ORF) 1 and ORF2/3 junction sequences of 230 nucleotides in length. Green squares denote pig liver samples and those collected in supermarket and wet market are labelled with a suffix S and W, respectively. Pink diamonds indicate human serum samples and the indigo-blue triangle refers to the World Health Organization HEV RNA standard 6329/10. Reference sequences of 29 known HEV subtypes are labelled in the format of genotype and subtype, followed by GenBank accession number. Bootstrap values with a cut-off value of 50% are shown at nodes on the phylogenetic tree. The tree is mid-point rooted. Scale bar indicates the number of nucleotide substitutions per site. (Reproduced with permission from: Chan MCV, Kwok K, Hung TN, Chan PKS. Molecular Epidemiology and Strain Comparison between Hepatitis E Viruses in Human Sera and Pig Livers during 2014 to 2016 in Hong Kong. J Clin Microbiol 2017;55:1408-15).

samples during the study period are genetically indistinguishable from those isolated from swine samples, suggesting that contaminated pig liver is one possible source of local human cases of autochthonous HEV infections. Food-borne transmission may play a role in HEV infections in Hong Kong.⁵

Acknowledgements

This study was supported by the Health and Medical Research Fund, Food and Health Bureau, Hong Kong SAR Government (#13120172). We are also grateful for funding support provided by the Department of Microbiology, The Chinese University of Hong Kong, to carry out virus sequencing work on clinical samples described in this report.

References

1. Meng XJ, Wiseman B, Elvinger F, et al. Prevalence of antibodies to hepatitis E virus in veterinarians working with swine and in normal blood donors in the United States and other countries. *J Clin Microbiol* 2002;40:117-22.
2. Tai AL, Cheng PK, Ip SM, Wong RM, Lim WW. Molecular epidemiology of hepatitis E virus in Hong Kong. *J Med Virol* 2009;81:1062-8.
3. Sayed IM, Vercauter AS, Abdelwahab SE, Vercauteren K, Meuleman P. Is hepatitis E virus an emerging problem in industrialized countries? *Hepatology* 2015;62:1883-92.
4. Liu P, Li L, Wang L, et al. Phylogenetic analysis of 626 hepatitis E virus (HEV) isolates from humans and animals in China (1986-2011) showing genotype diversity and zoonotic transmission. *Infect Genet Evol* 2012;12:428-34.
5. Meng XJ. Expanding host range and cross-species infection of hepatitis E virus. *PLoS Pathog* 2016;12:e1005695.

Antiviral activity of human $\gamma\delta$ -T cells against enterovirus 71

KT Lam, J Zheng, Z Xiang, YP Liu, YL Lau, WW Tu *

KEY MESSAGES

1. $V\gamma 9V\delta 2$ -T cells can directly kill enterovirus (EV) 71-infected cells.
2. The cytotoxicity of $V\gamma 9V\delta 2$ -T cells against EV71-infected cells is mediated by the Fas-FasL pathway.
3. $V\gamma 9V\delta 2$ -T cells have non-cytolytic antiviral activity against EV71 through their secreted IFN- γ .

Hong Kong Med J 2019;25(Suppl 9):S21-3

HMRP project number: 13120972

KT Lam, J Zheng, Z Xiang, YP Liu, YL Lau, WW Tu

Department of Paediatrics and Adolescent Medicine, LKS Faculty of Medicine, The University of Hong Kong, Hong Kong SAR

* Principal applicant and corresponding author: wwtu@hku.hk

Introduction

Enterovirus 71 (EV71) is the most common cause of hand foot and mouth disease (HFMD).¹ Although the clinical manifestations of HFMD are usually mild and self-limiting, HFMD caused by EV71 is occasionally associated with severe complications such as encephalitis, aseptic meningitis, and brain stem encephalitis.¹ HFMD usually occurs in infants and young children and has become a major threat to public health in Southeast Asia (including Hong Kong) and mainland China.¹ Currently, there are no antiviral agents against EV71 infection. Therefore, there is a need for development of novel antiviral strategies for EV71 infection.

$\gamma\delta$ -T cells play an important role in the defence against pathogens and tumours.² Phosphoantigen pamidronate (PAM) and isopentenyl pyrophosphate (IPP) can selectively activate and expand by up to 50-fold the $V\gamma 9V\delta 2$ -T cells in human peripheral blood.^{3,4} PAM and IPP also trigger $\gamma\delta$ -T cells to produce IFN- γ and other cytokines and chemokines, hence displaying their antiviral activities.⁵ $V\gamma 9V\delta 2$ -T cells expanded by IPP or PAM can efficiently kill influenza virus-infected monocyte-derived macrophages (MDMs) thus reducing viral replication in vitro.^{3,4} $V\gamma 9V\delta 2$ -T cells can also inhibit human influenza virus replication by releasing IFN- γ .⁵ However, whether PAM-expanded $\gamma\delta$ -T cells can efficiently kill EV71-infected cells and inhibit the virus replication (and their underlying mechanisms) remain unknown.

We aimed to investigate the antiviral cytokine responses of human $V\gamma 9V\delta 2$ -T cells and the cytotoxic and non-cytolytic antiviral activities of $V\gamma 9V\delta 2$ -T cells against EV71.

Methods

Human EV71 were propagated in Vero cells with

DMEM and 5% FBS. The virus titre was also determined by Vero cell infection. The cytopathic effect of the infected cell was observed daily, and the TCID₅₀ was calculated according to the Reed-Muench formula.

PAM-expanded $V\gamma 9V\delta 2$ -T cells were generated from human peripheral blood mononuclear cells.³ MDM were generated from monocytes as described previously.⁴ Human peripheral blood mononuclear cells were infected with virus at multiplicity of infection of 2 or treated with mock; cells were harvested every 4 hours; brefeldin A was added at 4h before harvesting. Cells were stained for surface markers (V $\delta 2$, CD3, Fas, and FasL from Biolegend) and then fixed and permeabilised and stained with intracellular cytokines (IFN- γ , TNF- α , perforin, granzyme A and B, or their respective isotype controls from Biolegend). All sample data were acquired by LSR II flow machine (BD Bioscience). The flow cytometry data was analysed by FlowJo software (8.8.6).

PAM-expanded $V\gamma 9V\delta 2$ -T cells (effector (E)) were co-cultured with EV71-infected MDM or mock-treated MDM (targets (T)) at different T:E ratios: 1:0, 1:10, 1:20, and 1:30 for 2 to 4 hours. The cell-free coculture medium was harvested for lactic dehydrogenase-based in vitro toxicology assay (Sigma-Aldrich) to determine $V\gamma 9V\delta 2$ -T cells cytotoxicity as described by supplier instructions. The percentage of dead MDM was calculated by sample optical density value divided by the optical density value of 100% lysed MDM. The blocking assay was performed by first incubated $V\gamma 9V\delta 2$ -T with neutralisation antibodies (mouse anti-human NKG2D, mouse anti TRAIL, Fas L, and standardised IgG1 isotype control antibodies at 10 μ g/mL) or perforin inhibitors concanamycin A and granzyme blocker, Bcl2 for 30 mins before co-culture with vMDM at different T:E ratios. After co-culture for 4

hrs, the cell free supernatant was assayed with lactic dehydrogenase method as above.

VP1 gene copies in the cells and supernatant were quantified by SYBR green real-time RT-PCR. The supernatant and infected cells were processed for RNA using RNA extraction kit (TAKARA) and same known amount of RNA of each samples were converted to cDNA for Q-PCR by TAKARA reverse transcription kit. The expression of viral VP1 gene was accessed by ABI Prism 7900 detection system. Results were expressed as the number of target gene copies per 10^5 MDMs.

To evaluate cell-cell contact requirement for the direct killing of V γ 9V δ 2-T cells, the Transwell (24 wells, pore size 0.45 μ m; Millipore) system was used. Target cells (T) in the bottom were infected by EV71 at multiplicity of infection of 2. V γ 9V δ 2-T cells (E) were added directly into the bottom wells or into Transwell inserts at a T: E ratio of 1: 10. After 4 h, the supernatant in the bottom wells were harvested and analysed for cell death by lactic dehydrogenase assay as above. To determine the non-cytolytic antiviral activity of V γ 9V δ 2-T cells, a 24-well Transwell culture system as described above with smaller pore size at 0.45 μ m was used. PAM-expanded V γ 9V δ 2-T cells were added in the upper wells, and 100 000 MDM were plated in lower wells with virus infection (multiplicity of infection of 2). The EV71 viral RNA copies in MDM and supernatants were quantified by Q PCR as described in the above. To investigate which soluble molecules were involved in the non-cytolytic antiviral activity of V γ 9V δ 2-T cells, the same Transwell system and blocking assay as described above were used.

Data were expressed as mean \pm SEM. Statistical significance was determined by paired or nonpaired parametric-test using GraphPad Prism 5 software. $P < 0.05$ was considered to be significant.

Results

To determine the magnitude and kinetics of the antiviral cytokine responses of human V γ 9V δ 2-T cells in response to EV71, human peripheral blood mononuclear cells were infected with EV71 virus at multiplicity of infection of 2 or mock for 24 hours, and surface expressions of Fas and FasL, and intracellular expressions IFN- γ , TNF- α , perforin, granzyme A and B were analysed at different time points by FACS. Human V γ 9V δ 2-T cells had optimal responses to EV71 after 16 hours of infection. V γ 9V δ 2-T cells had very strong responses to EV71 in terms of the induction of IFN- γ and TNF- α . However, EV71- and mock-treated groups did not differ significantly in terms of Fas, FasL, granzyme A and B, and perforin expressions in V γ 9V δ 2-T cells.

To determine whether V γ 9V δ 2-T cells could kill EV71-infected MDM, we used lactic dehydrogenase assay to examine their cytolytic activities during

the co-culture of PAM-expanded V γ 9V δ 2-T cells (effector, E) with EV71-infected autologous MDM (target, T). V γ 9V δ 2-T cells could kill EV71-infected MDM. Using the Transwell culture assay, we found that V γ 9V δ 2-T cells lost their cytotoxicity toward EV71-infected MDM when V γ 9V δ 2-T cells were physically separated from EV71-infected MDM. This result indicated that cell-cell contact is required for the direct killing of V γ 9V δ 2-T cells.

To understand mechanisms underlying the direct killing of PAM-expanded V γ 9V δ 2-T cells, neutralisation mAbs for NKG2D, FasL, TRAIL, perforin-specific inhibitor concanamycin A, and granzyme B inactivator Bcl-2 were used. Only the blockade of FasL significantly reduced the cytotoxicity of V γ 9V δ 2-T cells. However, the blockade of other pathways such as KGN2D, TRAIL, perforin, and granzyme B did not inhibit V γ 9V δ 2-T cells cytotoxicity. These results indicated that the direct killing of V γ 9V δ 2-T cells against EV71-infected cells was mediated through Fas/FasL pathway.

To evaluate whether PAM-expanded V γ 9V δ 2-T cells can inhibit EV71 replication through their released soluble molecules, the 24-well Transwell culture system was used. Even when V γ 9V δ 2-T cells were physically separated from EV71-infected MDM, the EV71 VP1 gene copies in EV71-infected MDM and culture supernatants were significantly reduced, indicating that the soluble molecules released from PAM-expanded V γ 9V δ 2-T cells can inhibit the EV71 replication. To understand which soluble molecules were involved in this inhibition, the IFN- γ neutralisation mAb, perforin-specific inhibitor concanamycin A, and granzyme B inactivator Bcl-2 were added into the Transwell culture system. Inhibition of EV71 viral replication was significantly abrogated only when IFN- γ neutralising mAb was added. These results indicated that the non-cytolytic antiviral activity of PAM-expanded V γ 9V δ 2 T cells against EV71 mainly depended on IFN- γ .

Discussion

We demonstrated that human V γ 9V δ 2-T cells have both cytotoxic and non-cytolytic antiviral activities against EV71. To the best of our knowledge, this is the first report to demonstrate that $\gamma\delta$ -T cells have a potent antiviral activity against EV71.

$\gamma\delta$ -T cells play an important role in the defence against pathogens and tumours.² They have broad antiviral activities against different viruses. In our previous studies, we demonstrated that phosphoantigen-expanded V γ 9V δ 2-T cells could efficiently kill influenza virus-infected MDM and thus reducing viral replication in vitro, and that this cytotoxicity against influenza virus-infected MDM depended on NKG2D activation and mediated by

Fas-FasL and perforin-granzyme B pathways.^{3,4} In this study, we showed that PAM-expanded V γ 9V δ 2-T cells could directly kill EV71-infected MDM and reduce EV71 replication. However, we found only Fas-FasL pathway was involved in the killing of V γ 9V δ 2-T cells against EV71-infected MDM. These data suggest that V γ 9V δ 2-T cells may use different pathways to kill different virus-infected cells.

In our previous study, we showed that V γ 9V δ 2-T cells can produce IFN- γ to inhibit human influenza H1N1 viral replication.⁵ In this study, we found that V γ 9V δ 2-T cells produced a large amount of IFN- γ in response to EV71 as compared to TNF- α . Using the Transwell culture system and IFN- γ neutralisation mAb, we demonstrated that V γ 9V δ 2-T cells may inhibit EV71 replication through their released IFN- γ . Therefore, V γ 9V δ 2-T cells have non-cytolytic antiviral activity against EV71.

Conclusion

V γ 9V δ 2-T cells have both cytotoxic and non-cytolytic antiviral activities against EV71. The cytotoxicity of V γ 9V δ 2-T cells against EV71-infected MDM is mediated by Fas-FasL pathway. IFN- γ released from V γ 9V δ 2-T cells can inhibit EV71 viral

replication. Our study suggests a novel approach by using pamidronate to activate and expand V γ 9V δ 2-T cells against EV71 infection.

Acknowledgement

This study was supported by the Health and Medical Research Fund, Food and Health Bureau, Hong Kong SAR Government (#13120972).

References

1. Hagiwara A, Tagaya I, Yoneyama T. Epidemic of hand, foot and mouth disease associated with enterovirus 71 infection. *Intervirology* 1978;9:60-3.
2. Born WK, Reardon CL, O'Brien RL. The function of gammadelta T cells in innate immunity. *Curr Opin Immunol* 2006;18:31-8.
3. Qin G, Mao H, Zheng J, et al. Phosphoantigen-expanded human gammadelta T cells display potent cytotoxicity against monocyte-derived macrophages infected with human and avian influenza viruses. *J Infect Dis* 2009;200:858-65.
4. Tu W, Zheng J, Liu Y, et al. The aminobisphosphonate pamidronate controls influenza pathogenesis by expanding a gammadelta T cell population in humanized mice. *J Exp Med* 2011;208:1511-22.
5. Qin G, Liu Y, Zheng J, et al: Type 1 responses of human V γ 9V δ 2 T cells to influenza A viruses. *J Virol* 2011;85:10109-16.

Pre-pandemic live-attenuated influenza vaccine

DH He *, APY Chiu, JTK Wu, BJ Cowling

KEY MESSAGES

1. During the 2009 influenza pandemic in Hong Kong, matched vaccines for the pandemic strain were not available until 8 months after its start. We described the potential use of pre-pandemic seasonal vaccine to mitigate the next pandemic.
2. We used an age-structured epidemic model to identify the optimal timing and age-specific allocation strategies for administration of vaccinations.
3. With a stockpile of 200000 doses, if we start vaccinating those aged 5 to 9 years and 15 to 19 years on day 1, the maximum peak time delayed is 17.4 days and the peak height reduction is 16.8%, compared with no vaccination.
4. If we start vaccinating on 98.8th day, the maximum reduction in death is 13.85% by vaccinating those aged 5 to 9 years and 15 to 19 years. The maximum reduction in hospitalisation is 15.00% by vaccinating those aged 5 to 19 years.
5. In future influenza pandemic with limited vaccine stockpile, vaccinating those aged 5 to 19 years one week before the major wave can minimise the number of hospitalisations and deaths. Vaccination campaign should be started early in order to delay the arrival of a major wave of infections and reduce its height.

Hong Kong Med J 2019;25(Suppl 9):S24-7
HMRF project number: 13121382

¹ DH He, ¹ APY Chiu, ² JTK Wu, ² BJ Cowling

¹ Department of Applied Mathematics, The Hong Kong Polytechnic University

² WHO Collaborating Centre for Infectious Disease Epidemiology and Control, School of Public Health, Li Ka Shing Faculty of Medicine, The University of Hong Kong

* Principal applicant and corresponding author: daihai.he@polyu.edu.hk

Introduction

During the 2009 influenza pandemic in Hong Kong, matched vaccines for the pandemic strain were not available until 8 months after its start. This study described the potential use of pre-pandemic seasonal vaccine to mitigate the next pandemic. A randomised trial of inactivated vaccine in Hong Kong suggested that seasonal influenza infection provides strong but possibly short-lived protection against pandemic influenza.¹ Children are protected against respiratory infections in general for the first few weeks after vaccination with live-attenuated influenza vaccine (LAIV). The strength and duration of this effect appears to be non-specific and may last a few weeks if associated with the innate immune response. This is known as temporary non-specific immunity (TNI).²

This study investigated strategies to use LAIV to mitigate a future influenza pandemic in Hong Kong. If LAIV is useful in mitigating a pandemic, this may support the idea of increasing seasonal coverage of LAIV. We expect that the TNI effect, the limited cross-protection post TNI, and the consequent interference (herd immunity, indirect benefit) at the population level may act together to slow the transmission and soften the impact to health services.

Assuming that LAIV can provide up to 2 weeks' protection against pandemic infection and

limited cross-protection post TNI, what are the optimal vaccination administration strategy, optimal age-specific allocation plan, and optimal timing of vaccination? This study aimed (1) to maximise the peak height reduction of hospitalisation rates and peak time delayed in order to reduce peak demand for healthcare services, and (2) to minimise the total number of hospitalisations or deaths. We would vaccinate core transmitters and high-risk persons if the stockpile is large enough to hinder transmission. Assuming post TNI cross-protection is negligible, the optimal timing is to have the 2-week TNI to cover the period during which the force of infection is the highest.

Methods

In our age-structured epidemic model,³ S denoted susceptible, E exposed, I infectious, R recovered, T those who have been given LAIV and have acquired TNI, P those who have lost TNI but have acquired limited immunity, H those who are hospitalised, and D deaths. Individuals aged 0 to 69 years were subdivided into fourteen 5-year groups plus an additional group of 70+ years (S_1 to S_{14}).

Without vaccination, a susceptible individual may go through: susceptible → exposed → infectious → (hospitalised) → recovered (or death). Stages with parentheses may be skipped. With vaccination, a susceptible individual may go through: susceptible →

TNI → (P: limited long-term immunity) → exposed → infectious → (hospitalised) → recovered (or death).

Infections can happen both within and between age-groups. We assume that transmissions happen from an infectious age-group i to a susceptible age-group j at a rate of $\beta_{ji}S_{ji}$. β_{ji} is called the transmission rate matrix. T and P individuals can also be infected but at reduced rates of $\eta\beta_{ji}S_{ji}$ and $\xi\beta_{ji}S_{ji}$, respectively. Exposed individuals become infectious at a rate σ , and the mean latent period is $1/\sigma$. Infectious becomes recovered at a rate γ , and the mean infectious period is $1/\gamma$. T becomes P at a rate of κ , which is chosen such that the duration of TNI is about 2 weeks. Infectious is diagnosed and hospitalised at an age-specific rate h_i (from I_i to H_i). Hospitalised die at an age-specific rate d_i (from H_i to D_i). The model diagram without age structure is shown in Fig 1.

Fitting model to observed infection attack rate

We incorporated reasonable epidemiological parameter values and the age structure of the Hong Kong population into the model. For the contact matrix, we used the PolyMOD data of United Kingdom.³ We re-scaled and altered part of the contact matrix, such that the yield age-profile of the attack rate may match the observed infection attack rate age-profile of the 2009 pandemic influenza in Hong Kong. We assumed that the prior immunity against the pandemic strain was linearly from 4% (age 0-4 years) to 39% (age ≥ 70 years).⁴

Infection peak time delayed and peak height reduced

We assumed that vaccine stockpile was sufficient for 200 000 individuals. For a targeted age class

i , susceptible patients were vaccinated on a first-come first-serve basis until the stockpile ran out. The vaccination campaign was assumed to last for about 10 days. According to Centers for Disease Control and Prevention, the LAIV is only suitable for individuals aged 5 to 49 years. Each age-group was either vaccinated or not vaccinated. We had 512 different scenarios of target age-groups.

Results

Through simulations, a late start of the vaccination campaign only led to short or no delay in the peak of the influenza infections. We fixed the vaccination campaign on day 1 (beginning of the pandemic). We assumed the pandemic was ignited by n (2 to 20) infectious individuals in the each of the three age-groups (30-34, 35-39, and 40-45 years). We simulated each scenario 100 times (with a random number of seeds) and then averaged the outcomes. We considered 512 combinations of vaccination for various age-groups. For instance, scenario 1 was vaccination for those aged 5 to 49 years and scenario 512 was no vaccination. The maximum delay of the peak time of 17.4 days was achieved if those aged 5 to 10 and 15 to 19 years were vaccinated starting from day 1 of the pandemic, with a stockpile of 200 000 (Fig 2). The second, third, and fourth optimal scenarios were vaccinating those aged 10 to 19, 5 to 14, and 5 to 19 years, respectively. Vaccinating all eligible ages (5-49 years) is less than ideal. The height of the peak was reduced by 16.78%, 15.86%, 15.76%, and 15% by vaccinating those aged 5 to 10 or 15 to 19, 10 to 19, 5 to 14, and 5 to 19 years, respectively. Fig 3 shows the effects of varying start dates of vaccination campaign on the numbers of hospitalisations and deaths secondary to the pandemic with a stockpile of 200 000 doses.

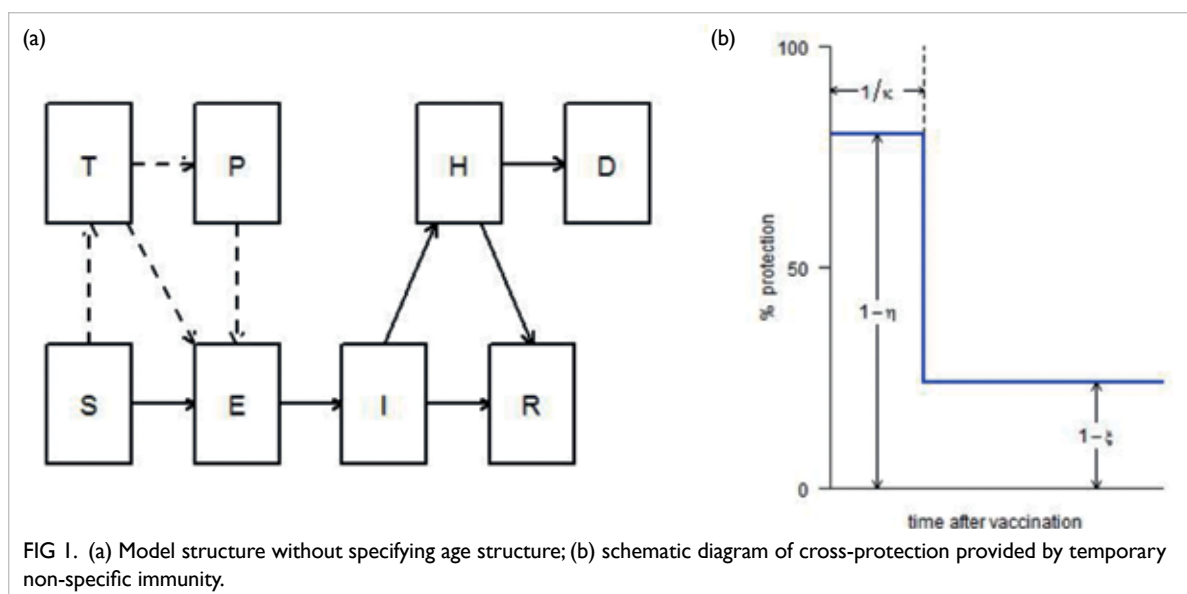


FIG 1. (a) Model structure without specifying age structure; (b) schematic diagram of cross-protection provided by temporary non-specific immunity.

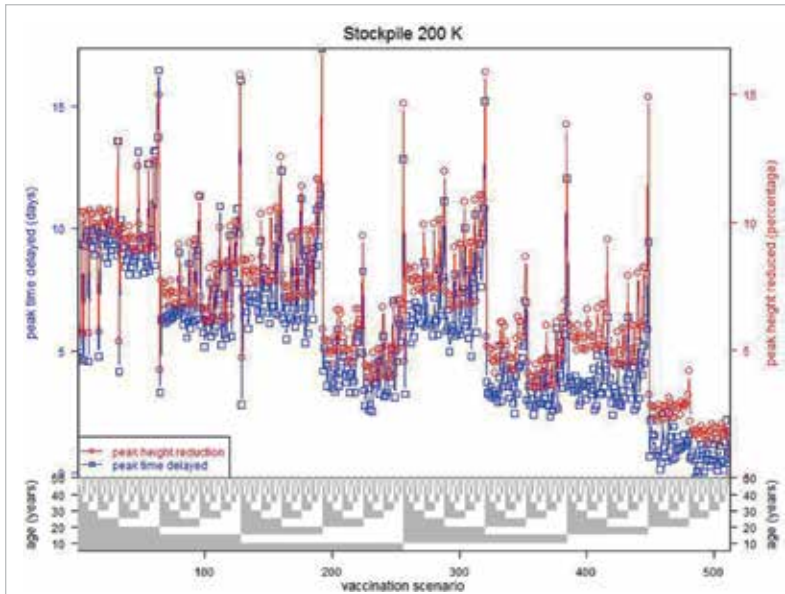


FIG 2. The impacts of temporary non-specific immunity on the infection peak time delayed and peak height reduction under different vaccination scenarios, with a stockpile of 200 000 doses and the campaign starting on day 1. The optimal strategy is to start vaccinating for those aged 5-10 and 15-19 years. The maximum peak time delayed is 17.4 days and the maximum peak height reduction is 16.78%.

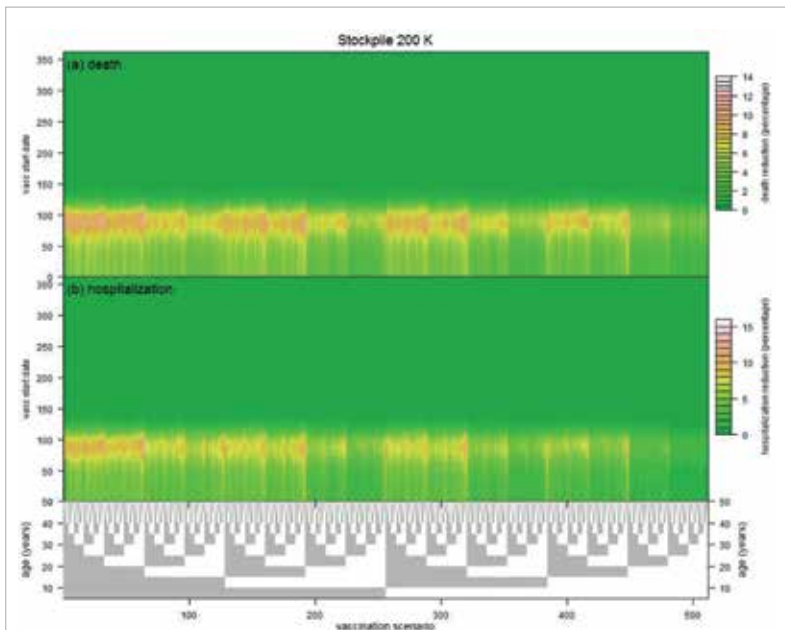


FIG 3. Effects of varying start dates of vaccination campaign on reduction of (a) death and (b) hospitalisation (in percentage) with a stockpile of 200 000 doses. The largest reduction is achieved on the 98.8th day for death when vaccinating those aged 5-9 and 15-19 years and for hospitalisation when vaccinating those aged 5-19 years, and maximum reduction is 13.85% for death and 15% for hospitalisation.

Discussion

Assuming a stockpile of 200 000 LAIV doses, if the goal is to reduce hospitalisations and deaths as much

as possible, vaccination should not be started until the arrival of the major wave (a week before the peak time) to maximise the effect of TNI. The target age-group should be those aged 5 to 19 years. If the goal is to delay the arrival time of the major wave of infections and to reduce its height, the vaccination campaign should be started as early as possible, because the initial development stage plays a crucial role on the arrival time of the major wave.

Our models are calibrated to the observed infection attack rates in a Hong Kong study by Wu et al.⁵ We have considered several plausible scenarios to make our model more applicable for policymakers' decision making. Previous studies on optimal strategies for mitigating an influenza pandemic showed that school-age children should be the priority groups for vaccination because they have higher contact rates and higher secondary attack rate of household transmission.

Our study has limitations. We made simplifying assumptions about several epidemiological features the pandemic influenza: we did not consider (1) the possibility of multiple waves of pandemic influenza, (2) the impact of co-circulation of seasonal influenza during a pandemic, and (3) cross-subtype immunity and age-variations of vaccine efficacy. In addition, we did not consider the impacts of multifaceted intervention strategies in our mathematical model. During an influenza pandemic, both non-pharmaceutical and pharmaceutical intervention strategies are likely to be applied. Furthermore, the age-structured epidemic model did not consider other risk groups such as people with chronic respiratory disease, those aged ≥ 65 years, and healthcare workers.

Conclusion

An age-specific compartmental model is useful for studying pandemic influenza transmission and determining the optimal mitigation strategies. We highlight the use of seasonal LAIV and an age-specific allocation process.

Acknowledgement

This study was supported by the Health and Medical Research Fund, Food and Health Bureau, Hong Kong SAR Government (#13121382).

Results from this study have been published in:

(1) He D, Chiu APY, Lin QY, Cowling BJ. Differences in the seasonality of MERS-CoV and influenza in the Middle East. *Int J Infect Dis* 2015;40:15-16.

(2) He D, Lui R, Wang L, Tse CK, Yang L, Stone L. Global spatio-temporal patterns of influenza in the post-pandemic era. *Sci Rep* 2015;5:11013.

(3) Yang L, Chan KH, Suen LK, et al. Impact of the 2009 H1N1 pandemic on age-specific epidemic

curves of other respiratory viruses: a comparison of pre-pandemic, pandemic and post-pandemic periods in a subtropical City. *PLoS One* 2015;10:e0125447.

References

1. Cowling BJ, Ng S, Ma ES, et al. Protective efficacy of seasonal influenza vaccination against seasonal and pandemic influenza virus infection during 2009 in Hong Kong. *Clin Infect Dis* 2010;51:1370-9.
2. Kelly H, Barry S, Laurie K, Mercer G. Seasonal influenza vaccination and the risk of infection with pandemic influenza: a possible illustration of non-specific temporary immunity following infection. *Euro Surveill* 2010;15:pii:19722.
3. Wallinga J, Teunis P, Kretzschmar M. Using data on social contacts to estimate age-specific transmission parameters for respiratory-spread infectious agents. *Am J Epidemiol* 2006;164:936-44.
4. Dorigatti I, Cauchemez S, Ferguson NM. Increased transmissibility explains the third wave of infection by the 2009 H1N1 pandemic virus in England. *Proc Natl Acad Sci U S A* 2013;110:13422-7.
5. Wu JT, Leung K, Perera RA, et al. Inferring influenza infection attack rate from seroprevalence data. *PLoS Pathog* 2014;10:e1004054.

PEGylated recombinant human arginase as a drug for breast cancer

SL Leung *, MK Ho, YM Lam, HY Chow, YH So, YC Leung

KEY MESSAGES

1. rhArg-PEG is highly potent and kills all breast cancer cell lines (including 'triple-negative' and highly aggressive metastatic cells) in vitro and in vivo in a receptor-independent manner.
2. rhArg-PEG induces multiple cancer cell death pathways that are cell-line dependent.
3. rhArg-PEG inhibits mTOR, activates AMPK, and induces a novel type of biphasic autophagic response in cancer cells, leading to autophagic cell death.
4. rhArg-PEG kills cancer cells lacking ornithine transcarbamylase and/or argininosuccinate

synthetase and inhibits more tumours than arginine deiminase-PEG does. It is a promising personalised medicine.

Hong Kong Med J 2019;25(Suppl 9):S28-31
HMRP project number: 01121936

SL Leung, MK Ho, YM Lam, HY Chow, YH So, YC Leung

Department of Applied Biology and Chemical Technology, and Lo Ka Chung Centre for Natural Anti-Cancer Drug Development, The Hong Kong Polytechnic University

* Principal applicant and corresponding author:
thomas.yun-chung.leung@polyu.edu.hk

Introduction

Breast cancer is the most common cancer in women and accounts for the highest female cancer death. As of 2008, approximately 207 500 of 1 383 500 breast cancer patients worldwide are resistant to hormone receptor- or HER2-targeting therapies. Safe and effective treatments against 'triple-negative' breast cancer (not expressing oestrogen receptor, progesterone receptor, or HER2) are in demand.

Arginine is essential for the growth of a variety of tumours, including hepatocellular carcinomas (HCCs) and melanomas. Depletion of arginine (using arginine-degrading enzymes or arginine-free growth medium) leads to massive growth retardation, cell cycle arrest, and/or apoptosis in many cancer cell lines.¹⁻⁴ In contrast, normal cells arrest at G0 phase under arginine deprivation and resume cycling once arginine is replenished. This selective anti-tumour property makes arginine deprivation a valuable means for cancer treatment. Our laboratory has shown that human hepatic arginase (arginase I), which catabolises arginine to form ornithine and urea, possesses anti-proliferative properties against HCC and melanoma cells in vitro and in vivo. Patients with HCC who underwent transhepatic arterial embolisation exhibited remarkable remission, as a result of the systemic release of endogenous arginase I induced by the treatment. We first reported that a recombinant form of human arginase I (rhArg) is highly potent against HCC and melanoma cell lines.^{1,2} Covalent modification of rhArg, using polyethylene glycol (PEG) with a molecular weight of 5000, gives the enzyme a longer half-life without

reducing its enzyme activity or anti-tumour efficacy. This PEGylated form of rhArg (rhArg-PEG) is highly effective in inhibiting the growth of HCC and melanoma xenografts in nude mice, and thus is a potential treatment for these cancers.^{1,2} Other studies have reported on anti-tumour properties of rhArg and its bioengineered derivatives. rhArg-PEG has been proved to be safe and effective in a phase 1a dose finding and phase 1b efficacy study in 35 advanced liver cancer patients at The University of Hong Kong.⁵

Depletion of arginine using the arginine deiminase (ADI) enzyme is effective against several cancer cell types in vitro and in vivo and is under extensive clinical trials for several cancer types. However, expression of the urea cycle enzyme argininosuccinate synthetase (ASS) in tumour cells can lead to resistance towards ADI treatment by allowing recycling of arginine from its enzymatic product, citrulline (Fig 1). ASS expression is commonly observed in cancer cell lines and tumour biopsies from patients. ADI enhances the sensitivity of MCF-7 towards ionising radiation treatment and kills MDA-MB-231, which is ASS-deficient.³ Only upon the knockdown of ASS expression using RNAi, was MCF-7 rendered susceptible to ADI-induced growth inhibition, thus proving that ASS expression and ADI resistance of breast cancer are closely linked. Immunohistochemistry revealed that >90% of the breast cancer biopsies sampled were ASS-positive, which could be resistant towards ADI treatment. Arginase is effective against breast cancers, because ASS expression alone cannot

render tumour cells resistant to its inhibitory effects, as shown in our study on ASS-expressing HCC cell lines.¹ Only cancer cells that simultaneously express the urea cycle enzymes of ASS, argininosuccinate lyase, and ornithine transcarbamylase were resistant to arginase treatment, whereas the co-expression of the first two could lead to ADI resistance (Fig 1). Arginase, therefore, can potentially inhibit the growth of a larger subset of tumours when compared with ADI. As rhArg-PEG is derived from human arginase, it should be a safer drug with less immunogenicity problems, compared with the bacterial enzyme ADI.

Methods

MDA-MB-231 human breast tumour cell xenograft mouse model

Female nude mice aged 5 to 6 weeks were used. They were kept in groups of five per cage and provided food and water ad libitum. MDA-MB-231 cells were harvested by trypsinisation and washed twice with 1× phosphate-buffered saline (PBS). The cell number was counted by trypan blue method. 1×10^7 cells of MDA-MB-231 were resuspended in 100 μ L PBS-matrigel mixture (with a ratio of 1:1) and injected subcutaneously into the right flank of the mice. The tumour growth was monitored by measuring length and width of the tumour by digital caliper regularly. The estimated tumour volume was calculated by the equation: Tumour volume (mm^3) = (length \times width²)/2. When the tumour volume grew to around 500 mm^3 , the mice were sacrificed and dissected. Tumours were collected and excised to around 10 mm^3 each. Each small tumour was transplanted into a new female nude mouse after anaesthesia by ketamine and xylazine. The dissected tumours were transplanted to the right flank of the mice. For MDA-MB-231 xenograft studies, 40 female nude mice transplanted with MDA-MB-231 solid tumours were used. The mice were separated into four groups randomly

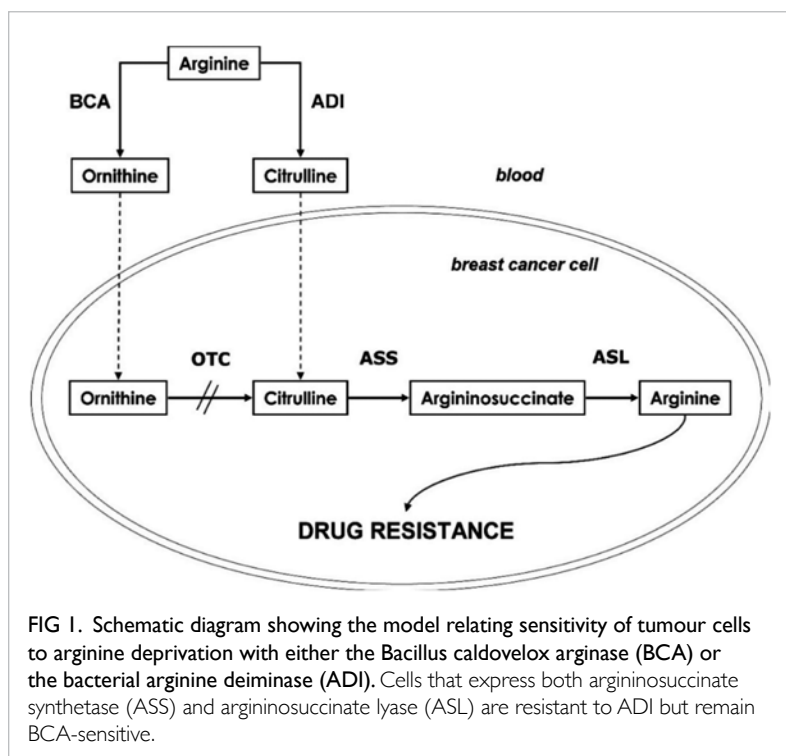


FIG 1. Schematic diagram showing the model relating sensitivity of tumour cells to arginine deprivation with either the *Bacillus caldovelox* arginase (BCA) or the bacterial arginine deiminase (ADI). Cells that express both argininosuccinate synthetase (ASS) and argininosuccinate lyase (ASL) are resistant to ADI but remain BCA-sensitive.

when the tumour volume reached an average of 50 mm^3 . Mice in the control group were injected with 1× PBS once a week; mice in the rhArg-PEG group were injected with 500 U rhArg-PEG (290 μ L, 2 mg) once a week; mice in the chloroquine (CQ) group were injected with 40 mg/kg CQ once every 2 days; and mice in the combination group (rhArg-PEG plus CQ) were injected with both 500 U rhArg-PEG once a week and 40 mg/kg CQ once every 2 days. The two drugs were injected separately with a 4-hour gap when both rhArg-PEG and CQ were injected to the

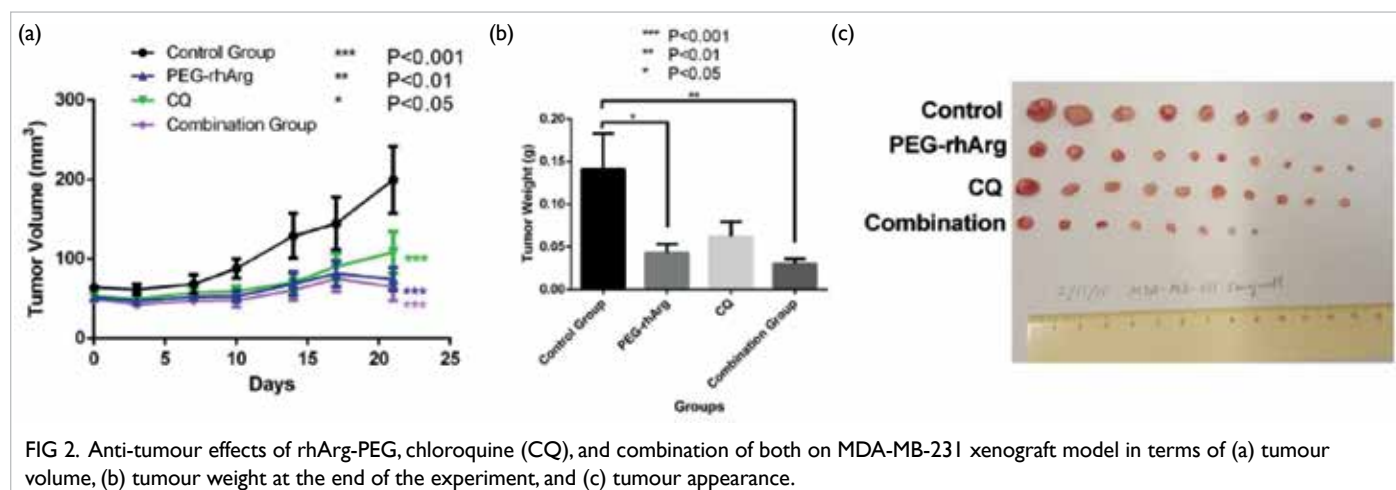


FIG 2. Anti-tumour effects of rhArg-PEG, chloroquine (CQ), and combination of both on MDA-MB-231 xenograft model in terms of (a) tumour volume, (b) tumour weight at the end of the experiment, and (c) tumour appearance.

mice within the same day. During the experiment, blood samples were collected from the saphenous vein. Tumour volume and the weight of mice were monitored regularly. The mice were then sacrificed and dissected to collect and weigh the tumours.

4T1 metastatic cell allograft mouse model

For 4T1 allograft studies, female Balb/c nude mice (5-6 weeks of age) were used. They were kept in groups of five per cage and provided food and water ad libitum. 4T1 cells were harvested by trypsinisation and washed twice with 1× PBS. The cell number was counted by the trypan blue method. Cells (1×10^5) of 4T1 were resuspended in 100 μ L 1× PBS and injected subcutaneously into the right flank. Mice were separated into two groups by random when the tumour had a mean length of 8 mm after 11 days of inoculation. Mice in the control group were injected with 1× PBS weekly. Mice in the rhArg-PEG group

were injected with 500 U (2.4 mg, 400 μ L) rhArg-PEG weekly. Blood samples were collected from the saphenous vein before injecting drug/PBS. The amino acid content of the serum was analysed by amino acid analyser (Biochrome). Tumour size and the weight of mice were monitored regularly. The mice were then sacrificed and dissected to collect and weigh the tumours. Lungs were also collected and washed with 1× PBS and fixed in Bouin solution overnight and then washed with 1× PBS. Lung metastatic nodules were counted.

Statistical analysis

Statistical analyses were performed using Student's *t*-test, Mann-Whitney *U* test, or analysis of variance. For multiple comparisons after analysis of variance, the Tukey post hoc pairwise comparison approach was used. A *P* value of <0.05 was considered significantly different.

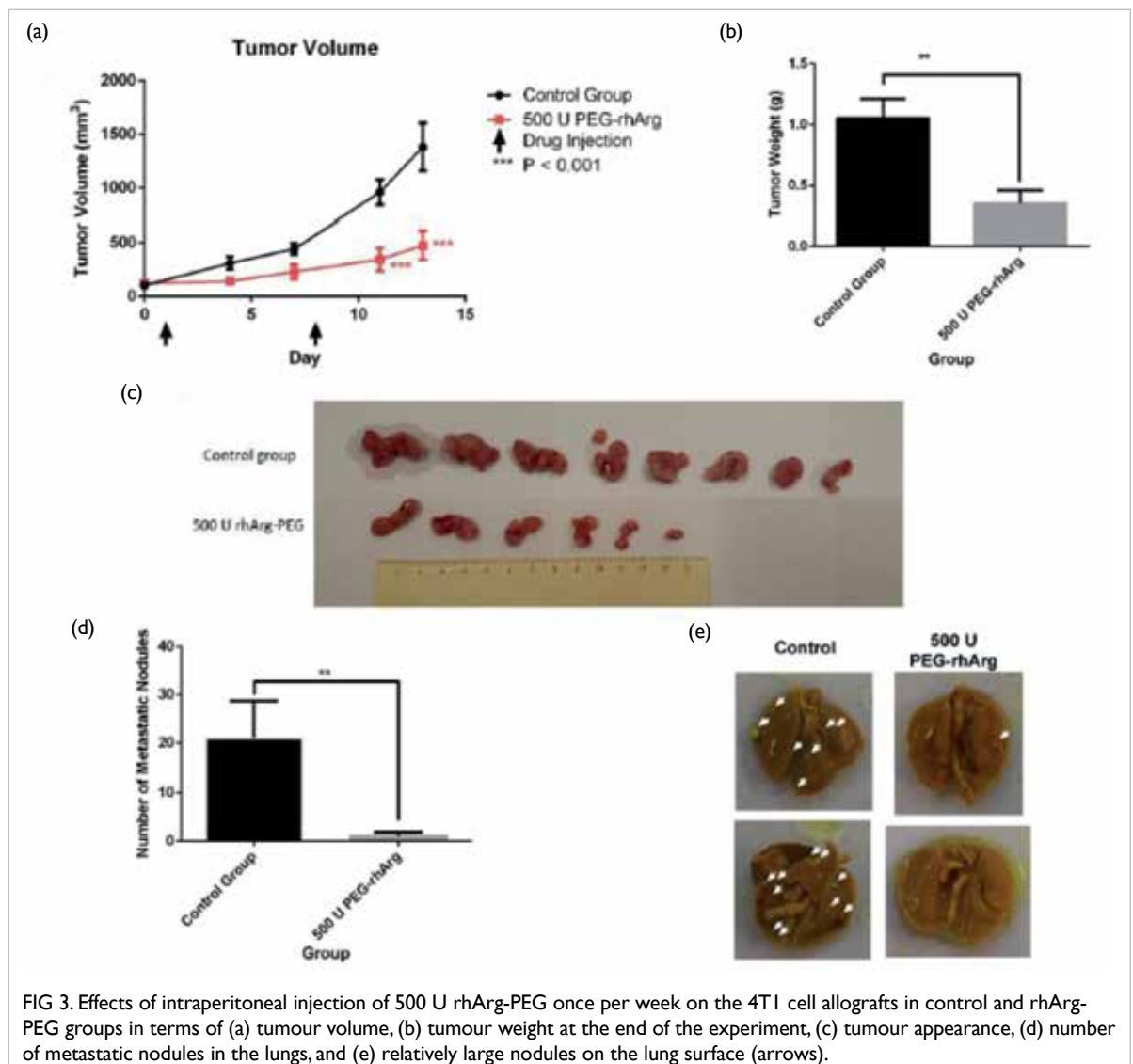


FIG 3. Effects of intraperitoneal injection of 500 U rhArg-PEG once per week on the 4T1 cell allografts in control and rhArg-PEG groups in terms of (a) tumour volume, (b) tumour weight at the end of the experiment, (c) tumour appearance, (d) number of metastatic nodules in the lungs, and (e) relatively large nodules on the lung surface (arrows).

Results

rhArg-PEG inhibits tumour growth in the MDA-MB-231 xenograft model

Chloroquine can bind with lysosome and prevents endosomal acidification. It can prevent degradation of autophagosomes and thus inhibit autophagy. In vitro data showed that CQ caused synergistic effects against MDA-MB-231 when it was combined with rhArg. Injecting 500 U of rhArg-PEG once per week significantly inhibited the growth of MDA-MB-231 xenograft (Fig 2). We tested whether CQ had synergistic effects when combined with rhArg-PEG. CQ alone inhibited the growth of the tumour, but it did not significantly improve efficacy of rhArg-PEG when combined with rhArg-PEG, consistent with data from Qiu et al.³

rhArg-PEG inhibits tumour growth and metastasis in the 4T1 cell allograft model

The efficacy of rhArg-PEG was tested in the 4T1 cell allograft metastasis mouse model. A dosage of 500 U of rhArg-PEG once per week significantly inhibited the growth of 4T1 solid tumour when compared with the control group (PBS group) [Fig 3]. 500 U of rhArg-PEG was sufficient to deplete all the serum arginine in mice for at least 7 days. The growth of the 4T1 allograft was significantly inhibited by the arginine depletion caused by rhArg-PEG. The aggressive 4T1 cancer cells have great potential to metastasise to distant organs. The lungs of the mice were evaluated for the anti-metastatic effects of rhArg-PEG (Fig 3). All mice in the control group of the 4T1 allograft contained the metastatic nodules in their lungs, whereas only 25% of the mice in the rhArg-PEG treatment group contained visible metastatic nodules. rhArg-PEG significantly reduced the number and the size of metastatic nodules.

Discussion

In our study, rhArg-PEG inhibited the tumour growth in the 'triple-negative' MDA-MB-231 xenograft model. PEGylation extended the serum half-life of protein drugs and reduced their immunogenicity. rhArg-PEG did not show immunogenicity or neutralising antibody problems. rhArg-PEG depleted serum arginine level, although some anti-drug antibodies were detected. Arginine

depletion by 500 U rhArg-PEG injected once per week inhibited the growth of 4T1 tumour cells in nude mice significantly and the drug was tolerable.

In addition, arginine starvation by rhArg-PEG inhibited the 4T1 tumour cell metastasis. Arginine is a precursor of polyamines, which are important for formation of lamellipodia and stress fibres during cell migration. Arginine plays an important role in cell migration and tumour metastasis. Depletion of arginine by rhArg-PEG may inhibit the production of polyamines and therefore inhibit metastasis of the aggressive 4T1 breast cancer cells in the mouse model. As cancer metastasis is the major cause of death, our finding may open up new possibilities for a more effective cancer therapy.

Conclusion

rhArg-PEG is safe and effective treatment against 'triple-negative' or highly metastatic breast cancer. rhArg-PEG is derived from human arginase and should be a safer drug with less immunogenicity problems, compared with bacterial enzyme ADI.

Acknowledgement

This study was supported by the Health and Medical Research Fund, Food and Health Bureau, Hong Kong SAR Government (#01121936).

References

1. Cheng PN, Lam TL, Lam WM, et al. Pegylated recombinant human arginase (rhArg-peg5,000mw) inhibits the in vitro and in vivo proliferation of human hepatocellular carcinoma through arginine depletion. *Cancer Res* 2007;67:309-17.
2. Lam TL, Wong GK, Chow HY, et al. Recombinant human arginase inhibits the in vitro and in vivo proliferation of human melanoma by inducing cell cycle arrest and apoptosis. *Pigment Cell Melanoma Res* 2011;24:366-76.
3. Qiu F, Chen YR, Liu X, et al. Arginine starvation impairs mitochondrial respiratory function in ASS1-deficient breast cancer cells. *Sci Signal* 2014;7:ra31.
4. Changou CA, Chen YR, Xing L, et al. Arginine starvation-associated atypical cellular death involves mitochondrial dysfunction, nuclear DNA leakage, and chromatin autophagy. *Proc Natl Acad Sci U S A* 2014;111:14147-52.
5. Yau T, Cheng PN, Chan P, et al. A phase 1 dose-escalating study of pegylated recombinant human arginase 1 (Peg-rhArg1) in patients with advanced hepatocellular carcinoma. *Invest New Drugs* 2013;31:99-107.

Detection of methylated septin 9 DNA in blood for diagnosis, prognosis, and surveillance of colorectal cancer

WK Leung *, VY Shin, WL Law

KEY MESSAGES

1. The sensitivity of methylated septin9 (mSEPT9) in blood was significantly higher than carcinoembryonic antigen (CEA) in detecting colorectal cancer (CRC) [73.9% vs 48.2%, $P < 0.001$]. However, both were not sensitive enough for detecting colorectal adenoma (<28%).
2. In patients with colorectal cancer, increased number of positive mSEPT9 PCR reactions in plasma samples after surgery was associated with higher rates of mortality (26.3% vs 4.2%, $P < 0.01$), recurrence (47.4% vs 14.1%, $P < 0.01$), and metastasis (36.8% vs 8.5%, $P < 0.01$).
3. In patients with colorectal cancer, the proportion

of those with negative CEA was higher than that of those with negative mSEPT9 at 6 months (71.8% vs 55.3%, $P = 0.035$) and 12 months (68.1% vs 48.1%, $P = 0.028$) after surgery.

Hong Kong Med J 2019;25(Suppl 9):S32-4
HMRF project number: 01121026

¹ WK Leung, ² VY Shin, ² WL Law

Queen Mary Hospital, The University of Hong Kong:

¹ Department of Medicine

² Department of Surgery

* Principal applicant and corresponding author: waikleung@hku.hk

Introduction

In Hong Kong, colorectal cancer (CRC) has surpassed lung cancer to become the most common cancer.¹ Colonoscopy is the most direct method to detect colorectal neoplasm, but it has potential risk and discomfort. Non-invasive blood test is simpler and have higher compliance, but there is no reliable blood biomarker for screening of CRC.

Aberrant methylation is a regulatory mechanism of gene expressions commonly found in tumour suppressor genes of cancers, including CRC. Various epigenetic biomarkers have been identified for diagnosis and prognosis of CRC. Methylated septin9 (mSEPT9) has high sensitivity for serological diagnosis of CRC. Detection of mSEPT9 DNA in blood has been approved by the Food and Drug Administration of the United States as a non-invasive screening test for CRC. However, no study has investigated the role of mSEPT9 on monitoring CRC patients after curative resection, particularly in comparison with carcinoembryonic antigen (CEA). The American Society of Clinical Oncology recommends that CEA be measured every 3 months for at least 3 years after surgery in patients with stage II or III CRC.

This prospective study aimed to (1) compare the diagnostic accuracy of mSEPT9 DNA in the plasma and CEA among patients with different stages of colorectal neoplasm, and (2) compare mSEPT9 with CEA in monitoring CRC patients who had undergone surgical resection of tumour.

Methods

This prospective study was approved by the Institutional Review Board of the Hospital Authority Hong Kong West Cluster and University of Hong Kong (UW 12-489). Informed consent was obtained from all patients. We prospectively enrolled symptomatic patients who were referred to have colonoscopy for bowel symptoms or diagnostic workup for iron deficiency anaemia as well as patients undergoing screening colonoscopy. We excluded patients with previous bowel resection, familial CRC syndrome, inflammatory bowel disease, or diagnosis of any other malignancy in the past.

During colonoscopy, all polyps were removed for histological examination and lesions suspicious of CRC were biopsied. Histological samples were reviewed by experienced pathologists and classified into (1) adenocarcinoma, (2) advanced adenoma, (3) non-advanced adenoma, or (4) normal colonoscopy without any polyp or adenoma. Advanced adenoma was defined as lesion with a diameter of ≥ 10 mm, with villous histology or the presence of high-grade dysplasia.

We prospectively recruited patients who were newly diagnosed as having adenocarcinoma of the colon or rectum and scheduled for curative resection. Blood sample was taken immediately before surgery (baseline) and after surgery at 3-month intervals for up to 2 years. We excluded patients who had received preoperative chemotherapy or radiotherapy or patients with other non-colonic malignancy. Tumour

staging was classified according to the seventh edition of the American Joint Committee on Cancer TNM Classification. Clinical relapse or recurrence was determined by history, physical examination, and relevant investigation findings. Imaging (including computed tomography or positron emission tomography-computed tomography) was arranged to confirm the presence of distant or regional recurrence. Surveillance colonoscopy after surgical resection was performed according to current recommendation.

Plasma samples were blinded to laboratory staff. mSEPT9 was determined by the Epi proColon 2.0 assay (Epigenomics AG, Berlin, Germany). Samples were analysed using real-time PCR in triplicate, and the mSEPT9 assay was considered positive when more than one PCR reactions was positive.

CEA levels were determined by enzyme-linked immunoassay. Abnormal or positive CEA level was defined as >3 ng/mL. Increased CEA level was defined as any increase in subsequent follow-up (compared with baseline) and was >3 ng/mL.

The sensitivity and specificity of mSEPT9 and CEA were computed with the 95% confidence intervals. Chi-squared test or Fisher Exact test was used to compare categorical data. All statistical analyses were two-sided and a statistically significant difference was set at $P < 0.05$. All analyses were performed by the SPSS (Windows version 21; IBM Corp, Armonk [NY], US).

Results

Of 282 patients included (62.8% male; mean age, 66.1 ± 11.5 years), 117 had confirmed CRC, 45 had advanced adenoma, 50 had non-advanced adenoma, and 70 had normal colonoscopy. Among the 117 confirmed CRC patients, 98 had serial blood taken before and after surgical resection.

The sensitivity of mSEPT9 and CEA for different diagnoses and tumour stages is shown in Fig 1. In patients with confirmed CRC, the overall positive rate was 73.9% (95% CI=65.8%-82.0%) for mSEPT9 and 48.2% (95% CI=39.1%-57.3%) for CEA ($P < 0.001$). The detection rate increased with higher tumour staging for mSEPT9 ($P = 0.003$) and CEA ($P = 0.033$). The positive rate increased from 52.6% (stage I cancer) to 100% (stage IV cancer) for mSEPT9 and from 26.3% to 100% for CEA. The positive rate differed significantly between mSEPT9 and CEA in stage II ($P = 0.001$) and stage III ($P = 0.004$) cancers but not in stage I and IV cancers. However, the sensitivity of both mSEPT9 and CEA was low (<28%) in advanced and non-advanced adenoma, with no significant difference in positive rate. In colonoscopy-negative subjects, the overall specificity of mSEPT9 and CEA was comparable (72.5% vs 79.3%, $P = 0.412$).

After surgery, the proportion of patients with negative CEA was higher than the proportion of patients with negative mSEPT9 at 6 months (71.8% vs 55.3%, $P = 0.035$), 12 months (68.1% vs 48.1%, $P = 0.028$), 18 months (67.9% vs 53.1%, $P = 0.18$), and 24 months (65.9% vs 30.0%, $P = 0.07$).

Among cancer patients with positive mSEPT9 or CEA at baseline, 46.8% and 46.7% ($P = 1.0$) turned negative at 6 months after surgery, respectively, whereas 47.2% and 39.3% ($P = 0.62$) turned negative at 12 months after surgery, respectively. For patients with non-advanced cancer (stage I/II), 79.2% and 55.6% ($P = 0.013$) had negative CEA and mSEPT9 at 6 months, respectively. For patients with advanced cancer stage (stage III/IV), 68.0% and 52.0% ($P = 0.39$) had negative CEA and mSEPT9 at 6 months, respectively. For patients with no clinical recurrence, mSEPT9 or CEA was negative at 6 months (55.3% vs 72.9%, $P = 0.038$), 12 months (49.0% vs 69.7%, $P = 0.033$), 18 months (59.3% vs 65.9%, $P = 0.316$), and 24 months (30.0% vs 65.9%, $P = 0.07$), respectively.

Most patients had a decline in the number of positive mSEPT9 reactions after surgery (Fig 2). An increased number of positive reactions was associated with higher rates of mortality (26.3% vs 4.2%, $P < 0.01$), recurrence (47.4% vs 14.1%, $P < 0.01$), and metastasis (36.8% vs 8.5%, $P < 0.01$).

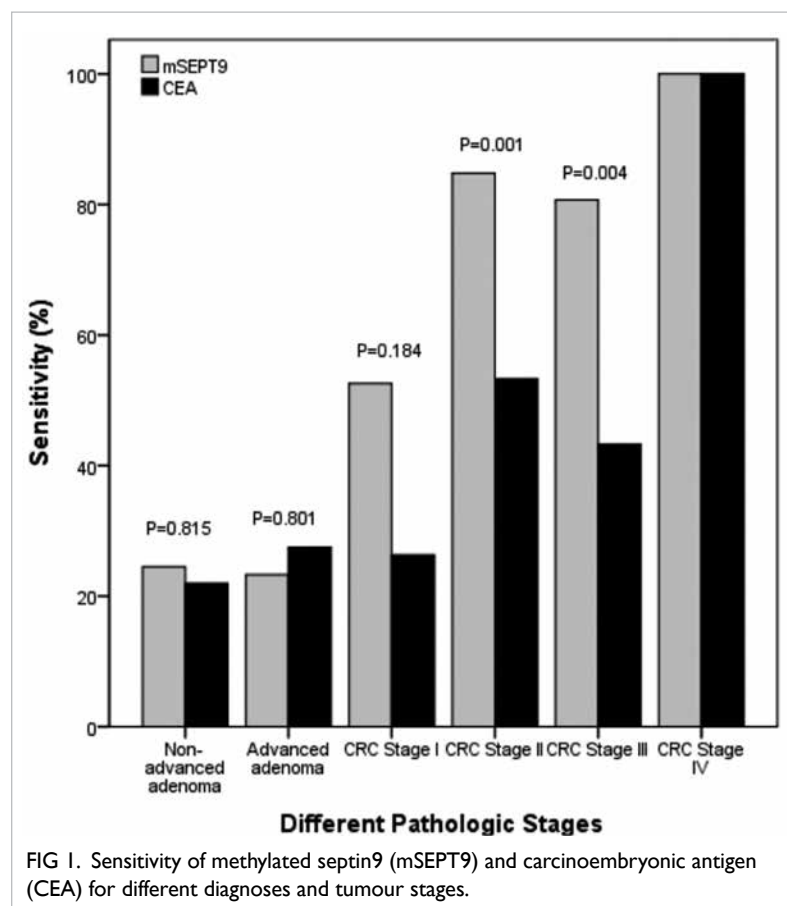
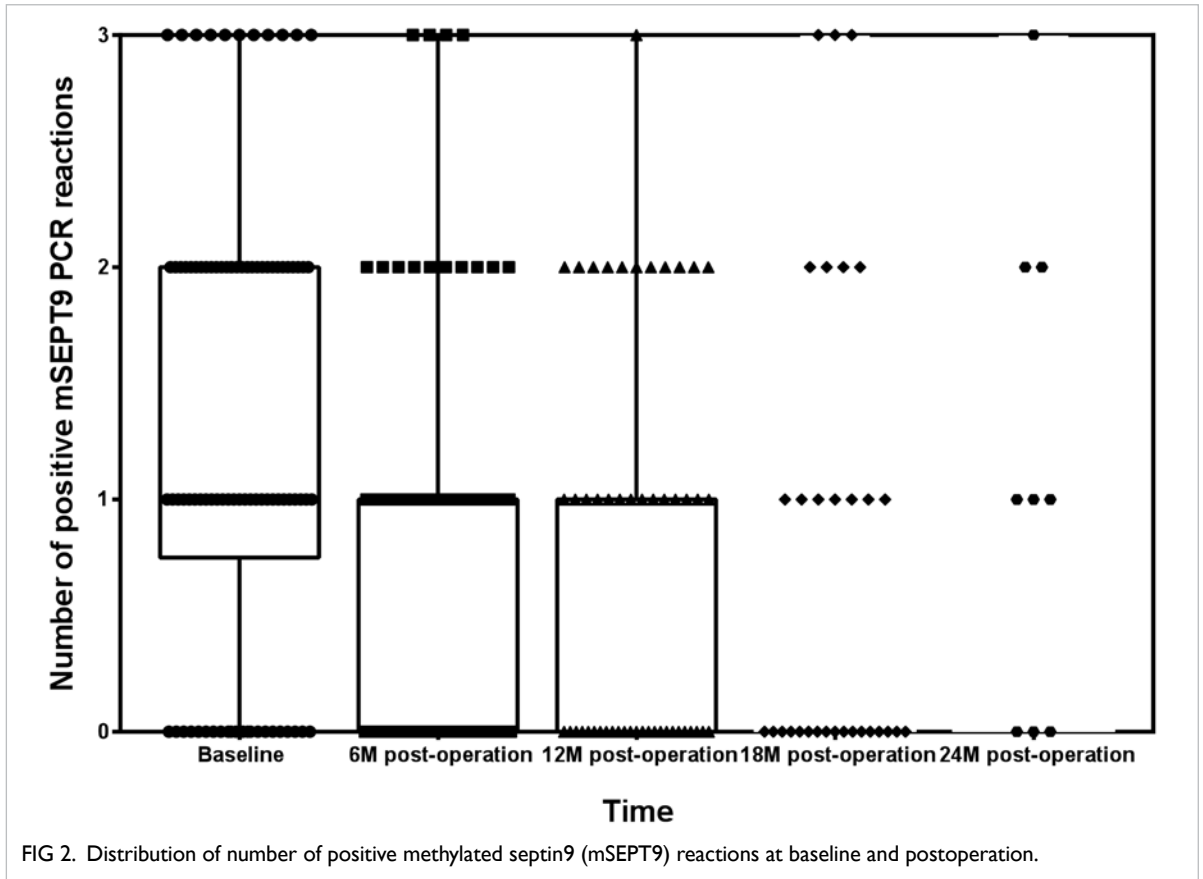


FIG 1. Sensitivity of methylated septin9 (mSEPT9) and carcinoembryonic antigen (CEA) for different diagnoses and tumour stages.



Conclusion

Sensitivity was higher for mSEPT than CEA in diagnosing CRC; sensitivity of mSEPT9 increased with higher tumour staging. An increased number of positive mSEPT9 PCR reactions in blood samples was associated with higher rates of recurrence, metastases, and mortality. After surgery, the negative rate was lower for mSEPT9 than CEA. As both mSEPT9 and CEA decline very slowly after surgery, further studies are needed to identify a more sensitive way to detect subtle changes in mSEPT9 concentration in blood for detection of early CRC recurrence.

Acknowledgements

This study was supported by the Health and Medical Research Fund, Food and Health Bureau, Hong Kong

SAR Government (#01121026). We also thank all colorectal surgeons and endoscopists in the Queen Mary Hospital for patient recruitment.

References

1. Hong Kong Cancer Registry, Hospital Authority. Available at <http://www3.ha.org.hk/cancereg/facts.html>. Accessed 28 February 2017.
2. Church TR, Wandell M, Lofton-Day C, et al. Prospective evaluation of methylated SEPT9 in plasma for detection of asymptomatic colorectal cancer. *Gut* 2014;63:317-25.
3. Potter NT, Hurban P, White MN, et al. Validation of a real-time PCR-based qualitative assay for the detection of methylated SEPT9 DNA in human plasma. *Clin Chem* 2014;60:1183-91.
4. Song L, Jia J, Peng X, Xiao W, Li Y. The performance of the SEPT9 gene methylation assay and a comparison with other CRC screening tests: a meta-analysis. *Sci Rep* 2017;7:3032.

M2 macrophages on tumour growth and metastasis in hepatocellular carcinoma

K Man *, CM Lo, XB Liu

KEY MESSAGES

1. M2 macrophages contributed to poor survival outcome in liver cancer patients. An increase in the number of immune cells within the tumour correlated with reduction in the overall and relapse-free survival period.
2. An increase in M2 macrophages correlated with larger tumour size, increased venous infiltration, and higher tumour stage.
3. M2 macrophages secreted a chemokine CCL22 that promoted invasiveness of liver cancer cells and increased the incidence of metastasis.

4. Targeting the tumour-promoting macrophages is a potential therapeutic strategy against liver cancer.

Hong Kong Med J 2019;25(Suppl 9):S35-9
HMRF project number: 01122266

K Man, CM Lo, XB Liu

Department of Surgery, The University of Hong Kong

* Principal applicant and corresponding author: kwanman@hku.hk

Introduction

Hepatocellular carcinoma (HCC) is the fifth most commonly diagnosed malignancy and the second most common cause of death from cancer worldwide. Over 500 000 new cases and deaths are estimated to occur every year. HCC is characterised by rapid disease progression and high postsurgical recurrence and high metastatic rate (50% to 70% over 5 years) and often results in poor clinical outcomes.¹ One major risk factor of recurrence and metastasis is sustained inflammation, which is found in up to 80% of cancer patients. Therefore, understanding the roles of inflammatory-related immune cells, particularly macrophages, in cancers is important. It remains controversial whether macrophages contribute to better or poorer clinical outcomes in HCC.

Macrophages can be sub-classified into classically (M1) and alternatively (M2) activated phenotypes based on surface receptors and functional characteristics. With a distinct secretory profile consisting of cytokines and growth factors, M2 macrophages are responsible for mediating wound healing processes via extracellular matrix remodelling, angiogenesis, and immunosuppression. In human cancers, these wound-healing features are exploited to facilitate tumour growth and dissemination. Collective evidence demonstrates that intratumoural macrophages known as tumour-associated macrophages exhibit M2 phenotypes and are correlated with poor prognosis in numerous malignancies.²

Methods

The present study comprised a clinical study, an in

vivo study, and an in vitro study (Fig 1). The study was approved by the Institutional Review Board of the University of Hong Kong. Informed written consent was obtained from all patients. Animals (Control of Experiments) Ordinance (Hong Kong) and the institute's guidance on animal experimentation were strictly followed.

For clinical study, tumorous liver tissues (intra-tumour) and peritumoural liver tissues within 2 cm proximal to the tumour margin (peri-tumour) were collected from 95 patients (aged 18-83 years, 78% male) who underwent curative surgery for HCC in Queen Mary Hospital from 2004 to 2008.

For in vivo study, male athymic nude mice (BALB/c nu/nu, 4-6 weeks old) were used. Surgical procedures have been described in previous reports by our group. Briefly, 3×10^5 MHCC97L cells suspended in 0.2 mL DMEM were injected subcutaneously into the flanks of mice. After 4 weeks, the subcutaneous tumours were resected and diced into 1 mm³ cubes, which were then implanted in the left lobes of the livers of another group of nude mice. Simultaneously, 5×10^5 M1 or M2 polarised THP-1 macrophages suspended in 0.2 mL DMEM were injected into the portal vein of the same group of mice. Nine mice were used for both the negative control and the M2 macrophage treatment group, whereas six mice were used for the M1 macrophage treatment group. Mice injected with pure DMEM were served as negative control. Tumour size and metastasis of MHCC97L xenograft were monitored weekly by Xenogen IVIS (Xenogen IVIS 100, Caliper Life Sciences). All mice were sacrificed at week 5 and the size of liver tumour was measured.

For in vitro study, to examine the direct effect on cell growth and migration of HCC, macrophages

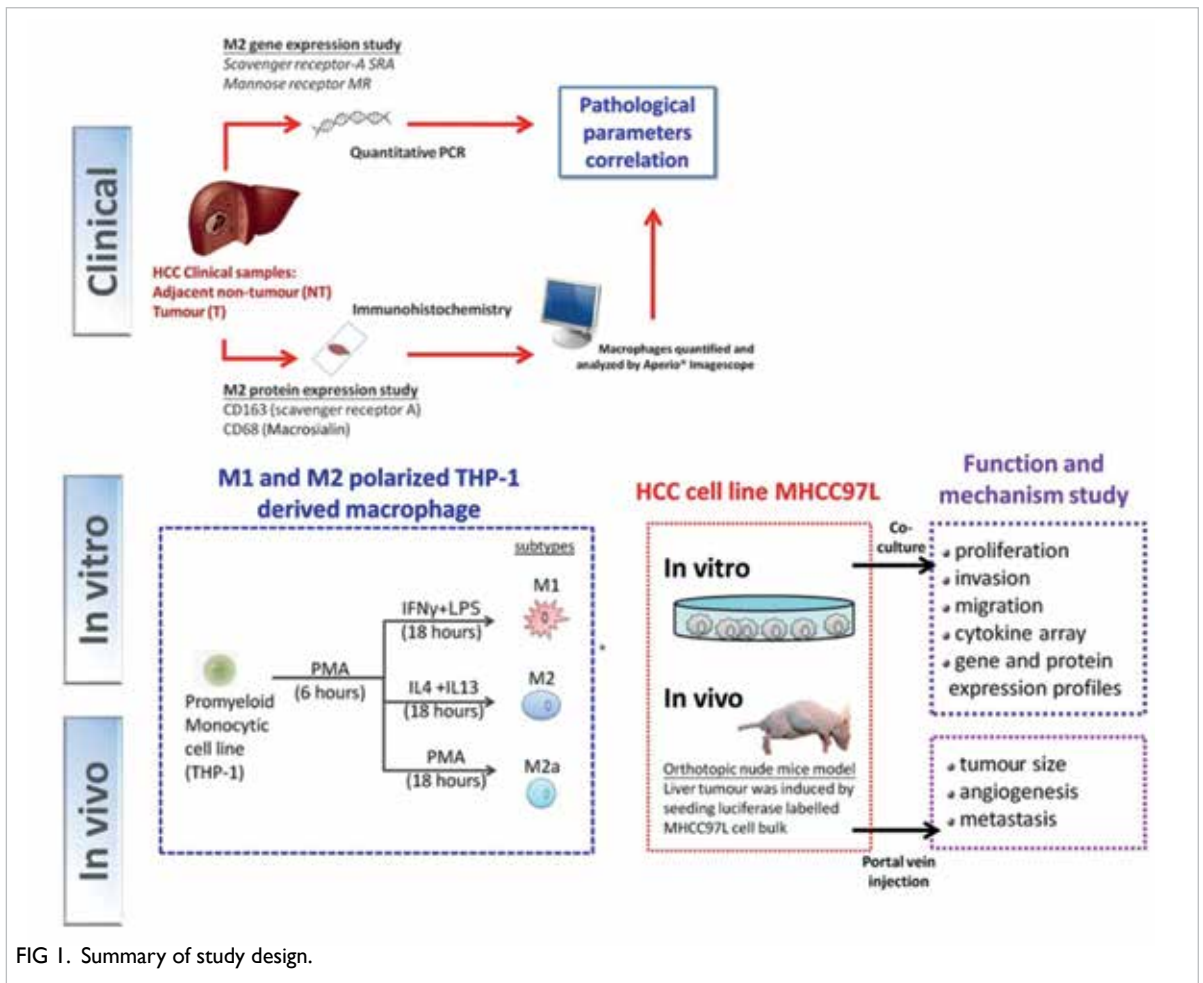


FIG 1. Summary of study design.

and MHCC97L cells cocultivation was conducted using the non-contact coculture transwell system (Corning). For cell growth, 1×10^5 , 3×10^5 , or 5×10^5 THP-1 cells were seeded in 0.4- μ m sized pores inserts and polarised into M1 and M2 macrophages. Culture medium was then replaced by FBS-free RPMI 1640 medium for further 24 hours. Inserts containing M1 or M2 polarised THP-1 macrophages were transferred to 6-well cell culture plate seeded with MHCC97L cells (1×10^5 cells per well) in advance and cocultured for 72 hours. Inserts were discarded and the MHCC97L cells were washed with PBS three times and trypsinised with 0.05% Trypsin-EDTA (Invitrogen). The total number of MHCC97L cells after coculture with macrophages in each well was measured by the FC500 flow cytometer (Beckman Coulter). To evaluate the status of MHCC97L cells after co-culture, 1 mg/mL of D-luciferin was added to each well and visualised by In Vivo Imaging System (IVIS; Xenogen IVIS 100).

Statistical analysis was performed using GraphPad Prism 5.0 and PASW Statistics 18.0 (SPSS Inc.). A P value of ≤ 0.05 was considered statistically significant. Unpaired Student's *t* test and Fisher's

exact test for dual comparison and log-rank test for comparison of survival in Kaplan-Meier survival plot were used. Prognostic value of each clinicopathologic parameter and expression level of macrophage marker was tested by univariate Cox proportional hazards regression analysis. The prognostic power of significant predictors in the univariate analysis was then evaluated by a multivariate survival model.

Results

We analysed the level of M2 macrophages in tumour tissue collected from 80 HCC patients. Three antibody targeting surface receptors: monocyte/macrophage (CD14), macrophage (CD68), and M2 macrophage (CD163) were used to identify distinct subpopulation residing in the intratumoural and peritumoural regions of HCC tissues via immunohistochemistry. The ratio of positively stained macrophages to total cell population in each sample was determined. All macrophages were highly expressed in the tumoural region, and most of the populations demonstrated M2 subtype. Consistent results were observed in the mRNA expression study involving two M2

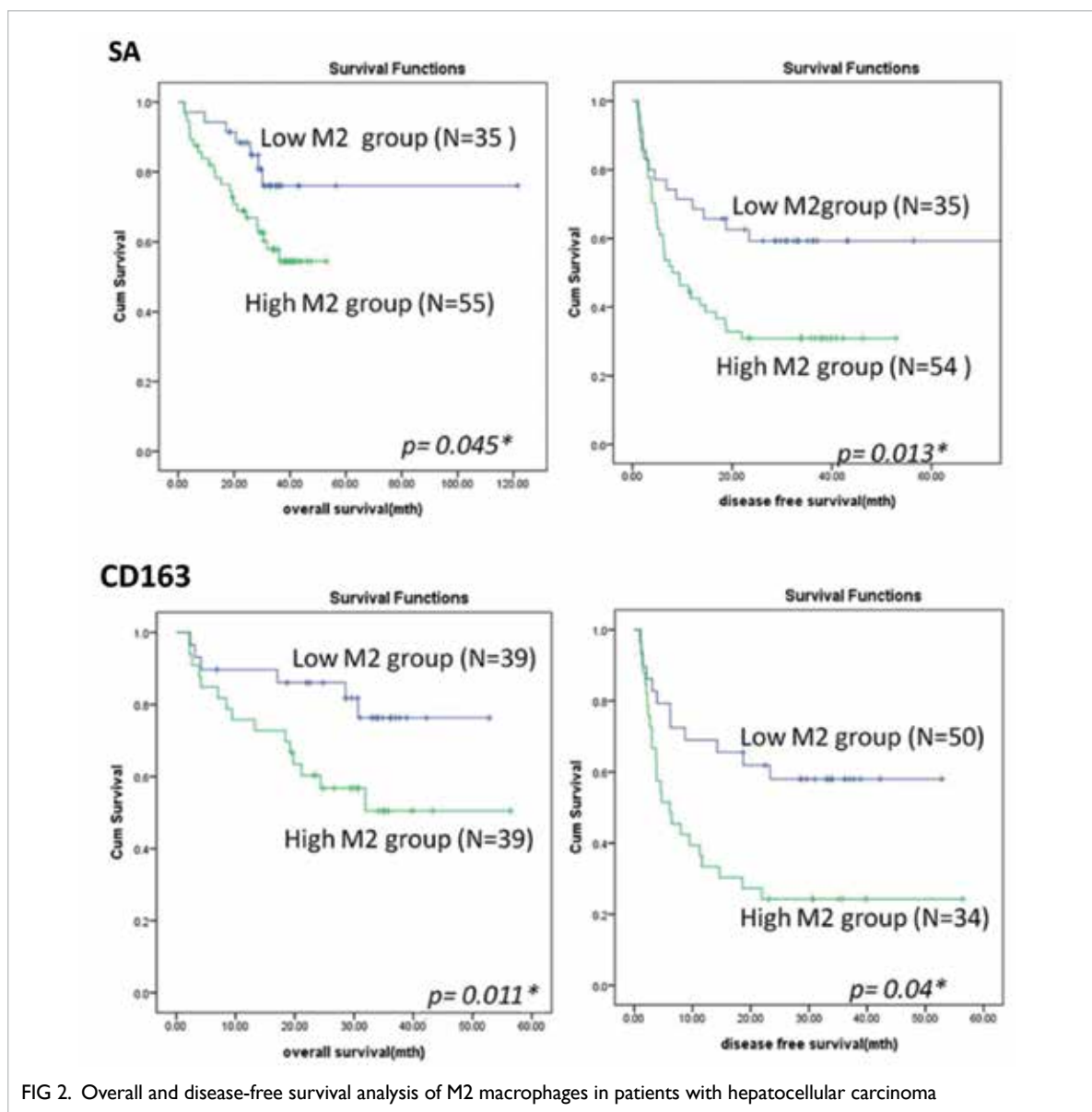


FIG 2. Overall and disease-free survival analysis of M2 macrophages in patients with hepatocellular carcinoma

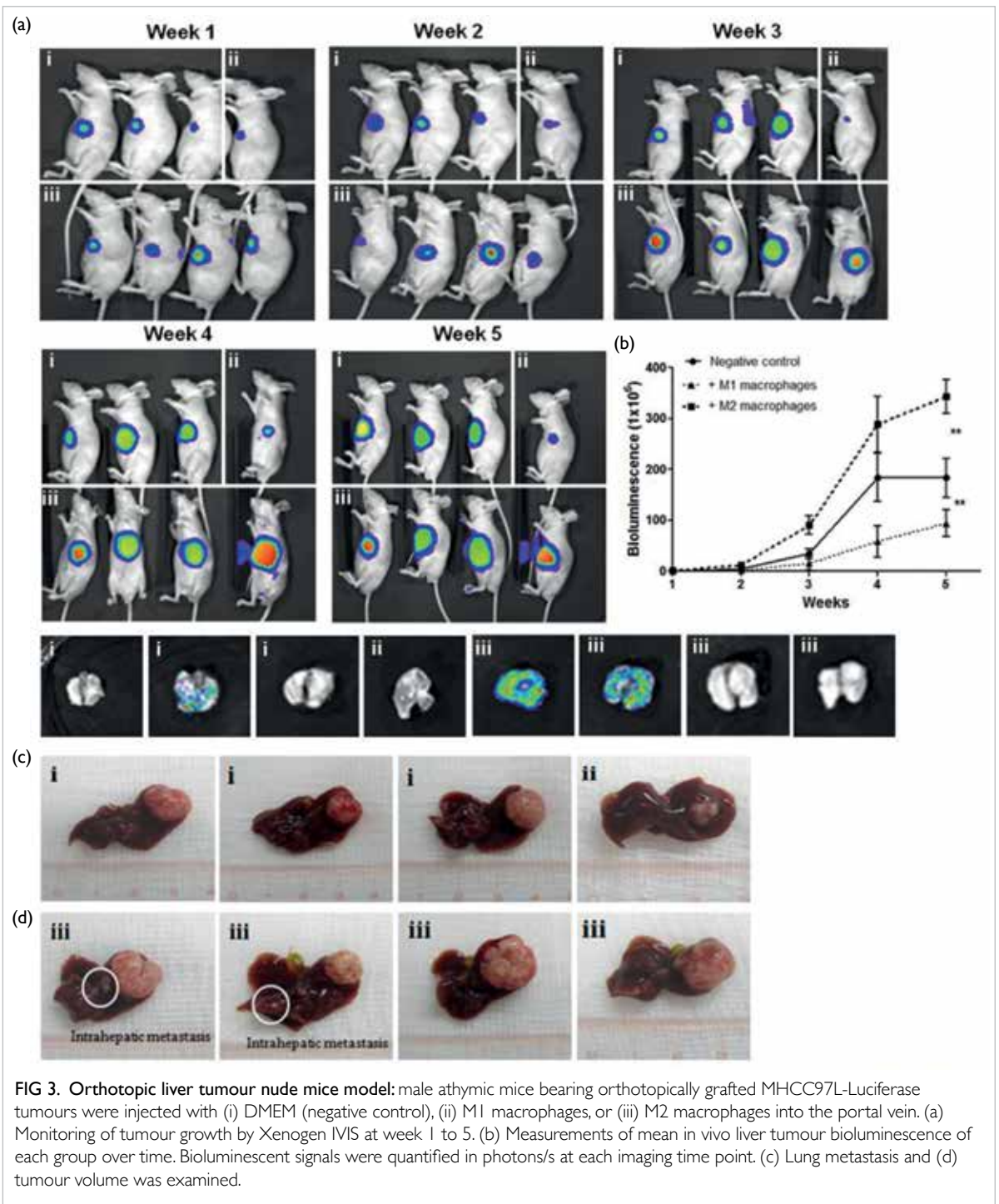
macrophage-specific transcripts: class A scavenger receptor (SA) and mannose receptor (MR).

High expression levels of M2 macrophage markers SA and CD163 in tumour area significantly correlated with shortened overall and disease-free survival in HCC patients (Fig 2). Using multivariate Cox proportional hazards analyses, only the M2 macrophage markers CD163⁺ and SA were significant independent prognosis factors in overall survival (CD163⁺: hazard ratio [HR]=3.14, 95% confidence interval [CI]=1.2-8.2, P<0.05) and disease-free survival (CD163⁺: HR=3.64, 95% CI=1.0-7.0, P=0.043; SA: HR=3.56, 95% CI=1.0-12.2, P=0.044).

Increased levels of CD163 and SA were significantly associated with late tumour stages, venous infiltration, and multiple tumour nodules

(P<0.05) in HCC patients. High levels of M2 macrophages induced invasiveness in tumour cells.

To validate the tumour-promoting effects of M2 macrophages, we tested M2 macrophages on an orthotopic nude mice model of liver cancer. 5 × 10⁵ THP-1-derived M1 or M2 macrophages were introduced into the liver of nude mice via portal vein injection immediately after orthotopic liver transplantation. Tumour growth and metastasis were monitored using Xenogen IVIS100, and the mice were sacrificed at week 5 after transplantation. The tumour volume in the mice injected with M2 macrophages increased 3.26-fold compared with the control group (1.27±0.36 cm³ vs 0.39±0.05 cm³, P=0.032, Fig 3a). By contrast, the mice injected with M1 macrophages exhibited a significant 2.79-fold reduction in tumour volume (0.14±0.02 cm³,



P=0.044). An increased rate of lung metastases was observed in the M2-treated group compared with the control (57% vs 25%, P<0.05, Fig 3b and c). To identify the location of the injected M2 macrophages, immunohistochemistry with anti-human CD163 antibody was applied, and positively stained cells were observed in the peritumoural region (Fig 3d). M2 macrophages stimulated the growth of tumour as well as increased the metastasis incidents in liver cancer.

To further verify whether M2 macrophages directly induce the growth and invasiveness of HCC cells, in vitro studies were conducted by co-culturing HCC cell line MHCC97L with M2 macrophages. After 72 hours, the cell number of MHCC97L significantly increased 1.3-fold compared with the single MHCC97L culture (P<0.05). M2 macrophages were found to enhance the migration of HCC cells. Applying a similar co-cultivation methodology but with 8 µm inserts and 24 hours of incubation to allow

cell migration across the membrane, the number of migrated MHCC97L increased by 3.2-fold upon co-cultivation with M2 macrophages compared with the control ($P < 0.01$).

Given that cytokines and chemokines represent the major functional responses of macrophages, a signalling mechanism between M2 macrophages and HCC cells may account for the pro-tumoural activities. The expression level of 42 cytokines in M1 and M2 monoculture supernatants as well as M1/MHCC97L and M2/MHCC97L co-culture supernatants were examined using an antibody cytokine array. Only the cytokine C-C motif chemokine 22 (CCL22) known as macrophage-derived chemoattractant was significantly up-regulated in M2–MHCC97L, in contrast to the other three configurations (Fig 3d). To exclude the possibility that CCL22 may derive from MHCC97L before or after co-cultivation with M2 macrophages, transcript and protein analysis were performed; no CCL22 mRNA and protein were detected in both cases (data not shown).

Discussion

M2 macrophages in tumour area significantly contributed to the disease progression. The level of peritumoural M2 macrophages was a

predictor of the survival in HCC. In vivo and in vitro experimental evidences showed a significant increase in tumour growth and migration in the presence of M2 macrophages confirming their pro-tumour functions. One underlying mechanism identified was CCL22/CCR4, which enhanced HCC invasiveness through epithelial-mesenchymal transition activation.

Acknowledgements

This study was supported by the Health and Medical Research Fund, Food and Health Bureau, Hong Kong SAR Government (#01122266). We also thank our lab members for their technical assistance.

Results from this study have been published in: Yeung OW, Lo CM, Ling CC, et al. Alternatively activated (m2) macrophages promote tumour growth and invasiveness in hepatocellular carcinoma. *J Hepatol* 2015;62:607-16.

References

1. Gish RG, Porta C, Lazar L, et al. Phase III randomized controlled trial comparing the survival of patients with unresectable hepatocellular carcinoma treated with nolatrexed or doxorubicin. *J Clin Oncol* 2007;25:3069-75.
2. Talmadge JE, Donkor M, Scholar E. Inflammatory cell infiltration of tumors: Jekyll or Hyde. *Cancer Metastasis Rev* 2007;26:373-400.

Computational platform for modelling, analysis, and prediction of anti-EGFR drug resistance for lung cancer

H Yan *, GY Zhu, M Wong, V Lee

KEY MESSAGES

1. Epidermal growth factor receptor (EGFR) mutation is an important cause of drug resistance in non-small cell lung cancer (NSCLC). We conducted computational modelling of EGFR mutants and analysis of EGFR-drug interaction patterns.
2. Any observed EGFR mutation can be modelled mathematically, and its 3D structure can be predicted computationally. The fundamental cause of drug resistance can be found at the atomic level.
3. Different drugs can be analysed. Based on our computer model, the binding strength between an EGFR mutant and a drug can be calculated.
4. Drug resistance can be evaluated for each mutation and each drug. Thus, a comprehensive database of EGFR mutation and drug effectiveness

is established and is available online. The database provides a useful reference to medical doctors.

5. Our computational framework is less expensive than wet-lab experiments. It can also be used to study drug resistance related to other diseases.

Hong Kong Med J 2019;25(Suppl 9):S40-2
HMRF project number: 01121986

¹ H Yan, ² GY Zhu, M Wong, ⁴ V Lee

¹ Department of Electrical Engineering, City University of Hong Kong

² Department of Chemistry, City University of Hong Kong

³ Department of Pathology, Li Ka Shing Faculty of Medicine, The University of Hong Kong

⁴ Department of Clinical Oncology, Li Ka Shing Faculty of Medicine, The University of Hong Kong

* Principal applicant and corresponding author: h.yan@cityu.edu.hk

Introduction

Lung cancer has the highest mortality rate among all cancer types and results in 1.6 million deaths each year worldwide.¹ In Hong Kong, lung, liver, and colorectal cancers are the three leading causes of cancer deaths. Lung cancer accounts for more deaths than liver and colorectal cancers combined. About 85% of lung cancer patients have non-small cell lung cancer (NSCLC); many NSCLC cases are caused by a mutation of the epidermal growth factor receptor (EGFR), especially in Asia.² Several commercially available drugs are effective to shrink the tumour initially, but almost all patients develop drug resistance over time owing to mutations of EGFR.²⁻⁵

We studied EGFR mutations at the molecular and atomic levels. We collected EGFR mutations from research publications and from clinical cases at Queen Mary Hospital. Some of the mutations observed locally were rare and had never been reported. Based on computational models, we analysed how the 3D structure of EGFR changed secondary to a mutation. We then computed the binding strength of each drug with EGFR before and after the secondary mutation. The reduction in the binding strength reflected the degradation of the drug effectiveness. We built a 3D structural database of EGFR mutants and analysed the characteristics

of all known EGFR mutations at the atomic level. Our work can provide a useful reference to medical doctors for assessment of drug resistance level and planning personalised treatment.

Results

Computational platform and EGFR mutant structural database

Our outcomes are summarised in the website <http://bcc.ee.cityu.edu.hk/SFBG/>. Under 'Computational Platform', all known EGFR mutations that cause NSCLC and drug resistance are listed. Each mutant is displayed interactively; users can adjust its rotation and scale, and download the PDB file of the mutant. Users can report any new EGFR mutation to us for analysis by clicking 'Report New EGFR Mutations'. Summaries of all these mutants are shown in 'EGFR Mutant Structural Database: Computationally predicted 3D structures and the corresponding binding free energies with gefitinib and erlotinib' under 'Research and Publications' at http://bcc.ee.cityu.edu.hk/SFBG/research_and_publications.html.

Personalised prediction of NSCLC drug resistance

The effectiveness of a cancer drug can be measured

based on the patient survival time and the response level. We built a prediction model based on the extreme learning machines. Leave-one-out was used for cross-validation. Training data included personal attributes (such as the physical condition and smoke history) of 168 patients from Hong Kong hospitals. We also used the binding free energy, which was computed based on the computer predicted 3D structures of EGFR mutants and molecular dynamics simulations. The prediction model was then applied to unseen testing data. We have achieved about 90% accuracy for testing samples.

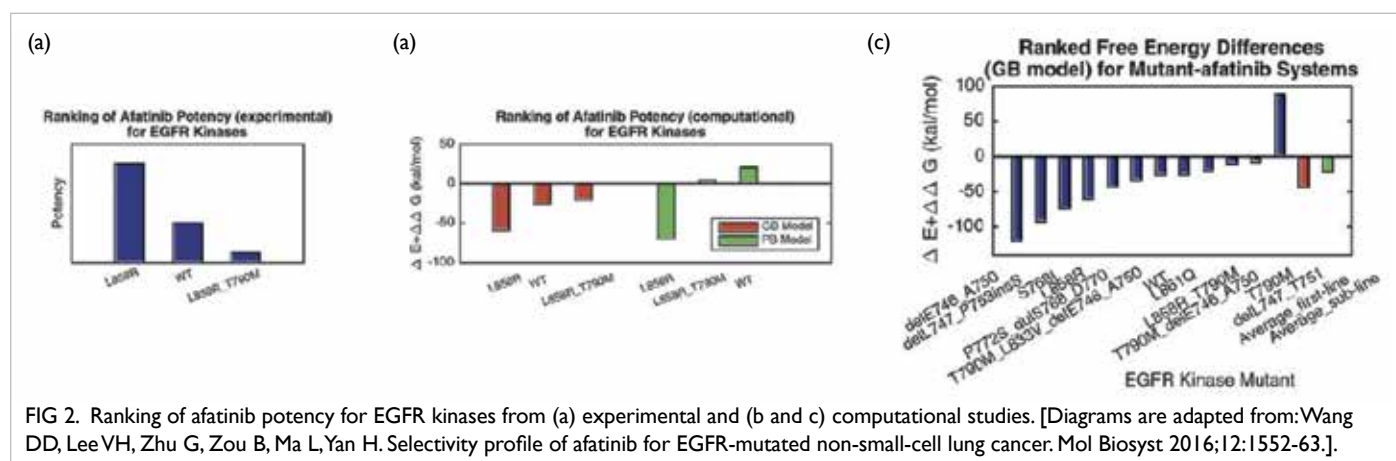
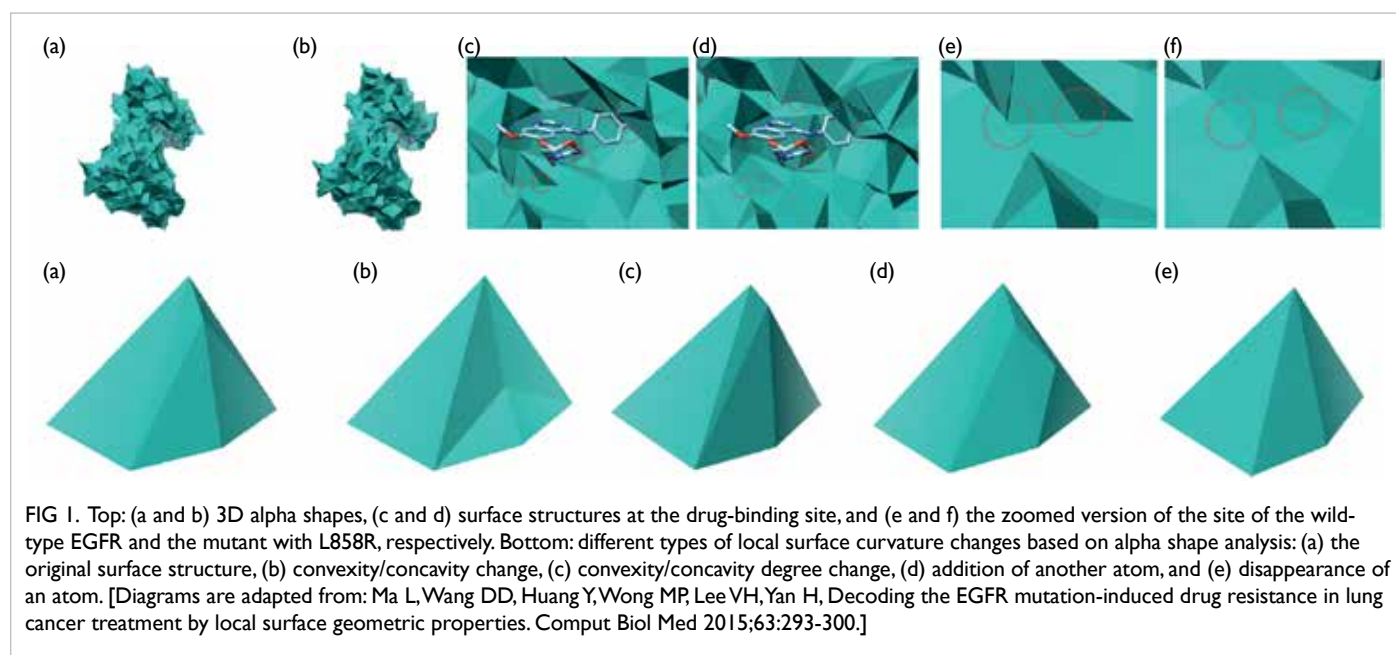
EGFR mutant surface characteristics

We developed a 3D alpha shape-based model to characterise the surface structure of a biomolecule or the interaction complex of two biomolecules. We can determine the convexity or concavity of

a molecular surface. We used the alpha shapes to analyse all known EGFR mutants and found that four types of surface curvature changes can result in weaker EGFR mutant-inhibitor binding and drug resistance (Fig 1). Our analysis provided physical reasons for drug resistance secondary to EGFR mutations.

Selectivity profile of afatinib

Afatinib is a second-generation NSCLC drug that forms covalent binding to an EGFR mutant. We analysed the potency of afatinib for different types of EGFR mutants computationally and experimentally. In clinical studies, the mutation type of each patient was determined before treatment with oral afatinib,⁵ and then the disease progression was observed. Fig 2 shows a potency ranking of afatinib for different EGFR mutations.



Characterisation of EGFR and ErbB-3 heterodimerisation

Based on data from 168 NSCLC patients, we characterised the interaction patterns of the EGFR mutants of these patients with three other proteins in the downstream EGFR signalling pathway: ErbB-2, IGF-1R, and c-Met,^{3,4} as well as the interaction patterns with NSCLC drug molecules (gefitinib and erlotinib), particularly c-Met and ErbB-3 had a very high binding strength, which implies c-Met plays an important role in regulating ErbB-3.

Acknowledgements

This study was supported by the Health and Medical Research Fund, Food and Health Bureau, Hong Kong SAR Government (#01121986). We also thank the staff at the Signal Processing and Biocomputing Lab, City University of Hong Kong, for their help with computer hardware and software and maintenance of our website.

Results from this research have been published in:

- (1) Ma L, Wang DD, Huang Y, Yan H, Wong MP, Lee VH. EGFR Mutant Structural Database: computationally predicted 3D structures and the corresponding binding free energies with gefitinib and erlotinib. *BMC Bioinformatics* 2015;16:85.
- (2) Wang DD, Zhou W, Yan H, Wong M, Lee V. Personalized prediction of EGFR mutation-induced drug resistance in lung cancer. *Sci Rep* 2013;3:2855.

- (3) Ma L, Wang DD, Huang Y, Wong MP, Lee VH, Yan H, Decoding the EGFR mutation-induced drug resistance in lung cancer treatment by local surface geometric properties. *Comput Biol Med* 2015;63:293-300.
- (4) Wang DD, Lee VH, Zhu G, Zou B, Ma L, Yan H. Selectivity profile of afatinib for EGFR-mutated non-small-cell lung cancer. *Mol Biosyst* 2016;12:1552-63.
- (5) Wang DD, Ma L, Wong MP, Lee VH, Yan H. Contribution of EGFR and ErbB-3 heterodimerization to the EGFR mutation-induced gefitinib- and erlotinib-resistance in non-small-cell lung carcinoma treatment. *PLoS One* 2015;10:e0128360.

References

1. Stewart BW, Wild CP, editors. *World Cancer Report 2014*. WHO Press; 2014. Available from: <https://www.who.int/en/news-room/fact-sheets/detail/cancer>.
2. Haley JD, Gullick WJ. *Cancer Drug Discovery and Development: EGFR Signaling Networks in Cancer Therapy*. Springer; 2008.
3. Singh I, Amin H, Rah B, Goswami A. Targeting EGFR and IGF 1R: a promising combination therapy for metastatic cancer. *Front Biosci (Schol Ed)* 2013;5:231-46.
4. Temraz S, Mukherji D, Shamseddine A. Dual targeting of HER3 and EGFR in colorectal tumors might overcome anti-EGFR resistance. *Crit Rev Oncol Hematol* 2016;101:151-7.
5. Liao BC, Lin CC, Yang JC. Novel EGFR inhibitors in non-small cell lung cancer: current status of Afatinib. *Curr Oncol Rep* 2017;19:4.

Combined use of *Andrographis paniculata* and chemotherapeutics for metastatic oesophageal cancer: a pre-clinical study

L Li, GGL Yue, KP Fung, J Yu, CBS Lau, PWY Chiu *

KEY MESSAGES

1. The combined use of water extract of *Andrographis paniculata* (APW) and chemotherapeutics (cisplatin plus 5-fluorouracil) reduced the metastasis of oesophageal tumour to lung in mouse models.
2. The combined use of APW and chemotherapeutics significantly suppressed the oesophageal xenograft growth by enhancing apoptosis.
3. Combined use of APW and chemotherapeutics had additional immunomodulatory benefit of APW.
4. The absorbed components of APW possessed

anti-migratory activities in oesophageal cancer cells.

Hong Kong Med J 2019;25(Suppl 9):S43-6
HMRP project number: 11120981

¹ L Li, ² GGL Yue, ^{2,3} KP Fung, ⁴ J Yu, ² CBS Lau, ¹ PWY Chiu

The Chinese University of Hong Kong:

¹ Department of Surgery

² Institute of Chinese Medicine and State Key Laboratory of Bioactivities and Clinical Applications of Medicinal Plants

³ School of Biomedical Sciences

⁴ Department of Medicine and Therapeutics

* Principal applicant and corresponding author:
philipchiu@surgery.cuhk.edu.hk

Introduction

Oesophageal cancer (OC) is the fourth and sixth leading cause of cancer-related death in China and United States, respectively. Surgery is the main treatment option for OC but has high recurrence rate owing to metastasis. Surgery followed by adjuvant chemotherapy and concurrent radiotherapy is a more effective treatment. The standard chemotherapeutics are cisplatin and 5-fluorouracil (5-FU).¹ Nevertheless, chemotherapy may cause a number of adverse effects that hamper efficacious treatment.

Many cancer patients use herbal prescriptions and supplements to combat cancer, strengthen the immune system, and counter some side-effects of the conventional treatments. A systematic review on Chinese herbal medicine for OC has shown improvement in immune system, extension of survival, reduction of adverse reactions to chemotherapy and radiotherapy, and the holistic function of the patients.² More scientific evidence of using Chinese herbal medicine for metastatic OC should be further explored.

The water extract of *Andrographis paniculata* (AP) has been shown to have anti-tumour effects in human OC cells. This study aimed to evaluate the anti-tumour and anti-metastatic activities of AP water extract (APW) combined with OC chemotherapeutics (cisplatin and 5-fluorouracil) in an OC metastatic mouse model. The immunomodulatory effect of APW was investigated in immune-competent mice. The gastrointestinal

absorption characteristics of APW were determined in a human intestinal Caco-2 cell transport model, which is a pre-clinical integral component of the Biopharmaceutics Classification System and can be used to investigate the gastrointestinal absorption, permeability, and drug-drug interactions.⁴ The anti-metastasis effects of the absorbed AP components (AAPC) through the Caco-2 transport model were verified in human oesophageal cancer cells in vitro.

Materials and Methods

A single lot of dried whole plant of AP (about 10 kg) was purchased from a renowned supplier in Hong Kong. Morphological and chemical authentications were accomplished in accordance with the Chinese Pharmacopoeia 2010. Authenticated voucher specimen (number: 3435) was deposited in the museum of the Institute of Chinese Medicine, CUHK. Dried whole plant of AP was extracted under reflux using water for 1 h and the extraction was repeated once. Following filtration, the crude water extract was centrifuged to remove undissolved particles. The extract was freeze-dried into powder.

The human OC cells EC-109 were obtained from Cell Bank of Type Culture Collection of Chinese Academy of Sciences (Beijing, China) and human intestinal Caco-2 cells were obtained from the American Type Culture Collection (MD, USA). Cell culture media and supplements were purchased from Life Technologies (NY, USA). BALB/c nude mice and C57BL/6 mice were provided by Laboratory Animal Services Centre, The Chinese University of

Hong Kong, and were housed under pathogen-free conditions. The experiments were approved by the Animal Experimentation Ethics Committee of The Chinese University of Hong Kong (Ref. No. 12-078-MIS).

Nude mice (6-8 weeks of age) were inoculated intraperitoneally with 5×10^6 EC-109 cells in 200 μ L PBS on day 0. On day 1, animals were randomised into four groups: (1) control, (2) APW (1600 mg/kg), (3) combination of cisplatin (1.5 mg/kg) and 5-FU (42.5 mg/kg), and (4) combination of APW (1600 mg/kg), cisplatin (1.5 mg/kg), and 5-FU (42.5 mg/kg). APW was orally administered daily for 21 days, and cisplatin and 5-FU were injected intraperitoneally on days 13 and 19. On day 22, the mice were anaesthetised and whole blood was obtained by cardiac puncture. The animals were sacrificed by cervical dislocation. Lungs of the mice were dissected out after cervical dislocation and fixed in 10% buffered formalin. The samples were stained with haematoxylin and eosin. Stained sections were examined and photographed under a light microscope (Olympus IX71, Japan). Evaluation of lung metastasis was carried out according to a previous study.³

Nude mice (6-8 weeks of age) were inoculated subcutaneously into the flank with EC-109 (1×10^6 cells per 100 μ L PBS) on day 1. The mice were randomised into the four groups when the tumour reached the volume of 70 mm³. Treatment period was 21 days, with the same treatment protocol mentioned above. Body weight was monitored and the size of tumour was measured with a caliper every 3-4 days and were calculated with the formula: $(\text{length} \times \text{width})^2/2$. At the end of treatment (day 22), tumours were excised from mice after sacrifice. Sections were subjected to TUNEL staining to determine the number of apoptotic cells. Blinded assessments were performed in four randomly chosen sections from each mouse using Image J software (NIH).

Immune responses of mice towards APW and/or chemotherapeutics were evaluated in a carcinogen-induced oesophageal dysplasia mouse model (protocol modified from Tang et al.⁵). In brief, C57BL/6 mice (4 weeks of age) were fed ad libitum with a zinc-deficiency diet (Envigo, CA, USA) for 3 weeks and then provided with drinking water containing 60 μ g/mL 4-nitroquinoline 1-oxide (NQO, Sigma, MO, USA) for 11 weeks. Treatments started at week 8 and the treatment protocol was the same as that mentioned above. At the end of treatment, the animals were sacrificed and spleens were excised. The isolated spleen leucocytes were subjected to T-cells subsets (eg CD3e⁺, CD4⁺, CD8⁺) measurement using flow cytometry.

Caco-2 cells were seeded at 3×10^5 cells/well in six-well plates with Transwell inserts (0.4 μ m pore size; Corning, USA) and cultured for 21 days prior to transport experiments. Transport experiments were

carried out as described previously.⁴ The APW at 400, 800, 1600, 3200, or 6400 μ g/mL were added on the apical side of the monolayer and incubated at 37°C for 2 h. The buffer in the basolateral compartment that contains the AAPC was collected and blow dried by termovap nitrogen sample concentrator and redissolved in culture medium for cell assays.

The viability of EC-109 cells was examined by trypan blue exclusion assay. Briefly, EC-109 cells (2.5×10^5 /well) were seeded in 24-well plates and allowed adhesion overnight. The medium was changed to 10% v/v FBS medium with AAPC (APW at 800, 1600, and 3200 μ g/mL) for 48 h. Subsequently, the adherent cells and floating cells were collected. The cell suspension was mixed with trypan blue dye. The number of viable cells was counted under a light microscope (Olympus IX-71, Japan). The motility of EC-109 was assessed by the scratch wound assay as described in previous study.³ In brief, EC-109 cell layers scraped with wounds were incubated with medium containing AAPC (APW at 800, 1600, and 3200 μ g/mL) for 24 h and each well was photographed at 40 \times magnification under a light microscope. The wound area was blindly assessed using Image J software (NIH).

Data were expressed as mean \pm standard deviation for in vitro studies, and as mean \pm standard error of the mean for in vivo studies. One-way analysis of variance followed by post-hoc Dunnett test were used to compare the treatment groups and the control group. One-way analysis of variance followed by post-hoc Tukey multiple comparison test were used to determine significant differences among all groups. Statistical analyses were conducted using GraphPad Prism 5.0 (GraphPad Software Inc, San Diego, CA, USA). In all comparisons, $P < 0.05$ was considered statistically significant.

Results

Lung metastasis was observed after intraperitoneal inoculation of EC-109 cells for 22 days. Tumours were found in lung sections; treatments with APW, cisplatin plus 5-FU, or both could inhibit the lung metastasis in intraperitoneal xenograft-bearing nude mice (Fig 1).

Combined use of APW with cisplatin plus 5-FU showed inhibitory effects on EC-109 tumour growth (Fig 2). There was no significant change in body weight in all treatment groups. The number of the apoptotic cells was significantly higher in combined treatment groups than that in control group.

The number of cytotoxic T-lymphocytes (CD3e⁺, CD8a⁺) and T-helper lymphocytes (CD3e⁺, CD4⁺) from spleen increased after combined treatment of APW and cisplatin plus 5-FU. The number of cytotoxic T-lymphocytes in combined treatment group was significantly greater than in chemotherapeutic alone group.

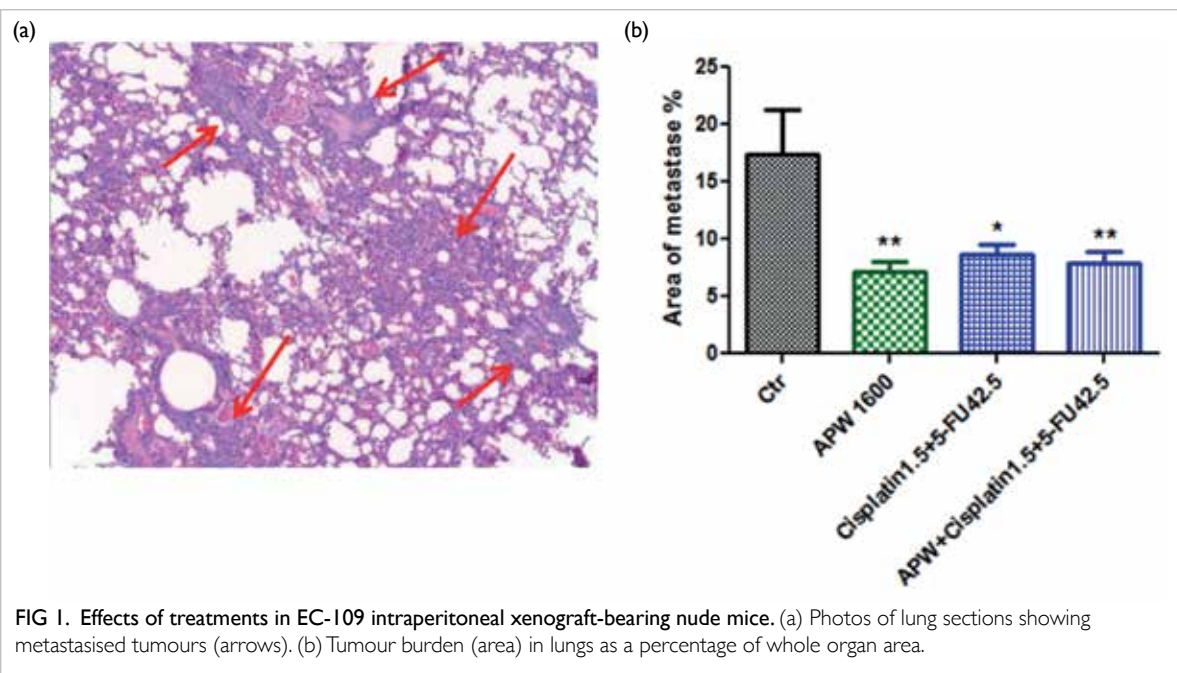


FIG 1. Effects of treatments in EC-109 intraperitoneal xenograft-bearing nude mice. (a) Photos of lung sections showing metastasised tumours (arrows). (b) Tumour burden (area) in lungs as a percentage of whole organ area.

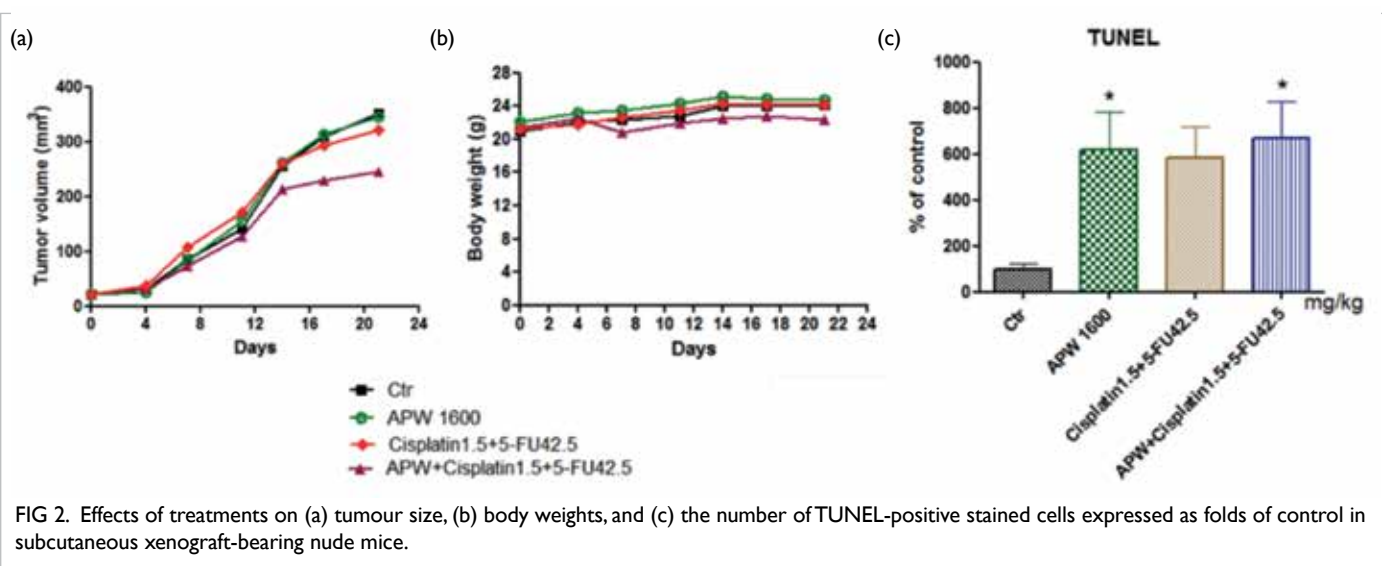


FIG 2. Effects of treatments on (a) tumour size, (b) body weights, and (c) the number of TUNEL-positive stained cells expressed as folds of control in subcutaneous xenograft-bearing nude mice.

AAPC from 800, 1600, and 3200 µg/mL APW did not affect the viability of EC-109 cells after 48 h incubation (Fig 3). The open wound area in wells treated with AAPC from 800, 1600, and 3200 µg/mL APW were larger than those of control wells after incubation for 24 h, suggesting the cell motility was suppressed by AAPC.

Discussion

The present studies involved three mouse models. The intraperitoneal xenograft-bearing nude mice model demonstrated the anti-metastatic activities of APW and/or chemotherapeutics. The effects may be

responsible for the prolongation of survival attained after the combined treatment (data not shown). The enhanced anti-tumour effects in combined treatment were observed. The combined treatment significantly increased the number of apoptotic cancer cells in tumour. A reduction of number of proliferative cancer cells was observed in tumour sections from combined treated mice (data not shown), suggesting the proliferation of cancer cells was also inhibited by combined treatment.

To investigate the immunomodulatory effect of APW, the NQO-induced oesophageal dysplasia mouse model showed significant alterations of T-cell populations after treatments. The combined

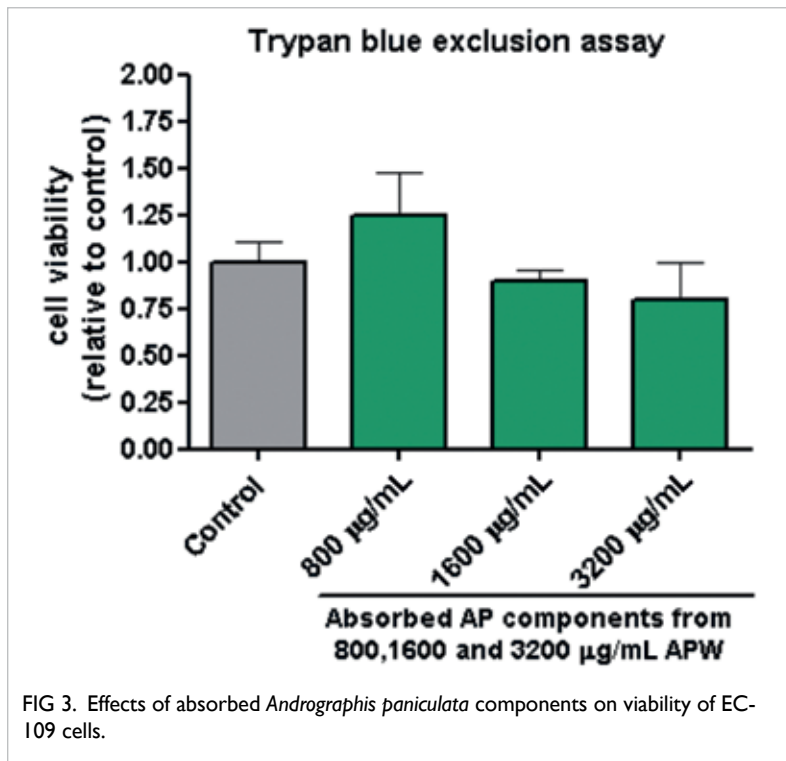


FIG 3. Effects of absorbed *Andrographis paniculata* components on viability of EC-109 cells.

treatments significantly increased T cytotoxic lymphocytes. The cytokine productions from spleen lymphocytes of mice were affected by the APW and/or chemotherapeutics treatments.

The in vitro activities of APW on metastasis were investigated. The bioavailability of andrographolide, which was expected to be the active component of AP, was reported to be poor. Nonetheless, the absorption of the water extract of AP, which is the traditional way to use Chinese herbal medicine, has not been reported. The Caco-2 transport model was used to mimic the gastrointestinal absorption and permeability and to investigate the absorption of APW. The absorbed AP components were found to suppress the motility of OC cells without cytotoxicity. Cancer cell motility and invasion are essential processes in cancer metastasis. These findings suggested that the absorbed components of APW are capable to inhibit the metastasis of cancer cells in vitro.

Conclusion

Combined use of APW and chemotherapeutics exerted anti-tumour and anti-metastatic effects in metastatic OC mouse models, with additional

immunomodulatory benefit of APW observed. The in vitro anti-migratory activity of absorbed components of APW could partly explain the efficacies in mouse models. Taking together, the combined treatment (APW plus cisplatin and 5-FU) has more beneficial effects against metastatic OC than chemotherapeutics alone.

Acknowledgements

This study was supported by the Health and Medical Research Fund, Food and Health Bureau, Hong Kong SAR Government (#11120981). We would like to thank Prof Anthony Wing-Hung Chan, Department of Anatomical and Cellular Pathology, The Chinese University of Hong Kong, for assessment of histological samples. We also thank Dr Kar-Man Chan, Ms Si Gao, Mr Hin-Fai Kwok, Mr Ching-Po Lau, Ms Julia Kin-Ming Lee, Miss Ceci Lok-Sze Wong, and Mr Eric Chun-Wai Wong for technical support.

Results from this study have been published in:

- (1) Yue GG, Lee JK, Li L, et al. *Andrographis paniculata* elicits anti-invasion activities by suppressing TM4SF3 gene expression and by anoikis-sensitization in esophageal cancer cells. *Am J Cancer Res* 2015;5:3570-87.
- (2) Li L, Yue GGL, Lee JMK, et al. Investigation of the combination effects of *Andrographis paniculata* with chemotherapeutics for esophageal cancer treatment. *Clin Gastroenterol Hepatol* 2015;13:e80.
- (3) Li L, Yue GG, Lee JK, et al. The adjuvant value of *Andrographis paniculata* in metastatic esophageal cancer treatment – from preclinical perspectives. *Sci Rep* 2017;7:854.

References

1. Yun T, Han JY, Lee JS, et al. Phase II study of weekly paclitaxel and capecitabine in patients with metastatic or recurrent esophageal squamous cell carcinoma. *BMC Cancer* 2011;11:385.
2. Wei X, Chen ZY, Yang XY, Wu TX. Medicinal herbs for esophageal cancer. *Cochrane Database Syst Rev* 2007;2:CD004520.
3. Yue GG, Lee JK, Li L, et al. *Andrographis paniculata* elicits anti-invasion activities by suppressing TM4SF3 gene expression and by anoikis-sensitization in esophageal cancer cells. *Am J Cancer Res* 2015;5:3570-87.
4. Awortwe C, Fasinu PS, Rosenkranz B. Application of Caco-2 cell line in herb-drug interaction studies: current approaches and challenges. *J Pharm Pharm Sci* 2014;17:1-19.
5. Tang XH, Knudsen B, Bemis D, Tickoo S, Gudas LJ. Oral cavity and esophageal carcinogenesis modeled in carcinogen-treated mice. *Clin Cancer Res* 2004;10:301-13.

AUTHOR INDEX

| | | | |
|------------|------|-----------|----|
| Chan MCW | 17 | Li L | 43 |
| Chan PKS | 17 | Lian JX | 4 |
| Chen LJ | 12 | Liu XB | 35 |
| Chiu APY | 24 | Liu YP | 21 |
| Chiu PWY | 43 | Lo CM | 35 |
| Chong V | 8 | Man K | 35 |
| Chow HY | 28 | McGhee SM | 4 |
| Cowling BJ | 24 | Pang CP | 12 |
| Fung KP | 43 | Shin VY | 32 |
| Gangwani R | 4, 8 | So YH | 28 |
| He DH | 24 | Tham CCY | 12 |
| Ho MK | 28 | Tu WW | 21 |
| Kam YW | 4 | Wong DSH | 4 |
| Kawasaki R | 8 | Wong I | 8 |
| Lam KT | 21 | Wong L | 4 |
| Lam YM | 28 | Wong M | 40 |
| Lau CBS | 43 | Wong R | 8 |
| Lau YL | 21 | Wu JTK | 24 |
| Law WL | 32 | Xiang Z | 21 |
| Lee V | 40 | Yan H | 40 |
| Leung CKS | 12 | Yu J | 43 |
| Leung SL | 28 | Yue GGL | 43 |
| Leung WK | 32 | Zheng J | 21 |
| Leung YC | 28 | Zhu GY | 40 |
| Li KKW | 4 | | |

Disclaimer

The reports contained in this publication are for reference only and should not be regarded as a substitute for professional advice. The Government shall not be liable for any loss or damage, howsoever caused, arising from any information contained in these reports. The Government shall not be liable for any inaccuracies, incompleteness, omissions, mistakes or errors in these reports, or for any loss or damage arising from information presented herein. The opinions, findings, conclusions and recommendations expressed in this publication are those of the authors of the reports, and do not necessarily reflect the views of the Government. Nothing herein shall affect the copyright and other intellectual property rights in the information and material contained in these reports. All intellectual property rights and any other rights, if any, in relation to the contents of these reports are hereby reserved. The material herein may be reproduced for personal use but may not be reproduced or distributed for commercial purposes or any other exploitation without the prior written consent of the Government. Nothing contained in these reports shall constitute any of the authors of these reports an employer, employee, servant, agent or partner of the Government.

Published by the Hong Kong Academy of Medicine Press for the Government of the Hong Kong Special Administrative Region. The opinions expressed in the *Hong Kong Medical Journal* and its supplements are those of the authors and do not reflect the official policies of the Hong Kong Academy of Medicine, the Hong Kong Medical Association, the institutions to which the authors are affiliated, or those of the publisher.